AN ABSTRACT OF THE DISSERTATION OF

Elizabeth R. Axton for the degree of Doctor of Philosophy in Pharmaceutical Sciences and Toxicology presented on August 2, 2017

Title: Mass Spectrometry Techniques to Assess the Metabolism and Toxicity of Pharmaceutical and Dietary Nitrates

Abstract approved: _____

Jan F. Stevens and Robert Tanguay

Nitric oxide (NO) is a signaling molecule that regulates blood pressure and vascular tone. Humans produce NO by endothelial nitric oxide synthase (eNOS), which is impaired in patients with cardiovascular disease leading to increased blood pressure, endothelial dysfunction, and an increased risk of adverse cardiovascular outcomes. Maintaining optimal levels of NO is critical for human health. Inorganic nitrate (NO_3^-) is reduced to NO and can be an alternate pathway to restore NO production. Diets high in nitrate reduce blood pressure and improve exercise performance in humans. In patients with advanced cardiovascular disease, organic nitrates such as nitroglycerin (glyceryl trinitrate, GTN) release NO and are essential for managing symptoms. This dissertation emphasizes mass spectrometry techniques to elucidate novel mechanisms for the effects of both organic and inorganic nitrate on cardiovascular health and exercise performance.

Pharmaceutical Nitrate. Patients develop tolerance to GTN after several weeks of continuous use, limiting the potential for long-term therapy. The cause of nitrate tolerance is relatively unknown. I developed a cell culture model of nitrate tolerance that utilizes stable isotopes to measure metabolism of $^{15}N_3$-GTN into ^{15}N-nitrite. I performed global metabolomics to identify

the mechanism of GTN-induced nitrate tolerance and to elucidate the protective role of vitamin C. Metabolomics demonstrated that GTN impaired purine metabolism and depleted intracellular ATP and GTP. GTN inactivated the enzyme xanthine oxidase (XO), an enzyme that is critical for the metabolism of GTN into NO. Vitamin C prevented inactivation of XO, resulting in increased NO production from GTN. Vitamin C supplementation should be further investigated as a simple and inexpensive strategy to prevent nitrate tolerance.

Dietary Nitrate. Inorganic nitrate improves exercise performance by reducing the oxygen cost of exercise. Although previous research has suggested that nitrate improves mitochondrial efficiency and stimulates mitochondrial biogenesis, we have an incomplete understanding of the mechanism. In a zebrafish (*Danio rerio*) model, nitrate reduced the oxygen cost of exercise during a vigorous 2-hour exercise test. Although there were no significant differences in mitochondrial function between control and nitrate-treated zebrafish, nitrate treatment increased resting ADP, ATP, and cyclic AMP levels. Metabolomics analysis of whole fish illustrated that nitrate stimulated glycolysis and ketogenesis. I conclude that nitrate reduces the oxygen cost of exercise by favoring glycolysis for energy production, thereby producing more ATP while consuming less oxygen. Nitrate-stimulated alteration of metabolic fuels for energy production is a novel mechanism for the improvement in exercise performance.

Summary. This dissertation is a significant contribution to scientific knowledge because of the development of a novel assay to measure ^{15}N-labeled nitrate and nitrite, which I have applied to study the metabolism of pharmaceutical and dietary nitrates. Using metabolomics, I elucidated the novel mechanism that vitamin C prevents nitrate tolerance by protecting XO from inactivation. Furthermore, I demonstrated that nitrate alters the utilization of metabolic fuels, leading to reduced oxygen consumption during exercise.

Mass Spectrometry Techniques to Assess the Metabolism and Toxicity of Pharmaceutical and Dietary Nitrates

by
Elizabeth R. Axton

A DISSERTATION

submitted to

Oregon State University

in partial fulfillment of
the requirements for the
degree of

Doctor of Philosophy

Presented August 2, 2017
Commencement June 2018

Doctor of Philosophy dissertation of Elizabeth R. Axton presented on August 2, 2017

APPROVED:

Co-Major Professor, representing Pharmaceutical Sciences

Co-Major Professor, representing Toxicology

Dean of the College of Pharmacy

Head of the Department of Environmental and Molecular Toxicology

Dean of the Graduate School

I understand that my dissertation will become part of the permanent collection of Oregon State University libraries. My signature below authorizes release of my dissertation to any reader upon request.

Elizabeth R. Axton, Author

ACKNOWLEDGEMENTS

I would like to acknowledge my advisor, Fred Stevens, for his continued support in my development as a scientist. You gave me the independence to pursue my ideas, while always maintaining high expectations and providing me with valuable feedback. I would like to thank my committee members Robert Tanguay, Susan Tilton, Jane Ishmael, Chrissa Kioussi, and Adrian Fritz Gombart for their helpful feedback, support, and guidance.

Thank you to all members of the lab, including Cristobal Miranda and David Yu for their support with cell culture and molecular biology assays, Ralph Reed for his HPLC expertise and critical eye, Jaewoo Choi for his assistance with organic chemistry and mass spectrometry, and Manuel Garcia-Jaramillo for hands-on assistance. In particular, I acknowledge the undergraduate students that have made this work possible: Eleonso Cristobal, Jackilyn Toftner, Eunice Lee, Joshua Hay, and Erik McEntire. I acknowledge all past and present lab members for their support and friendship throughout the years. In addition, I would like to thank Jeffrey Morré for assistance with mass spectrometry. Thank you to Norm Hord and Laura Beaver for their support and assistance, especially through the nitrate zebrafish collaboration. You have both been excellent mentors to me, and it has been truly a joy to work with you throughout the last year. I would like to thank members of the Linus Pauling Institute - in particular, Scott Leonard, Alexander Michels, Sandra Uesuegi, Mary Fantacone, and Gerd Bobe have provided technical assistance, feedback on scientific writing, and general advice and support.

Finally, thank you to my family and friends for proving emotional support throughout the years. A doctoral degree takes a village, and I would not have been able to do it without all of you.

CONTRIBUTION OF AUTHORS

Elizabeth A. Hardardt contributed to the development of the LC-MS/MS method in Chapter 2. Chapter 4 was co-authored with Laura M. Beaver, with contributions by Lindsey St. Mary, Lisa Truong, Christiana Logan, Sean Spagnoli, Mary Catherine Prater, Rosa Moon Keller, Manuel Garcia-Jaramillo, Sean Newsom, Matt Robinson, Robert Tanguay, and Norman Hord. Jan F. Stevens was the principal investigator of all manuscripts.

TABLE OF CONTENTS

TABLE OF CONTENTS (Continued)

LIST OF FIGURES

LIST OF FIGURES (Continued)

Figure Page

LIST OF TABLES

Table Page

CHAPTER 1: INTRODUCTION

Nitric oxide (NO) is a free radical signaling molecule that regulates several physiological and pathological pathways, including blood pressure and vascular tone. Humans produce NO from L-arginine by the enzyme endothelial nitric oxide synthase (eNOS) within the endothelial cell layer of blood vessels. Once generated, NO diffuses into the smooth muscle cell layer to induce vasodilation. The pathway of NO-stimulated cGMP-dependent vasodilation is summarized in Figure 1.1. NO production by eNOS is impaired in patients with cardiovascular disease (2). Furthermore, NO can react with other free radicals such as superoxide (O_2^-), resulting in increased oxidative stress and reduced NO levels. This reduction in NO increases blood pressure, causes endothelial dysfunction, and increases the risk of adverse cardiovascular outcomes (2). For these reasons, maintaining optimal levels of NO is critical for human health.

Nitrate (NO_3^-) is a polyatomic ion that is ubiquitous in nature. Although nitrate itself is relatively inert, it is enzymatically reduced to NO in humans and can be used as an alternate pathway to restore NO production. Present in high amounts in beets and leafy greens, diets high in nitrate reduce blood pressure and improve exercise performance in humans (3,4). In addition to inorganic nitrate in the diet, organic nitrates (R-ONO_2) are prodrugs used as pharmaceutical agents. In patients with advanced cardiovascular disease, organic nitrates such as nitroglycerin are metabolized into NO and are essential for managing symptoms and preventing heart attacks (5). Therefore, nitrates are beneficial for both preventing and treating cardiovascular disease.

In this introductory chapter, I review the literature on these two types of nitrates and their application to human health. First, pharmaceutical organic nitrates are used to treat chest pain resulting from insufficient blood flow (angina). However, patients develop tolerance to organic nitrates over time, which limits their efficacy and potential for long-term therapy. I review the literature on the metabolism of organic nitrates, and the state of the knowledge on the

development of nitrate tolerance. Next, I explore dietary nitrates and the relatively new discovery that they can improve exercise performance and reduce the oxygen cost of exercise. Some research suggests that nitrate improves mitochondrial efficiency and stimulates biogenesis; others suggest that the mechanism is extramitochondrial. We have an incomplete understanding of the mechanism by which nitrate improves exercise performance. Finally, I introduce mass spectrometry as a tool to bring insight into the gaps in literature surrounding both organic and inorganic nitrates and their effects on cardiovascular health and exercise performance. A mechanistic understanding of the functions of nitrate is essential to determine their long-term impact on human health.

1.1. PHARMACEUTICAL NITRATE

History and Use in the Clinic

Nitroglycerin is an organic nitrate that is used to treat chest pain resulting from insufficient blood flow to the heart (angina pectoris). Nitroglycerin was first synthesized as an explosive by the Italian chemist Ascanio Sobrero in 1847 by mixing glycerol with a mixture of nitric and sulfuric acid (6). Alfred Nobel sought to develop protocols for the safe use of nitroglycerin as a commercially available explosive. Sadly, Alfred Nobel's younger brother Emil Oskar Nobel, as well as several other workers in the Nobel lab, were killed in an accidental nitroglycerin explosion in 1864. Nobel's factory in Hamburg was destroyed twice during the development of "Blasting Oil", a liquid form of nitroglycerin. Blasting Oil was later banned due to its reactivity, and Nobel eventually used nitroglycerin as an active ingredient in the explosive dynamite.

In 1878, Dr. William Murrell experimented with using diluted nitroglycerin to reduce blood pressure and relieve angina. His work was published in *the Lancet* in 1879 (5). Ironically, Alfred

Nobel was prescribed nitroglycerin a few months before his death in 1896, although he refused to take it. Nitroglycerin was re-named glyceryl trinitrate or "Trinitrin" for clinical uses so as to not alarm the public. Although they are chemically identical, glyceryl trinitrate (GTN) is the preferred name for use in the clinic, and the term nitroglycerin is used to describe the explosive (6).

Until the 1980's, almost nothing was known about the mechanism of GTN. In 1980, Furchgott and Zawadzki discovered that vasodilation induced by acetylcholine was dependent on an intact endothelium, which released a diffusible and labile substance that was named the endothelium-derived relaxation factor (EDRF)(7,8). It was later determined that EDRF is in fact nitric oxide (NO), which regulates vascular tone, blood flow, blood pressure, inhibition of platelet aggregation and adhesion, and is involved in postischemic reperfusion, memory function, and central nervous system degenerative diseases (9,10). Furchgott was awarded a Nobel Prize in 1998 for his discovery of NO as a new cellular signaling molecule. Ferid Murad discovered that GTN releases NO (11), however the relevance of this finding was not understood until the discovery that EDRF was, in fact, NO (6). The history of the discovery of NO and its diverse role in vascular biology have been recently reviewed (12).

GTN was the first synthesized drug in the world (5). As such, it has been used in the clinic for almost 140 years. Today, GTN is most often prescribed as a sublingual pill or dermal patch. It is used to treat chest pain in patients suffering from stable angina caused by advanced cardiovascular disease. GTN releases NO, which diffuses into smooth muscle cells, inducing vasodilation and improving blood flow. GTN became a commonly prescribed drug because of its fast and potent effects: chest pain is relieved within minutes of a single sublingual dose of GTN. In more recent years, other nitrates have become available as slow-release alternatives to GTN

that are more suitable for long-term treatment. These include isosorbide mononitrate (ISMN), isosorbide dinitrate (ISDN), and pentaerythritol tetranitrate (PETN)(13). Although these GTN alternatives are less potent, patients develop tolerance at a slower rate.

Shortly after GTN was introduced as a cardiovascular drug, it became apparent that patients were suffering severe side effects. Notably, many patients developed migraines. Although vasodilation relieves chest pain, it also dilates blood vessels in the brain leading to severe headaches. This issue still persists in the clinic today. Migraines were also noticed in Alfred Nobel's factory: workers complained of headaches on Mondays, and the symptoms subsided throughout the remainder of the week. This was referred to as "Monday disease" and is indicative of withdrawal (6). Furthermore, patients reported having to take higher and higher doses of GTN to achieve the same effects. This observed nitrate tolerance is a phenomenon that researchers still do not fully understand (14,15).

Nitrate tolerance develops after only a few weeks of continuous GTN therapy, which reduces its potential for long-term treatment. To prevent nitrate tolerance, doctors instruct patients to implement 12-hour nitrate-free intervals, usually during the night. Though this strategy is effective at preventing nitrate tolerance, it increases the risk of an adverse cardiovascular event. Patients commonly have early morning heart attacks when the drug is at its lowest plasma concentration (16). GTN is now primarily prescribed as a short-term treatment in cases of severe chest pain. In addition to reducing the effectiveness of GTN, nitrate tolerance is associated with the development of endothelial dysfunction, which has the potential to worsen patient outcomes.

GTN Metabolism and Mechanism of Action

Critical to the biological effects of GTN is the metabolism into NO. The enzymatic mechanism for production of NO from GTN was not discovered until 2002 – over 120 years after GTN was put into clinical use. GTN is bioactivated into nitrite by mitochondrial aldehyde dehydrogenase (ALDH2). Chen et al. demonstrated that purified ALDH2 can bioactivate GTN into nitrite, leading to cGMP production and subsequent cGMP-dependent vasodilation (17). Several years later, the same group demonstrated that ALDH2 knockouts in mice reduced the vasodilatory response to GTN. Importantly, the mice still responded to treatment, but only at much higher concentrations (18). Their results suggested that ALDH2 is a high affinity pathway of GTN bioactivation, however there is another low-affinity pathway that may be physiologically relevant under certain conditions. Enzymatic bioactivation of GTN was demonstrated to preferentially produce 1,2-GDN, whereas non-enzymatic hydrolysis of GTN produces both 1,2-GDN and 1,3-GDN (17).

Not all researchers were convinced that ALDH2 is a major GTN-bioactivating enzyme. Nitrite must be reduced to NO – a reaction that ALDH2 is incapable of catalyzing. D'Souza et al. demonstrated that siRNA knockdowns and overexpression of ALDH2 in epithelial cells had no effect on the cells' response to GTN (19). In addition, diphenyleneiodonium (DPI), a potent inhibitor of ALDH2, did not decrease GTN-induced vasodilation of bovine coronary arteries (20,21). Recently, Miura et al. demonstrated that 3 different ALDH2 polymorphisms in Japanese subjects did not have altered vasodilatory response to GTN, or alter the rate of the development of nitrate tolerance (22). Often, no changes in NO production are detected after GTN treatment, and yet there is a significant vasodilatory response (23). Thus, clinical evidence suggests that ALDH2 activity alone cannot account for the potent vasodilatory response to GTN. These results suggest that there may be additional vasoactive mechanisms of GTN.

One enzyme that may be involved in the metabolism of GTN is xanthine oxidase (XO). XO is the enzyme that metabolizes hypoxanthine and xanthine into uric acid, and is the final step of purine metabolism in humans. In the year 2000, it was discovered that XO can metabolize GTN into nitrite, and subsequently into NO (24-27). The FAD site of XO bioactivates GTN into nitrite, producing superoxide as a reactive byproduct. Nitrite is then reduced to NO at the molybdenum site, using xanthine or NADH as a cofactor and electron donor (28). Originally, these early publications went unnoticed because this is a lower affinity pathway that is only significant in acidic or low oxygen conditions. However, this pathway may take on greater significance in the ischemic conditions of a diseased heart. This alternate pathway of GTN bioactivation by XO may be the lower affinity pathway responsible for GTN-induced vasodilation previously reported in the aforementioned publications (18-20).

Mechanisms of Nitrate Tolerance

Elucidating the cause of nitrate tolerance is no small feat. After 140 years of use in the clinic, many hypotheses have been proposed and yet there is no scientific consensus. One challenge with determining the cause of nitrate tolerance is the many steps required for GTN to have a physiological effect: GTN must be absorbed, reach its target site (the endothelial cells of blood vessels), be enzymatically metabolized into NO, and then NO must diffuse into the smooth muscle cells where an intact signaling pathway is needed to have a physiological response. If any of these steps are impaired with prolonged GTN treatment, there will be a reduced vasodilatory response. Here, I discuss some of the potential mechanisms for the development of nitrate tolerance.

Mechanisms of nitrate tolerance can be categorized into two potential causes: i) reduced bioactivation of GTN into NO, and ii) reduced physiological response to NO. An underlying theme to all mechanisms that lead to nitrate tolerance is oxidative stress. In 2005, Dr. Thomas Münzel developed the "oxidative stress hypothesis" which claims that the development of nitrate tolerance is due to increased intracellular oxidative stress (29,30). GTN bioactivation results in both superoxide and NO production. NO undergoes a rapid biradical reaction with superoxide (6.7×10^9 M^{-1} S^{-1}) to form peroxynitrite ($ONOO^-$), a highly reactive oxidative and nitrative species (31,32). Peroxynitrite can target DNA, lipids, proteins, and amino acids, leading to vascular and myocardial dysfunction (31). For these reasons, peroxynitrite is a double-edged sword: it causes deleterious effects in tissue due to its nitrative and oxidative capacity, yet also acts as a sink for bioavailable NO.

Some potential targets for peroxynitrite that may cause the development of nitrate tolerance are XO (33), ALDH2 (17), and eNOS (34). All of these enzymes are involved with either GTN bioactivation or endogenous NO production. Importantly, inactivation of these enzymes by peroxynitrite would further increase intracellular oxidative stress. XO produces superoxide in low oxygen and acidic conditions, such as in ischemic heart tissue (28,35). ALDH2 is a 4-hydroxy-2(*E*)-nonenal (HNE) metabolizing enzyme, and inactivation of ALDH2 will lead to increased levels of HNE and mitochondrial oxidative stress (36). Peroxynitrite can cause uncoupling of eNOS, which in turns produces more oxidative species instead of NO (34). For these reasons, even a very low concentration of peroxynitrite can cause significant intracellular oxidative stress.

In addition to increasing intracellular oxidative stress, inactivation of XO, ALDH2, and eNOS reduces GTN metabolism and endogenous NO production. The reduction in NO production is the hallmark characteristic of endothelial dysfunction (37). ALDH2 has previously been

demonstrated to be inactivated with GTN treatment, which leads to reduced GTN-induced vasodilation (17). XO has also been shown to be inactivated with GTN treatment, however the physiological significance of XO in nitrate tolerance has yet to be determined (28,35). Since GTN increases intracellular superoxide and peroxynitrite, it is feasible that these oxidative species inactivate GTN-bioactivating enzymes and lead to reduced reactivity to GTN.

Clinical Significance

It is important to elucidate the mechanism of nitrate tolerance because GTN is an essential drug for the treatment of angina. It remains one of the most often prescribed drugs, especially in the US. The development of nitrate tolerance not only limits the use of GTN long term, but it also may indicate the development of serious abnormalities such as endothelial dysfunction, which worsens patient outcomes (38). For these reasons, GTN is currently reserved for cases of emergency treatment during instances of severe chest pain. Diagnosis and management of nitrate tolerance relies solely on patients' reporting of chest pain and on treadmill stress tests. These assessments are difficult to interpret: increased chest pain can be due to advancing cardiovascular disease or to the development of nitrate tolerance. There is a need for a simple and non-invasive method to test for the development of nitrate tolerance.

An understanding of the mechanistic cause of nitrate tolerance will provide us with valuable information on how to prevent it. The unifying theme of oxidative stress suggests that co-treatments with antioxidants have the potential to prevent nitrate tolerance. Hydralazine, a potent antioxidant and antihypertensive drug, has been shown to decrease mitochondrial oxidative stress and maintain GTN-induced vasodilation (39,40). Clinical studies in the 1990's demonstrated that vitamin C supplements may attenuate the development of nitrate tolerance

(41-43). Interestingly, the studies on the effects of vitamin C on nitrate tolerance have suggested that it may act via a mechanism independent from its antioxidant properties. More research is needed to elucidate the mechanism of vitamin C in preventing nitrate tolerance, especially given that it would be a simple and inexpensive co-treatment strategy. If an effective co-treatment becomes available, GTN may be able to be used for long-term therapy.

1.2. DIETARY NITRATE

Dietary nitrate is inorganic (NO_3^-) and primarily consumed as a constituent in root vegetables and leafy greens. Nitrate is present in water (current limit 10 mg/L), which has been steadily increasing with the increased use of nitrogen-based fertilizers (44). Nitrate and nitrite salts are used as preservatives and coloring agents in processed meats such as bacon, hot dogs, sausage, and lunch meat. Despite common belief, the amount of nitrate that humans consume in vegetables greatly outweighs that in processed meats. A 100 g serving of spinach has 741 mg of nitrate, whereas 100 g of bacon contains 5.5 mg of nitrate (45). Vegetables with the highest amount of nitrate (> 250 mg nitrate per 100 g wet weight) are celery, cress, chervil, lettuce, spinach, and red beets (45). Approximately 80% of the human intake of nitrate comes from fruits and vegetables, and the remaining 20% comes from processed meat and drinking water (46).

Here, I review the literature on the metabolism of dietary nitrate and its known beneficial effects: reduction of blood pressure and improved exercise performance. Given that many perceive nitrate to be entirely harmful, I also discuss the perceived negative health effects of nitrate and whether they are a genuine health concern.

Metabolism of Dietary Nitrate

Nitrate and nitrite were long considered stable, inactive end products of NO production. Research in the 1990's demonstrated that nitrite is not a waste product because it can be recycled back into NO (47-49). Intravenous infusion of nitrite results in NO-dependent vasodilation, demonstrating that nitrite can be reduced into NO in vivo (50). For these reasons, inorganic nitrate and nitrite are now considered a bioavailable pool for NO instead of inert waste products (51). Given that NO can be spontaneously oxidized back into nitrite and nitrate, these species are in constant flux, and are often referred to as "NO_x".

Humans concentrate dietary nitrate in the saliva. Salivary nitrate levels can be as high as 10 mM, whereas nitrite is 1-2 mM after nitrate consumption (52). Once in the oral cavity, commensal facultative anaerobic bacteria use nitrate as an alternative electron acceptor to oxygen during respiration, effectively reducing salivary nitrate to nitrite by the action of nitrate reductases. It has been demonstrated that rinsing with antibacterial mouthwash prior to consuming nitrates abolishes the effects (53,54). If nitrate enters the oral cavity, then is spit instead of swallowed, there is no absorption of nitrate or nitrite (52).

Once swallowed, the acidic environment of the stomach protonates nitrite into nitrous acid (HNO_2), which spontaneously produces NO and nitrogen dioxides (47,48). The production of NO is greatly increased in the presence of vitamin C or polyphenols (55,56). The NO produced in the stomach then diffuses into the blood stream. NO is rapidly oxidized back into nitrate and nitrite in the blood (half-life 3-4 seconds). Nitrite and nitrate in the blood are absorbed into the intestines and excreted by the kidneys. In addition to NO formation in the stomach, nitrite can also be systemically reduced to NO in the blood by deoxyhemoglobin, myoglobin, xanthine

oxidase, and cytochrome c oxidases of the mitochondrial electron transport chain. Reduction of nitrite to NO is favored in low oxygen or acidic conditions, such as in ischemic heart tissue or contracting skeletal muscle (46).

See Figure 1.2 for the parallel pathways of NO production.

Dietary pathway vs. endogenous pathway of NO production. In addition to production of NO from dietary nitrate, there is an endogenous pathway of NO production from L-arginine. L-arginine reacts with O_2 to produce NO and L-citrulline, which is facilitated by the enzyme nitric oxide synthase (eNOS). NO production by eNOS is dependent on neutral pH and oxygen, whereas NO production from nitrite and NO is favored at acidic pH and low oxygen. It has been proposed that the nitrate-nitrite-NO pathway is a backup for NO production from L-arginine (57). The relative contribution of nitrate from endogenous vs. exogenous sources naturally varies depending on diet, exercise, drugs, and disease state (46).

Beneficial Effects of Dietary Nitrate

Nitrate and nitrite were previously perceived to be potentially harmful dietary components due to the early reports of carcinogenicity and infantile methemoglobinemia. However, in the 1990's new research emerged suggesting that nitrate consumption in the diet improves cardiovascular health, immune function, exercise performance, and is associated with a lower risk of cancer. The beneficial effects of dietary nitrate appear to be dependent on the in vivo metabolism into NO. The beneficial effects now appear to far outweigh any risk of adverse effects, demonstrating a need to re-investigate recommendations on dietary intake of nitrate. Here, I discuss the impacts and potential mechanisms of nitrate on both cardiovascular health and exercise performance.

Dietary nitrate improves cardiovascular health. Cardiovascular disease remains the leading cause of mortality in the US. Epidemiological evidence suggests that a diet high in nitrates can lower blood pressure and prevent heart disease. Japanese longevity is the highest in the world, and they have very low incidence of cardiovascular disease. Sobko et al. fed 25 healthy volunteers either a Japanese diet or a western-type diet for 10 days. The subjects who consumed the Japanese diet had higher levels of both salivary and plasma nitrite and nitrate, and lower diastolic blood pressure by 4.5 mmHg (58). In the US, the Dietary Approaches to Stop Hypertension (DASH) diet has been demonstrated to lower blood pressure. Interestingly, the DASH diet, which is rich in vegetables (8-10 servings per day), exceeds the recommended dietary intake of nitrate by 550% for a 60 kg adult (59). The results of these studies question the FDA's recommendation to limit nitrate and nitrite consumption.

Nitrate reduces blood pressure. Hypertension (increased blood pressure) is the most common risk factor for cardiovascular morbidity and mortality. NO is a key regulator of cardiovascular function, and its primary function is maintaining vascular homeostasis. Emerging evidence suggests that oxidative stress and subsequent NO deficiency are associated with the development of hypertension (60). Lundberg et al. performed a double-blind crossover study in healthy humans. The research subjects received 0.1 mmol/day sodium nitrate for 3 days, corresponding to approximately 100-300 g of nitrate-rich vegetables. Nitrate supplementation reduced diastolic blood pressure (DBP) by 4 mmHg (61). These results were later confirmed in a larger cohort, where the researchers also measured a significant decrease in systolic blood pressure (SBP)(62). Webb et al. demonstrated a similar reduction of blood pressure with a beetroot juice supplement (0.3 mmol nitrate/day)(DBP decreased by 8 mmHg, SBP decreased by 10 mmHg)(63). These results are striking because a 5 mmHG decrease in DBP over a 5-year

duration is associated with a 38% and 23% decrease in risk of stroke and heart disease, respectively. Most studies on the BP-lowering effects of nitrite and nitrate have been conducted on healthy young and middle-aged subjects, however the BP-reducing effects have also been demonstrated in older subjects with peripheral artery disease and in hypertensives (64). Long-term studies are needed to establish the clinical significance of BP-lowering effects of nitrate supplementation in hypertensive subjects.

This nitrate-nitrite-NO pathway may be particularly important when endogenous NO production is impaired in ischemic tissue. Chronic Inhibition of eNOS, the enzyme that catalyzes endogenous production of NO from arginine, leads to NO deficiency and causes severe hypertension and progressive kidney damage. This effect is recovered by oral nitrate and nitrite supplementation (65,66). These results demonstrate that in the absence of eNOS activity, nitrate can be used as an alternate NO source to prevent deficiency.

Dietary nitrate improves exercise performance. In addition to the cardioprotective benefits of nitrates, it was also recently discovered that nitrates can improve exercise performance. The first report of the beneficial effects of nitrates on exercise performance was published in 2007 by Larsen et al. 9 research subjects were exposed to 0.1 mmol nitrate per kg body weight for 3 days, then completed a continuous cycling ergometer test. The oxygen cost of exercise was significantly reduced with nitrate supplementation (mean VO_2 reduction of 5%). There were significant improvements in gross efficiency (work output per unit energy expended) and delta efficiency (change in work output per unit change in energy expenditure). There was no difference in VO_2 max (peak oxygen uptake), heat rate, ventilation, or respiratory exchange ratio (62). The results of this study suggest that nitrate supplementation increased the efficiency of muscle oxidative metabolism. The findings of Larsen et al. were profound because it contradicts

the basic tenet of human exercise physiology that oxygen cost of submaximal exercise is fixed irrespective of age, health, fitness, and is unresponsive to nutritional or pharmacological intervention (67). Assuming that other factors are held constant, an increase in muscle efficiency would yield a greater work output for the same energy cost. This would, in theory, translate to improved exercise performance.

The aforementioned studies measured several markers of exercise efficiency, however it remained to be seen whether these changes would translate to improved exercise performance. In the early nitrate studies, time to exhaustion or incremental tests were used as a marker of exercise performance (4). However, real-world competitive sports often require athletes to complete a given distance in the shortest amount of time. A 15% improvement in time to exhaustion could be expected to translate into a 1% improvement in time trial performance over a given duration (4). Though seemingly small, a 1% increase in exercise performance would be a significant improvement for elite athletes, and could feasibly make the difference between winning and being runner up.

Lansley at al. performed a study on 9 moderately fit cyclists, where they consumed a single dose of 0.5 L of beetroot juice (6.2 mmol). 2.5 hours later, the cyclists completed a 4-km and 16.1-km time trial on a cycle ergometer. VO_2 max was not different between the treatments, however the mean power output was higher in those who consumed the beetroot juice. Beetroot significantly improved the time trial performance in the 4-km (2.8% improvement) and the 16.1-km (2.7% improvement). This study was the first example of nitrate improving time-trial performance, with the added caveat that it was after only a single high dose of nitrate (68). This work was followed up by Cermak et al., dosing 12 trained male cyclists with concentrated beetroot juice (8 mmol/day) for 6 days. After the 6^{th} day, the athletes completed 60 minutes of

submaximal exercise, then a 10-km time trial performance. The beetroot juice improved both time trial performance and power output (69).

In the years since these original studies on the effect of nitrate on exercise performance, there have been many publications attempting to characterize these effects. Several studies have shown that acute or short-term supplementation with nitrate does not improve exercise performance in highly trained athletes (70-73). Wilkerson et al. gave 0.5 L (6.2 mmol) of beetroot juice to well-trained cyclists, and asked them to complete a 50-mile time trial. There was no significant difference in time trial performance between the beetroot juice treatment and the placebo (71). These results were supported by several others, demonstrating that a single or short-term nitrate treatment does not increase exercise performance in trained runners, cyclists, or cross-country skiers. Interestingly, in these studies in highly trained athletes, plasma levels of nitrite did not increase at the same magnitude as less trained athletes (71). These results could be explained by high eNOS activity in elite athletes, rendering nitrate reduction to NO a minor contribution to the overall NO pool.

Nitrate improves cognitive function during exercise. Fatigue during high-intensity exercise may be exacerbated by decreased blood flow into the brain (74-76). Low cerebral blood flow during exercise is associated with higher mental fatigue and increased effort perception, leading to earlier withdrawal from exercise (77). Nitrate supplementation has been shown to increase cerebral perfusion frontal lobe white matter in older adults at rest (78). Specifically, the regions affected by nitrate supplementation were the anterior cingulated cortex (ACC) and the dorso-lateral prefrontal cortex. The ACC and prefrontal cortex are associated with mental fatigue, perception of physical effort, and fatigue-related feedback, emotion, arousal states, and decision making. Interestingly, it has been demonstrating that mentally fatiguing subject for 90

minutes before exercise results in reduced time to exhaustion, even when there was no difference in physiological responses to exercise (77).

Thompson et al. measured cognitive performance before, during, and after exercise with either a beetroot juice supplement or a placebo. Nitrate supplementation decreased mental fatigue during exercise, but did not improve cognitive performance post exercise (79). Gilchrist et al. demonstrated that nitrate supplementation for 2 weeks in type 2 diabetics significantly improved reaction time during simple tasks (80). Wightman et al. supplemented 40 healthy young adults (median age 21.3 years) with a single dose of 5.5 mmol nitrate in a double-blind, placebo crossover trial. Cerebral blood flow increased after 90 minutes and was correlated with increased cognitive performance in 3 different tasks (81). These recent results suggest that nitrate improves cerebral blood flow to improve cognitive performance, both during exercise and at rest. These findings may have particular significance in team sports where players are required to make fast and accurate decisions.

Mechanistic studies suggest that the effects of nitrate on muscle and mitochondrial proteins takes at least 3-7 days (59, 61). Several of the aforementioned studies measured more drastic changes in exercise and cognitive performance with a longer duration of treatment (69,82). Interestingly, there were anecdotal reports that beetroot juice supplementation was used extensively by athletes in a wide variety of sports in the 2012 London Olympic and Paralympic games, with great success (4).

Mechanism of action of dietary nitrate. We have reasonable evidence to suggest that consumption of nitrate reduces blood pressure and improves exercise performance. The results of most studies demonstrate that these effects are mediated through the metabolism of nitrate

into NO, and subsequent cGMP-induced vasodilation. However, the observations that nitrate reduces the oxygen cost of exercise, increases time to exhaustion, and improves exercise performance cannot be explained solely by increased vasodilation. In fact, I postulate that increased vasodilation would increase oxygen availability in tissues, leading to increased oxygen consumption. Here, I discuss some of the potential mechanisms that nitrate and nitrite may have in improving exercise performance.

The nitrate-nitrite-NO pathway is supplementary to the L-arginine-NO pathway. eNOS-mediated production of NO from L-arginine is favored at neutral pH and in oxygen-rich tissues. During intense exercise, both pH and oxygen levels in contracting skeletal muscle decrease. In addition, cardiovascular disease is associated with cardiac ischemia – decreased oxygen and pH in the heart tissue. Under these conditions, eNOS activity is decreased, and conversion of L-arginine to NO is inhibited. The dietary nitrate-nitrite-NO pathway has been suggested to be a supplementary pathway to eNOS-arginine-NO pathway. In eNOS deficient mice, xanthine oxidoreductase expression and activity is increased, which increases the metabolism of nitrate into NO (83). This indicates that there is cross-talk between the nitrate-nitrite-NO pathway and the L-arginine-NO pathway. The changes in exercise and cognitive performance with nitrate supplementation may therefore be a result of increased NO production during physiological conditions where NO production from L-arginine is not favored. This increase in NO during exercise would lead to increased blood flow to contracting skeletal muscle and into cerebral tissue.

Nitrate improves mitochondrial efficiency. Research on the effect of dietary nitrate on exercise performance demonstrates that nitrate can decrease the oxygen cost of exercise. The oxygen-sparing effects indicate more efficient aerobic metabolism or improved mitochondrial efficiency.

Mitochondria could be a target for nitrate-induced effects on exercise performance. Mitochondrial oxidative phosphorylation is traditionally measured as the amount of oxygen consumed per ATP produced, or the P/O ratio. Larsen et al. demonstrated that nitrate supplementation improves the P/O ratio in humans (84). Some factors that can affect the P/O ratio are proton leak, proton slip, energetic cost of metabolite transport, or mitochondrial uncoupling (84). There are several possibilities on how nitrate, nitrite, or NO may interact with mitochondria. The most well-known of these mechanisms is that NO can bind cytochrome c oxidase (COX, Complex IV), which is the terminal electron acceptor in the electron transport chain (85). In addition, NO may increase mitochondrial biogenesis (86). The literature is conflicted because several studies demonstrate that nitrate increases mitochondrial efficiency and biogenesis, and yet others demonstrate that the effects of nitrate are extramitochondrial.

Calcium signaling. Bailey et al. demonstrated that the whole-body sparing of oxygen cost of exercise is due to changes in muscle energy metabolism. VO_2 and phosphocreatine (PCr) are spared with nitrate treatment, which may be due to reduced ATP cost of muscle power production (87). The authors suggested that this could be due to the effects of NO on the sarcoplasmic reticulum calcium (Ca^{2+}) ATPase or the actin-myosin ATPase (88,89). Decreased ATP cost of muscle activity would reduce changes in muscular substrates and metabolites that stimulate mitochondrial respiration (PCr, ADP, Pi). Hernandez et al. demonstrated improvements in muscle Ca^{2+} handling and contractile function in mice fed nitrate for 7 days. In fast twitch muscle fibers, nitrate increased myoplasmic free Ca^{2+} concentration, which was associated with increased expression of calsequestrin 1 and the dihydropyridine receptor – proteins that are involved in Ca^{2+} handling. These changes in Ca^{2+} handling resulted in increased contractile force. The authors concluded that dietary nitrate intake may increase muscle

function during normal movement (90). The results of these studies suggest that some effects of nitrate are independent of mitochondrial function.

We have an incomplete understanding of how nitrate reduces the oxygen cost of exercise and improves exercise performance. Some studies demonstrate that beetroot juice supplements are more effective than sodium nitrate at the same concentration, suggesting that there may be additional nutritional components in vegetables that potentiate the beneficial effects of nitrate. Furthermore, elite athletes are not as responsive to nitrate treatment compared to non-athletes, demonstrating that there may be physiological adaptations to exercise that reduce the benefits of nitrates. Finally, we have an incomplete understanding of how nitrate metabolism is altered during exercise conditions. New approaches are needed to determine the mechanisms of nitrate in improving both exercise and cognitive performance.

Adverse Effects of Dietary Nitrate

I have discussed many of the potential beneficial effects of nitrate, however nitrate can also cause adverse effects under certain situations. Public fear of nitrate and nitrite arose with reports that nitrate and nitrite increase the risk of gastric cancer (91-96) and infantile methemoglobinemia (97,98). These deleterious effects on human health have led to increasingly stringent limits on nitrate and nitrite levels in food, and a recommendation by the FDA to limit daily nitrate and nitrite intake. The current acceptable daily intake (ADI) for nitrate and nitrate as established by the World Health Organization (WHO) are 3.7 mg/kg/day and 0.07 mg/kg/day, respectively.

Carcinogenic effects of nitrite and nitrate. It was postulated that when nitrite is swallowed, it produces HNO_2 in the acidic environment of the stomach, which is capable of nitrosating

secondary amines consumed in the diet. This would produce nitrosamines, which are carcinogenic in animal models (99). While nitrosamines are undeniably carcinogenic (100), there is poor evidence that nitrosamines are formed with nitrate consumption. Nitrosamines form readily at pH 2.3-3.5 (101). Normally the pH of the stomach is 1.0-1.5, but it increases to pH 4.0-4.5 after ingesting a meal. At this pH, nitrosamines are not formed. Even after the acidic pH of the stomach is re-established, nitrite and NO production is favored over nitrosamine formation (101). Reducing agents found naturally in the diet, such as ascorbate and thiols, also prevent the formation of nitrosamines and favor the production of NO. These reducing substrates are at a high concentration in vegetables, and the stomach itself secretes ascorbic acid (102). Meat products with added nitrite or nitrate must add ascorbic acid or a similar reducing substance to prevent the formation of nitrosamines during cooking and before ingestion.

There is no epidemiological evidence suggesting that high intake of nitrate leads to increased rates of cancer (93,103-106). In actuality, diets high in leafy greens and vegetables, and therefore nitrates, have been shown to reduce the risk of several types of cancer, including gastric cancer (107-109). Vegetarians, who consume approximately 3 times the amount of nitrate as non-vegetarians, have lower mortality from gastric cancer (107,109). Although there is very little evidence that nitrate or nitrite causes cancer, processed meats such as bacon and sausage have been recently categorized as class 1 carcinogens, or “carcinogenic to humans” – the same class as asbestos and smoking tobacco. Finally, we observe that over time the worldwide incidence of gastric cancer is declining (110), whereas the consumption of nitrate and nitrite are both increasing.

Methemoglobinemia. Methemoglobinemia, or “blue baby syndrome” is characterized by increased levels of methemoglobin in the blood. Methemoglobin has a higher affinity for oxygen

than hemoglobin, resulting in lower delivery of oxygen to the tissues. The resulting hypoxia results in the characteristic blue color in infants. The first association between infantile methemoglobinemia and nitrate exposure was first reported in 1945 when baby formula was reconstituted in well water from rural areas (97,98). More recently it was discovered that methemoglobinemia only occurs when water with a high nitrate content has bacterial contamination, thereby producing high levels of nitrite (111), which can oxidize the Fe^{2+} of oxyhemoglobin to produce the Fe^{3+} of methemoglobin (112). Infants and young children are more susceptible to methemoglobinemia, and there have been no reports of methemoglobinemia in older children or adults. For these reasons, nitrate contamination in water is not considered a public health concern unless there is bacterial contamination of the water source.

Significance to Human Health

Nitrates are generally perceived to be entirely harmful and without any benefits. Negative perceptions are primarily due to the association of nitrates with cancer, however there is very little evidence demonstrating that nitrate consumption causes cancer. Research in the last 10 years has demonstrated that diets high in nitrate from vegetables can decrease blood pressure, improve blood flow to the muscles and brain, improve exercise and cognitive performance, and is associated with decreased risk of cardiovascular disease. For these reasons, nitrate-rich foods and dietary supplements are increasing in popularity among athletes (4). Therefore, it is important for us to characterize the metabolism and mechanism of action of nitrate to ensure that nitrates are not having unforeseen adverse effects. We have an incomplete understanding of how nitrate is metabolized during exercise, and the mechanism by which it improves exercise performance. In Chapter 4, I use zebrafish (*danio rerio*) as model to study the effect of nitrate

and nitrite on exercise performance. I demonstrate that this new model for nitrate research allows for multiple performance assays (oxygen consumption during exercise, swimming behavior, and cognitive performance) that can be correlated to biochemical endpoints to elucidate novel mechanisms of nitrate on exercise and cognitive performance.

1.3. MASS SPECTROMETRY AS AN ANALYTICAL TOOL TO STUDY NITRATE

I sought to determine the relative contribution of both pharmaceutical and dietary nitrates to total NO production in both the cell culture and zebrafish models. Nitrate metabolism is challenging to study because of several complicating factors. NO has a half-life of approximately 3-4 seconds in human plasma before it is readily oxidized back into nitrite or nitrate (113). Nitrate, nitrite, and NO (NO_x) are all capable of interconversion depending on the chemical and physiological environment. Cell culture analysis presents the additional challenge of having high background levels of nitrate and nitrite in the cell culture medium. For these reasons, analytical methods of measuring these NO_x species require high sensitivity and specificity, however must be fast and robust to prevent artifactual formation and sample degradation.

Measuring nitrate and nitrite as surrogates for NO is the preferred method for sensitive and accurate quantification (114). The most common method of measuring nitrite and nitrate is the Griess method. Although inexpensive and simple to perform, the Griess method has high detection limits and a narrow linear range (115), making it infeasible for most cell culture applications. More quantitative methods have since been developed, including chemiluminescence (CL), fluorometric assays, ultraviolet (UV) spectrophotometric methods, high-performance liquid chromatography (HPLC), capillary electrophoresis (CE), and gas

chromatography mass spectrometry (GCMS)(114-116). These methods also suffer from low detection limits, narrow linear range, or time-consuming reduction and derivatization steps.

In this dissertation, I present a novel method of measuring nitrate and nitrite that uses liquid chromatography tandem mass spectrometry (LC-MS/MS). Mass spectrometry is an analytical method that is used to identify and quantify chemical analytes. It is a useful technique because of its high sensitivity, ability to measure diverse classes of compounds, and high confidence in identification. This technique is based on initial ionization of the analyte by an ion source, then analysis of the mass-to-charge (m/z) ratio by a mass analyzer. Accurate mass measurements (measure the m/z to four decimal places) can be used to generate the molecular formula. Furthermore, tandem mass spectrometers (MS/MS) allow for the assessment of unique fragmentation patterns, which further increases confidence in the identification (117). Identification of the analytes is based on the chromatographic retention time, m/z value, isotope pattern, and fragmentation pattern. One benefit of mass spectrometry is that it allows for the use of stable isotopes (such as ^{13}C, ^{15}N, ^{18}O, and deuterium). By treating with stable isotope-labeled analytes and analyzing with mass spectrometry, the analyst can track the fate of the isotope. For these reasons, mass spectrometry has emerged as a promising new tool to measure NO_x species and their effects on biological systems.

The novelty of this method arises from using stable isotopes to track the fate of nitrate. I treated cells with ^{15}N-labeled GTN, and measured ^{15}N-nitrate and ^{15}N-nitrite production. This allowed me to quantify the nitrate and nitrite that are produced directly from GTN, and remove interference from the high background of nitrate and nitrite resulting from the cell culture media. In chapters 2 and 3, I utilize this method to measure GTN metabolism in a cell culture model of nitrate tolerance. In Chapter 4, this method is applied to measure the uptake and

metabolism of ^{15}N-nitrate in zebrafish. This stable isotope-assisted method has allowed us to quantify the relative weight of pharmaceutical, dietary, and endogenous pathways of NO production in biological samples.

In addition to quantifying nitrite and nitrate in biological matrices, I have also employed the use of untargeted mass spectrometry-based metabolomics to determine the biochemical effects of nitrate treatment. The collection of all chemical analytes, or "metabolites" in a biological system is referred to as the "metabolome". Metabolomics is a comprehensive method that allows for the detection and relative quantification of numerous metabolites. It is often referred to as an "untargeted" or "hypothesis generating" approach because the analysis is not limited to a subset of pre-defined targets. Metabolomics methods routinely identify several hundred metabolites in various biological samples, making it possible for the analyst to discover novel pathways that are affected by the treatment.

1.4. RESEARCH AIMS

The predominant goal of this dissertation is to utilize mass spectrometry techniques to bring insight into the metabolism, toxicity, and mechanism of action of pharmaceutical and dietary nitrates. Mass spectrometry can accomplish this goal by: 1) tracking stable isotopes of nitrate, and 2) performing untargeted metabolomics to identify pathways that are altered by nitrate treatment. The specific aims of this dissertation are:

1. **Track the metabolic fate of nitrate.** To address this aim, I develop a novel method of measuring ^{15}N-nitrate and ^{15}N-nitrite with mass spectrometry. In Chapter 2, I present this method and demonstrate its value in a cell culture model of nitrate tolerance. In Chapter 3, I use this method to test vitamin C as a co-treatment strategy to prevent nitrate tolerance. In Chapter 4, I utilize this method to quantify the uptake and metabolism of inorganic nitrate in zebrafish.

2. **Elucidate the mechanism by which vitamin C prevents GTN-induced nitrate tolerance**. In Chapter 3, I perform untargeted metabolomics on a cell culture model of nitrate tolerance, with vitamin C supplementation or deficiency. I present the metabolomics-driven elucidation of a novel mechanism by which vitamin C prevents nitrate tolerance. The results demonstrate that vitamin C should be re-investigated as a simple and inexpensive strategy to prevent nitrate tolerance.

3. **Determine the mechanism by which inorganic nitrate improves exercise performance.** In Chapter 4, I treat zebrafish with nitrate for 21 days and then test oxygen consumption during a 2-hour vigorous exercise test. I perform untargeted metabolomics on control or

nitrate-treated fish, either rested or exercised. I present a novel mechanism for the beneficial effects of nitrate on exercise performance.

The data outlined in this dissertation presents novel mechanisms for the effects of nitrate on human health. This dissertation has provided the scientific community with a new mechanism on the protective effects of vitamin C on nitrate tolerance, and a new mechanism on how nitrates can improve exercise performance. I perceive that these discoveries would not be possible without the use of mass spectrometry and metabolomics techniques. In the conclusion (Chapter 5) I confer how the techniques that I developed and/or applied in this dissertation can be utilized to further validate our findings in humans. Furthermore, I discuss the benefits and limitations of these approaches with the intent of allowing readers to determine whether these techniques would suit their individual research needs.

1.5. FIGURES

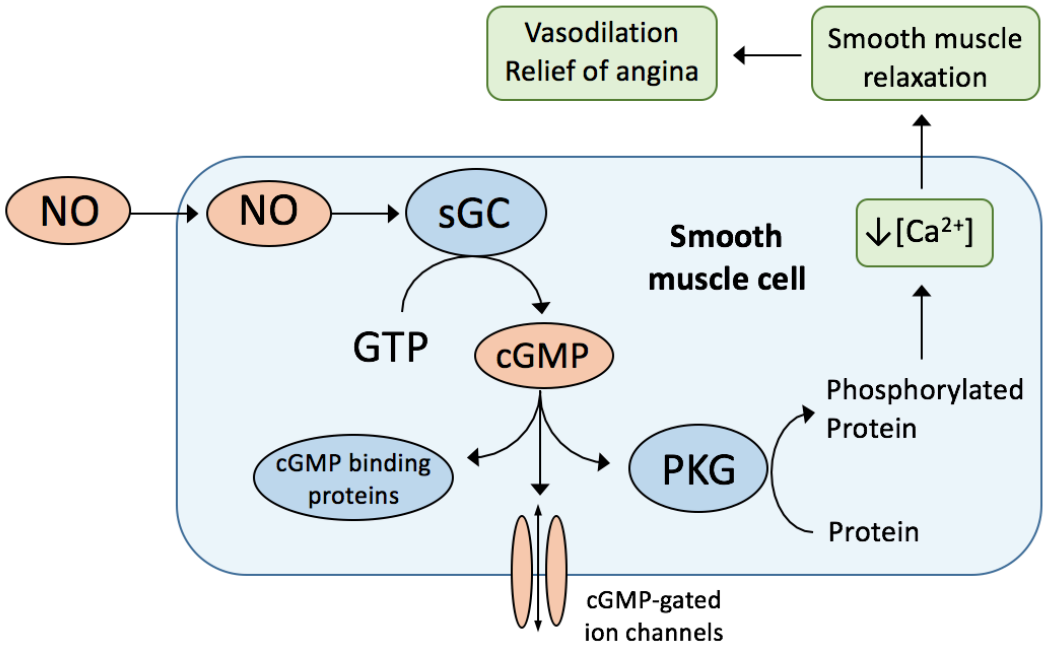

FIGURE 1.1: **cGMP-induced vasodilation**. NO stimulates a complex signaling cascade that results in vasodilation. The NO produced in endothelial cells passively diffuses into the smooth muscle cells within the blood vessel walls. NO binds to the heme center in soluble guanylate cyclase (sGC), which leads to the activation of sGC. Activated sGC catalyzes the conversion of guanosine 5'-triphosphate (GTP) into cyclic guanosine 3',5'-monophosphate (cGMP). cGMP is often measured as a biomarker for NO production in vivo. cGMP has three known physiological targets: cGMP-dependent protein kinase (PKG), cGMP-regulated phosphodiesterase, and cGMP-gated ion channels. The first of these, PKG, phosphorylates target proteins in response to an increase in cGMP concentration. In smooth muscle cells, cGMP-dependent protein kinase phosphorylates the inositol 1,4,5-triphosphate receptor, leading to a decrease in Ca^{2+} concentration and, ultimately, smooth muscle relaxation (1) and the relief of angina.

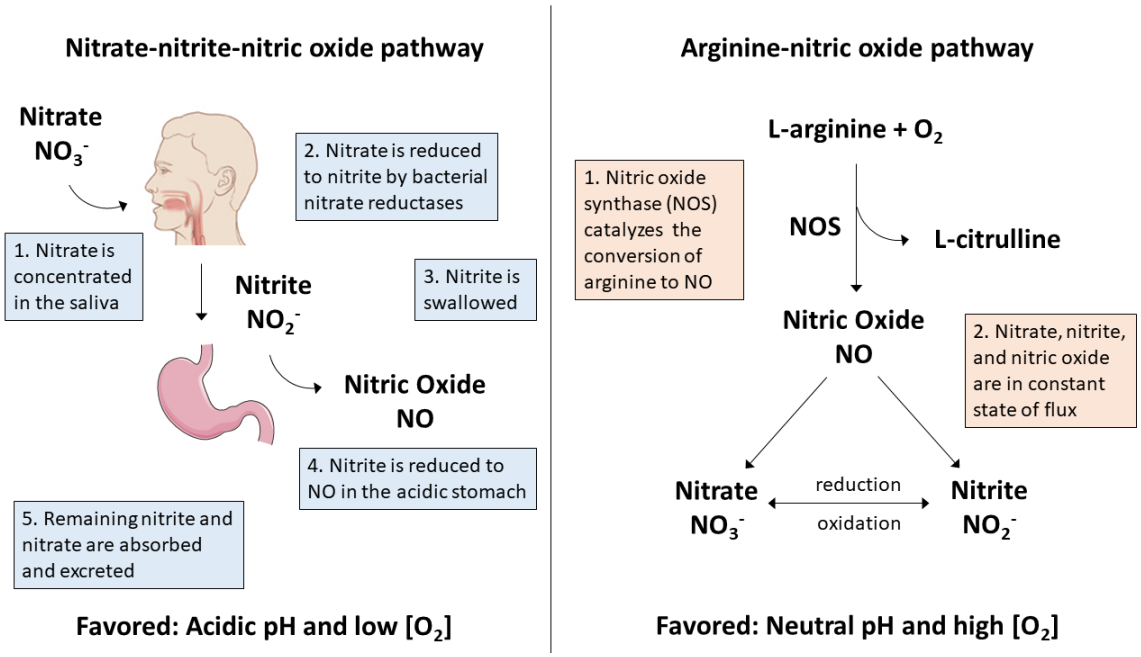

FIGURE 1.2: Pathways of NO production. In the nitrate-nitrite-nitric oxide pathway (left), nitrate is consumed in the diet and concentrated in the saliva. Bacterial nitrate reductases convert nitrate into nitrite in the saliva. Nitrite is swallowed and converted into NO in the low oxygen, acidic environment of the stomach. Remaining nitrate and nitrite are absorbed in the intestines and eventually excreted by the kidneys. Reduction of nitrate into nitrite and NO is favored in low oxygen and acidic conditions. In the arginine-nitric oxide pathway (right), L-arginine and oxygen are converted into L-citrulline and NO by nitric oxide synthase (NOS). This reaction is favored at neutral pH and is dependent on oxygen. In these conditions, NO is readily oxidized back into nitrite and nitrate.

CHAPTER 2

STABLE ISOTOPE-ASSISTED LC-MS/MS MONITORING OF GLYCERYL TRINITRATE BIOACTIVATION IN A CELL CULTURE MODEL OF NITRATE TOLERANCE

Elizabeth R. Axton, Elizabeth A. Hardardt, Jan F. Stevens

Journal of Chromatography B

Radarweg 29, 1043 NX Amsterdam, The Netherlands

Special Issue, Analytical Tools and Protocols in Oxidative Stress (2016) 1019: 156-163.

2.1. ABSTRACT

The nitric oxide (NO) metabolites nitrite (NO_2^-) and nitrate (NO_3^-) can be quantified as an endpoint of endothelial function. We developed a LC-MS/MS method of measuring nitrite and nitrate isotopologues, which has a lower limit of quantification (LLOQ) of 1 nM. This method allows for isotopic labeling to differentiate newly formed nitrite and nitrate from nanomolar to micromolar background levels of nitrite and nitrate in biological matrices. This method utilizes 2,3-diaminonaphthalene (DAN) derivatization, which reacts with nitrite under acidic conditions to produce 2,3-naphthotriazole (NAT). NAT was chromatographically separated on a Shimadzu LC System with an Agilent Extend-C_{18} 5 µm 2.1 x 150 mm column and detected using a multiple reaction monitoring (MRM) method on an ABSciex 3200 QTRAP mass spectrometer operated in positive mode. Mass spectrometry allows for the quantification of ^{14}N-NAT (m/z 170.1) and ^{15}N-NAT (m/z 171.1). Both nitrite and nitrate demonstrated a linear detector response (1 nM – 10 µM, 1 nM – 100 nM, respectively), and were unaffected by common interferences (Dulbecco's Modified Eagle Medium (DMEM), fetal bovine serum (FBS), phenol red, and NADPH). This method requires minimal sample preparation, making it ideal for most biological applications. We applied this method to develop a cell culture model to study the development of nitrate tolerance in human endothelial cells (EA.hy926).

2.2. INTRODUCTION

Nitric oxide (NO) is a signaling molecule and free radical that plays a diverse role in cardiovascular, immune, and nervous systems (118)(119). NO is produced from L-arginine by NO synthase (NOS) in mammals (118), yet it can also be produced via the reduction of nitrite (NO_2^-) and nitrate (NO_3^-) by xanthine oxidase (XO) (24-27,120). Nitrite and nitrate are present in the environment and diet. NO is released by cells in the picomolar to nanomolar range (121), and has an estimated in vivo half-life of 3-4 seconds in human blood (113). It is therefore very difficult to accurately measure, so its nitrite and nitrate metabolites are often measured as surrogates (122). Measurement of nitrite and nitrate is the most suitable and practical method to assess NO synthesis in vivo (114). Given that nitrite and nitrate can be reduced to NO by XO, nitrite and nitrate can be viewed as bioavailable storage pools for NO (51).

Nitrate tolerance. Glyceryl trinitrate (GTN), more commonly known as nitroglycerin, is used for the treatment of angina pectoris, coronary artery disease, acute myocardial infarction, hypertension, and congestive heart failure. GTN is a prodrug that must be bioactivated in endothelial cells to produce NO (Figure 2.1), which activates soluble guanylyl cyclase (sGC) to release the second messenger cyclic guanosine monophosphate (cGMP), stimulating the relaxation of smooth muscle cells (28,29). Continuous treatment with GTN results in nitrate tolerance after only a few weeks, which limits the long-term use and benefits of treatment (38). Currently, nitrate tolerance is managed by implementing nitrate-free intervals, but this strategy could become obsolete when co-therapies that effectively prevent nitrate tolerance become available. The cause of nitrate tolerance and the mechanism of GTN bioactivation remain relatively unknown. In the present study, we measure nitrite and nitrate as endpoints of GTN bioactivation in endothelial cells. Our intent is to determine whether cell culture and the

measurement of nitrite and nitrate isotopologues can be used as an appropriate model to determine the mechanism of GTN bioactivation and the cause of nitrate tolerance.

*Quantification of nitrite and nitrate***.** There are over 200 analytical methods for the measurement of nitrite and nitrate, yet a small portion of these can be applied to human biological fluids (114). Current methods that are used for nitrite and nitrate analysis include fluorescence, chemiluminescence, high performance liquid chromatography (HPLC), capillary electrophoresis, colorimetric and ultraviolet (UV) spectrophotometric methods, and gas chromatography-mass spectrometry (GC-MS). The current methods have been extensively reviewed (114,116,121,123,124). Mass spectrometry is the only analytical technique that is able to measure isotopologues of nitrite and nitrate, and is an indispensable analytical tool for reliable quantitative analysis of nitrite and nitrate (121). In the present study, we modify a method of measuring nitrite with LC-MS/MS (125,126), and expand upon it to include quantification of nitrate. We utilized the well-established 2,3-diaminonaphthalene (DAN) derivatization, which reacts with nitrite under acidic conditions to produce the highly fluorescent 2,3-naphthotriazole (NAT)(127)(Figure 2.2). Measuring NAT with LC-MS/MS, instead of by fluorescence, allows for the use of isotope labeling which reduces the impact of high background levels of nitrite and nitrate in biological matrices.

This LC-MS/MS method is a significant contribution to the field because it is a sensitive and reproducible method for quantifying nitrite and nitrate isotopologues as metabolic products of GTN. This method is used to investigate the mechanism of nitrate tolerance in human endothelial cells, which is made possible with the use of $^{15}N_3$-GTN.

2.3. MATERIALS AND METHODS

Chemicals. 2,3-diaminonaphthalene (DAN) was procured from TCI America (Portland, OR). $^{15}N_3$-glyceryl trinitate (GTN) in acetonitrile (^{15}N, 98%+), sodium ^{15}N-nitrite (^{15}N, 98%+), and sodium ^{15}N-nitrate (^{15}N, 98%+) were from Cambridge Isotope Laboratories (Tewksbery, MA). GTN, NADPH, sodium hydroxide, and nitrate reductase were from Sigma Aldrich (St. Louis, MO). Dulbecco's Modified Eagle Medium (DMEM), Hank's Buffered Sodium Salt (HBSS), trypsin-EDTA, fetal bovine serum (FBS), penicillin, and streptomycin were procured from Invitrogen (Carlsbad, CA). Ammonium bicarbonate, LCMS-grade water and methanol were purchased from J.T Baker (Center Valley, PA).

Endothelial cell culture and treatments with glyceryl trinitrate (GTN). EA.hy926 human hybrid endothelial cells (American Type Culture Collection; Manassas, VA) were maintained in culture in T75 flasks with DMEM medium containing 4.5 g/L glucose and 84 mg/L L-arginine, and supplemented with 10% FBS and 1% penicillin-streptomycin (PS) in a humidified incubator at 37°C with 5% CO_2. Endothelial cells were chosen because they have been previously shown to produce NO from nitrite, which caused changes in markers of intracellular nitrosation reactions (128). Endothelial cells express xanthine oxidase, mitochondrial aldehyde dehydrogenase, and nitric oxide synthase, among others.

EA.hy926 cells were plated at a density of 5.0×10^5 cells per well in 6-well plates with 2 mL medium following a trypsinization protocol. Cells were returned to the incubator for 24 hours before treatment. Nitrate tolerance was induced in cells using a modified method from Hinz and colleagues (129). In short, cells were given an initial 20 μM GTN challenge in phenol red-free DMEM with 1% FBS, and incubated for 5 hours. Medium was aspirated, washed once with 2 mL HBSS, then treated for 60 minutes at four concentration levels of ^{15}N-GTN (1 μM – 20 μM) in 1

mL phenol red-free DMEM with 1% FBS. Results were compared to control cells, which were treated with 5 µL of acetonitrile as a vehicle control. The entire final volume (1 mL) was transferred to Eppendorf tubes and immediately frozen at -80°C until analysis.

Enzymatic reduction of nitrate into nitrite. Nitrate was enzymatically converted to nitrite by incubating with nitrate reductase (130,131). The enzymatic method of reducing nitrate to nitrite is preferred to cadmium reduction because it is non-toxic, and offers high specificity, simplicity, rapidity, and complete conversion of nitrate into nitrite (130,131). One hundred µL of the cell medium, or ^{15}N-nitrate standard, was incubated with 10 µL of 1 U/mL nitrate reductase and 10 µL of 120 µM NADPH and incubated at room temperature for 60 minutes. There was complete conversion of nitrate into nitrite, as evidenced by conversion of known amounts of ^{15}N standards of sodium nitrite and sodium nitrate. After incubation, samples were immediately derivatized for nitrite analysis.

2,3-Diaminonaphthalene (DAN) derivatization. DAN reacts with nitrite under acidic conditions to form NAT (127), which is detectable with mass spectrometry. For mass spectrometric analysis of NAT, the protocol developed by Misko et al. (132) was adapted. No filtration is necessary because it was determined that our culture media is not a source of interference for the measurement of nitrite and nitrate. A 100 µL sample aliquot (culture medium, nitrite standards, or nitrate-derived standards) was incubated at 24°C for 60 minutes with 10 µL of 316 µM DAN in 50% EtOH with 0.62 M HCl. The reaction was quenched with 5 µL of 2.8 M NaOH. In alkaline conditions, NAT is stable for at least 24 hours (131). The samples were centrifuged at 16,000 x *g* for 1 minute, then transferred to glass LCMS vials (Microsolv, Eatontown, NJ) and analyzed for ^{14}N-NAT and ^{15}N-NAT.

Detection of 2,3-naphthotriazole (NAT) with LC-MS/MS. Mass spectrometric detection of ^{14}N-NAT and ^{15}N-NAT was performed on a Shimadzu Prominence LC system coupled to an AB Sciex 3200 QTRAP operated in positive ion mode. An Agilent Extend-C_{18} 5 µm 2.1 x 150 mm column was maintained at 40°C with a flow rate of 0.2 mL/min (0-13 minutes) and 0.4 mL/min (13-25 minutes). Mobile phase A was 5 mM aqueous NH_4HCO_3, mobile phase B was 100% methanol, and the needle wash solvent was 50% methanol. The total run time was 25 minutes, column eluent was directed to MS between 8-12 minutes only, and injections were 15 µL. The solvent gradient profile started at 5% B for 4 minutes, changed linearly to 50% B over 1 minute, was held at 50% B for 8 minutes, changed linearly to 95% over 3 minutes, was held at 95% B for 5 minutes, changed linearly to 5% B over 3 minutes, and remained at 5% B to equilibrate the column. Retention time was monitored, and no significant shifts were observed throughout sample sets. A multiple reaction monitoring (MRM) method monitored the following transitions over 100 ms for the analyte indicated: m/z 171.1 → 115.1 for ^{15}N-NAT, m/z 159.1 → 159.1for DAN, and m/z 170.1 → 115.1 for ^{14}N-NAT. The collision voltages were 33 V for all except DAN, which was 5 V. Declustering, entrance, and collision cell exit potentials were 51, 11.5 and 4 V, respectively. The IonSpray voltage was 5500 V and the ion source temperature was 550 °C. ^{14}N-NAT and ^{15}N-NAT concentrations were quantified by integrating the peaks in Analyst 1.5.1 to obtain peak area. Peak area was converted to concentration (nM) by using individual seven-point concentration curves of the analytes. Nitrate concentration was obtained after reduction with nitrate reductase.

Method validation and quality control. Seven-point concentration curves (1 nM – 10 µM) for sodium ^{15}N-nitrite and sodium ^{15}N-nitrate were made in combination and individually in Milli-Q water, 200 mM HEPES, and DMEM with 1% FBS. These were used to calculate LLOQ, linear

range, percent recovery in DMEM, and percent conversion of nitrate reduction to nitrite. Background levels of nitrate and nitrite were measured in water, HEPES, and DMEM. Three concentrations (10 nM, 100 nM, and 1000 nM) of nitrite and nitrate isotopologues were analyzed ten times in water and DMEM to determine precision and accuracy. For every day of analysis of cell culture or enzyme samples, a seven-point concentration curve of nitrite in water was run to assess instrument performance. If a decrease in sensitivity was observed, the instrument was cleaned and calibrated before analysis of samples. All samples were randomized to prevent batch effect, yet nitrite and nitrate samples were paired and run in sequence.

Statistical analysis. Results were analyzed using a one-way ANOVA, followed by Tukey post hoc analysis with a P-value of < 0.05 indicating significance. All statistical analyses were performed using GraphPad Prism 4.

2.4. RESULTS

Quantification of nitrite and nitrate. The derivatization product of NO_2^- is 2,3-naphthotriazole (NAT), which is detected by LC-MS/MS. ^{14}N-NAT has a parent mass of 169.1 Da, which has an $[M+H]^+$ mass of 170.1 Da. The major product ions of ^{14}N-NAT are $C_{10}H_8N^+$ (m/z 142.1) and $C_9H_7^+$ (m/z 115.1). The proposed fragmentation pattern of ^{14}N-NAT is in Figure 2.3. The transition of m/z 170.1→115.1 was chosen for quantitation because of the high abundance and specificity. ^{15}N-NAT has a m/z of 171.1 and a quantitation transition of m/z 171.1→115.1.

^{14}N-NAT and ^{15}N-NAT co-elute at 9.60 minutes. There is a significant peak at 10.04 minutes that was identified as a degradation product of ^{14}N-NAT and ^{15}N-NAT. ^{14}N-NAT and ^{15}N-NAT degrade into their N-oxide metabolites (m/z 186 and 187)(Supplemental Figure 2.1), which give rise to protonated ^{14}N-NAT and ^{15}N-NAT species upon in-source loss of •OH (m/z 169 and 170). This

"degradation peak" is larger in cell culture media samples, and increases over time if the samples remain at room temperature for several days. This demonstrates the necessity of measuring all derivatized samples within 24 hours of preparation.

Method Validation. The LC-MS/MS method of measuring nitrite and nitrate was analyzed for sensitivity, reproducibility, accuracy, precision, interferences, percent recovery, and carryover. Standard curves of nitrate and nitrite were used to determine LLOQ and the linear range. The LLOQ was defined as the lowest standard on the calibration curve at which the analyte peak was at least 5 times the response relative to blank response, with a precision of ≤ 20% RSD and an accuracy of 80-120%. ^{15}N-Nitrite and ^{15}N-nitrate had a LLOQ of 1 nM in both water and in DMEM (n=10). This value is within the same range as previous studies that have measured ^{15}N-nitrite with LC-MS/MS, which reported LLOQ of 4 nM (125) and 5 nM (126). We postulate that our quantitation limit is lower because different instrumentation and column, as well as our choice in solvent system. NAT is more stable under alkaline conditions, so using a solvent system with 0.1% formic acid (125,126) may lead to degradation of NAT and a reduction in sensitivity.

^{15}N-Nitrite had a linear range from 1 nM to 10 µM (correlation coefficient > 0.99, $P<0.01$), whereas ^{15}N-nitrate was linear from 1 nM – 100 nM (correlation coefficient > 0.99, $P<0.05$) (n=5). Though nitrate is detectable at very low concentrations, it demonstrated a low precision, high level of variability, and low recovery at concentrations greater than 100 nM (correlation coefficient = 0.72, $P>0.05$). This is most likely due to the saturation of nitrate reductase. For these reasons, this method is only suitable to measure nitrate at nanomolar levels without further method development. However, increasing the amount of enzyme was not desirable due to potential interferences with mass spectrometry.

Precision and accuracy were analyzed by spiking known amounts (10 nM, 100 nM, 1000 nM) of $^{15}NO_2^-$, NO_2^-, $^{15}NO_3^-$, and NO_3^- into water and DMEM (phenol red-free, with 1% FBS and PS), n=10. Individual calibration curves (seven points, 1 nM – 10 µM) were used for quantitation. Accuracy is determined as the percentage deviation of calculated concentration from the nominal concentrations, and was calculated with the equation: $\frac{calculated\ concentration - nominal\ concentration}{nominal\ concentration} * 100\%$. Precision is determined as the relative standard deviation (RSD) of the 10 measurements, and is calculated as $\frac{standard\ deviation}{mean} * 100\%$. Accuracy and precision is presented in Table 2.1. Satisfactory accuracies were obtained for ^{14}N-nitrite and ^{15}N-nitrite in both DMEM and water, with biases less than 7.5% and 5.6%, respectively. Accuracy for ^{14}N-nitrate and ^{15}N-nitrate was satisfactory up to 100 nM (less than 7.3% and 4.7%, respectively) but was not acceptable for 1000 nM (up to 20.4% and 17.9%, respectively). There was good precision for ^{14}N-nitrite (4.76 to 10.9%) and ^{15}N-nitrite (2.41 to 9.17%) in water and DMEM. Precision for ^{14}N-nitrate (6.32 to 9.43%) and ^{15}N-nitrate (5.16 to 8.51%) was high at 100 nM and lower, but was unacceptably low for the 1000 nM concentration (up to 19.2 and 15.6%, respectively). The results demonstrate that using ^{15}N labeled analytes improves accuracy and precision compared to the ^{14}N analytes. Nitrate has very low recovery above 100 nM, and should not be quantified at high nanomolar to micromolar concentrations without further method validation. This method is precise and accurate for the measurement of ^{15}N-nitrite and ^{15}N-nitrate in both water and DMEM.

Neither nitrite nor nitrate was found to interfere with each other. Percent recovery of nitrite and nitrate in the presence of the other analyte was 97% ± 4 and 98% ± 5, respectively. This demonstrates that we can measure nitrate and nitrite in a single sample without compromising the quantitation. Phenol-red free DMEM culture media with 1% FBS and PS was found to not be

a source of interference and caused minimal matrix effects. There was high recovery of spiked ^{15}N-nitrite and ^{15}N-nitrate within their linear range, n=10. The percent recovery of nitrite and nitrate in DMEM for all concentration points was 91% ± 3 and 99% ±11, respectively. This demonstrates that we can analyze nitrite and nitrate in cell culture medium with minimal sample preparation.

Both NADPH and nitrate reductase were added individually to ^{15}N-nitrite standards (5 points, 1 nM- 1 µM) to determine whether they would interfere with mass spectrometric detection of nitrite. NADPH and nitrate reductase did not affect either derivatization of nitrite, or mass spectrometric quantification of NAT. Samples incubated with 10 µL of 120 µM NADPH had a percent recovery of 100% ± 5, and samples with 10 µL of 1 U/mL nitrate reductase had a percent recovery of 99% ± 3. This indicates that at the concentrations tested, the presence of NADPH and nitrate reductase will not interfere with the recovery of nitrite from nitrate. In both water and DMEM, there was greater than 99% conversion of nitrate into nitrite within the linear range.

We quantified the concentration of nitrite in milli-Q water, 200 mM HEPES, phenol red-free DMEM with 1% FBS, and phenol red-free DMEM with 1% FBS that was used to culture 5 x 10^6 EA.hy926 cells in 2 mL medium for 24 hours at 37°C. The results are reported in Table 2.2. Background levels of nitrate exceeded our linear range of measurement, so these values are not reported. These high levels of nitrite and nitrate in both water and media demonstrate the necessity of using isotope labeling in cell culture experiments.

GTN dose-response: nitrate tolerant and control. Nitrate tolerance was induced in EA.hy926 cells with a 5-hour pre-treatment with GTN. The endothelial cells bioactivated GTN to produce

nitrite, whereas nitrate was not a significant product. Representative chromatograms are in Figure 2.4. A linear dose-response for ^{15}N-nitrite and ^{15}N-nitrate production was measured. GTN pre-treatment caused decreased production of ^{15}N-nitrite compared to the vehicle control, at all 4 concentrations tested (1, 5, 10, 20 μM) (P= 0.006, 0.014, 0.047, 0.029) (Figure 2.5a). However, ^{15}N-nitrate production was not altered by pre-treatment with GTN (P>0.05 for all concentration points) (Figure 2.5b). The concentration of nitrate was near the LLOQ, indicating that nitrate is not a significant metabolic product of GTN. There was no difference in ^{14}N-nitrite and ^{14}N-nitrate concentration between nitrate tolerant cells and control cells, demonstrating that there was no competition between GTN and $^{15}N_3$-GTN that would invalidate results (Figure 2.5c and 2.5d). ^{14}N-nitrite levels were similar for all concentration points, ranging from 411 to 487 nM, whereas ^{14}N-nitrate was 150 to 184 nM. The lower levels of ^{14}N-nitrate can be explained by the observation that these values were above our detection limit for nitrate, and thus suffer from incomplete conversion. This demonstrates that EA.hy926 cells can become nitrate tolerant, and may be a model for measuring the development of nitrate tolerance. This is a significant finding because it suggests that nitrate tolerance develops at the level of GTN bioactivation. The results indicate that the enzymes that are responsible for GTN metabolism may be inactivated or damaged by continuous GTN treatment.

These results are supported by the MTT cell viability assay, which determined that 24-hour treatment with a wide range of GTN treatments (0.1 μM – 50 μM) does not cause significant levels of cell death (Supplemental Information Figure 2.2a). In addition, the ATP Glo Assay to measure cell proliferation showed no significant differences between controls and multiple concentrations of GTN (1, 5, 10, 20 μM) (Supplemental Information Figure 2.2b). Both assays demonstrated minor, yet insignificant, increases in cell viability/proliferation with GTN

treatment. Therefore, the reduction in nitrite and nitrate production in nitrate tolerant cells is not caused by a reduced amount of viable cells.

2.5. DISCUSSION

The results demonstrate that our method of measuring nitrite and nitrate is highly sensitive, can differentiate between isotopologues of nitrite and nitrate, is accurate and precise, is free of common interferences, and requires minimal sample preparation. HPLC methods that use fluorescence detection have detection limits in low nanomolar levels, however they are not able to distinguish between newly formed and pre-existing (i.e., background) nitrite and nitrate (131) (133),(134). The ability of these methods to measure minute changes in nitrite and nitrate is questionable, particularly in light of the fact that we measured high nanomolar background levels of nitrite in cell culture media. Small changes in NO, and its metabolites, can have large physiological effects. We demonstrated that LC-MS/MS can measure changes in ^{15}N-nitrite and ^{15}N-nitrate concentrations in low nanomolar concentrations, which would undoubtedly be obscured without isotope labeling. Measuring NAT with LC-MS/MS, instead of by fluorescence, has the additional benefit of increased stability, because fluorescence quenching by biological components is not a concern. Though the merit of measuring nitrite and nitrate as surrogates for NO synthesis has been recently questioned (135), it remains the most suitable and practical method to assess NO production from GTN.

Despite the numerous benefits of measuring nitrite and nitrate with LC-MS/MS, there is one limitation that should be considered. This method requires for separate analysis of nitrite and nitrate, which increases sample preparation and analysis time. For many applications, this may not be a concern. We have demonstrated that nitrite is a better marker of GTN metabolism than

nitrate, thus it may suffice to measure nitrite only. Human and mammalian in vivo studies indicate that circulating nitrite, rather than nitrate, reflect endothelial-dependent NO synthesis (136). We acknowledge that methods that allow for simultaneous quantification of nitrite and nitrate may be preferable for human biological fluids. The GCMS method developed by Tsikas and coworkers, which uses pentafluorobenzyl (PFB) derivatization, allows for the measurement of isotopes and has the benefit of being able to measure nitrite and nitrate simultaneously (137). However, this GCMS method requires extensive sample preparation. The sensitivity of our LC-MS/MS method, as well as the ability to use isotope labeling, is necessary for mechanistic cell cultures studies.

One source of concern with this method could be that ^{15}N-NAT and ^{14}N-NAT only differ by a single mass unit. In theory, this could lead to issues with quantitation and interference with natural isotope abundance. We determined that ^{15}N-NAT is not detectable in cell culture samples with no treatment, indicating that the natural abundance of ^{15}N (0.36%) will not affect quantification. In addition, natural abundance of ^{13}C could not be mistaken for ^{15}N labeling because of the fragmentation pattern of NAT. There is a significant mass fragment peak at m/z 116.0, which results from the natural abundance of ^{13}C labeled NAT (9.7%). Since we measure the m/z 171.1→115.1 transition for ^{15}N-NAT, ^{13}C labeling is excluded from detection.

The cell culture results demonstrate that endothelial cells are capable of metabolizing GTN into nitrite. Pre-treatment with GTN resulted in nitrate tolerance, as evidenced by reduced ^{15}N-nitrite production. However, only low nanomolar levels of ^{15}N-nitrate were measured, suggesting that it is not a significant metabolic product of GTN. These results indicate that this may be a good model to determine the mechanism of GTN bioactivation, as well as the cause of nitrate tolerance. Measuring nitrite as an endpoint of GTN metabolism is a valuable tool to

determine the cause of nitrate tolerance. We hypothesize that inactivation of GTN-metabolizing enzymes, such as xanthine oxidase (XO), is the cause of nitrate tolerance.

2.6. CONCLUSION

LC-MS/MS is a sensitive and reproducible method of quantifying isotopologues of nitrite and nitrate, which will bring new insight into the phenomena of nitrate tolerance. We demonstrated that nitrate tolerance is associated with a significant decrease in nitrite production in human endothelial cells, which indicates inactivation of GTN-metabolizing enzymes.

2.7. ACKNOWLEDGMENTS

This research was supported in part by the National Institute of Health Grant T32ES007060, the College of Pharmacy, and the Linus Pauling Institute at Oregon State University. We would like to acknowledge Jeffrey Morré for his help with mass spectrometry, Dr. Cristobal Miranda for his assistance with cell culture techniques, and Eunice Lee, Erik McEntire, and Eleonso Cristobal for their technical assistance.

2.8. FIGURES

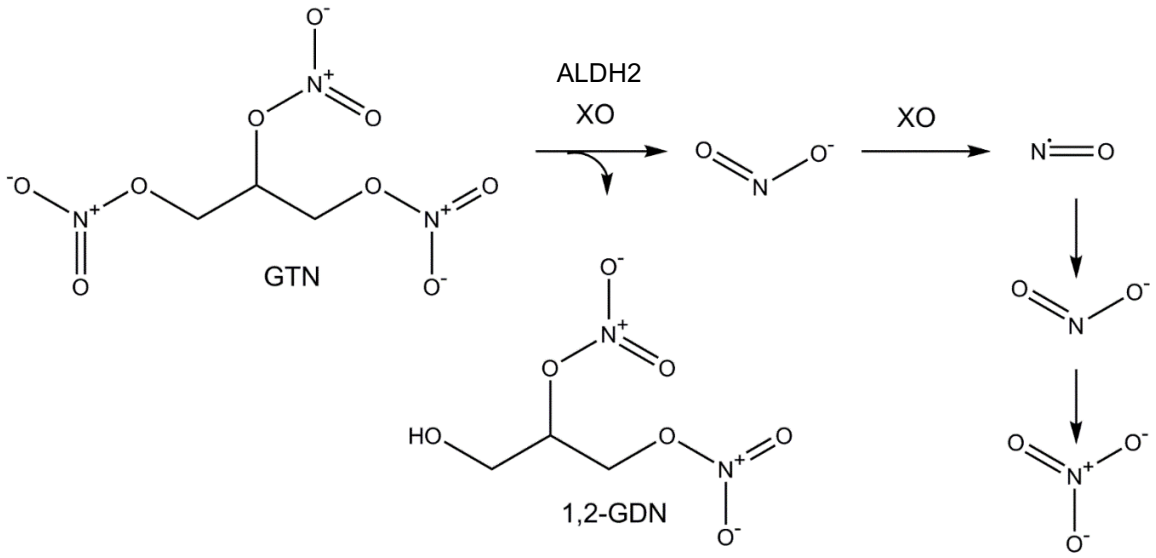

FIGURE 2.1: Bioactivation of glyceryl trinitrate (GTN) into NO. GTN is denitrified by xanthine oxidase (XO) and mitochondrial aldehyde dehydrogenase (ALDH2) in endothelial cells to produce 1,2-glyceryl dinitrate (1,2-GDN) and NO_2^-, which is reduced into NO and subsequently non-enzymatically oxidized to NO_2^- and NO_3^-.

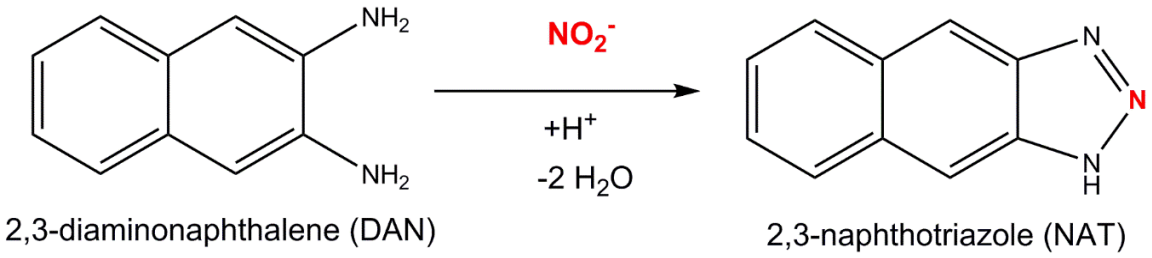

FIGURE 2.2: 2,3-diaminonaphthalene (DAN) derivatization. NO_2^- reacts with DAN under acidic conditions to produce 2,3-naphthotriazole (NAT).

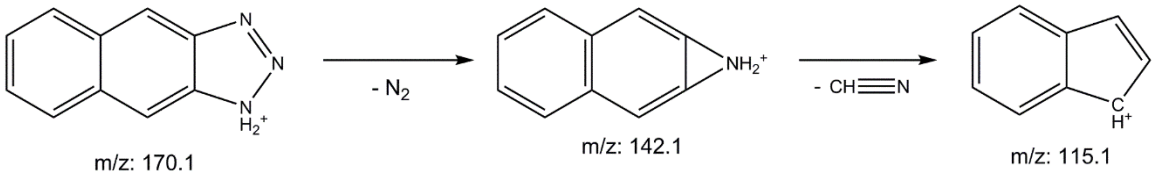

FIGURE 2.3: Proposed fragmentation pattern of 2,3-naphthotriazole (NAT). The molecular cation of ^{14}N-NAT (m/z 170.1) is fragmented into the qualifier ion $C_{10}H_8N^+$ (m/z 142.1), and undergoes additional fragmentation into $C_9H_7^+$ (m/z 115.1) which is used for quantification.

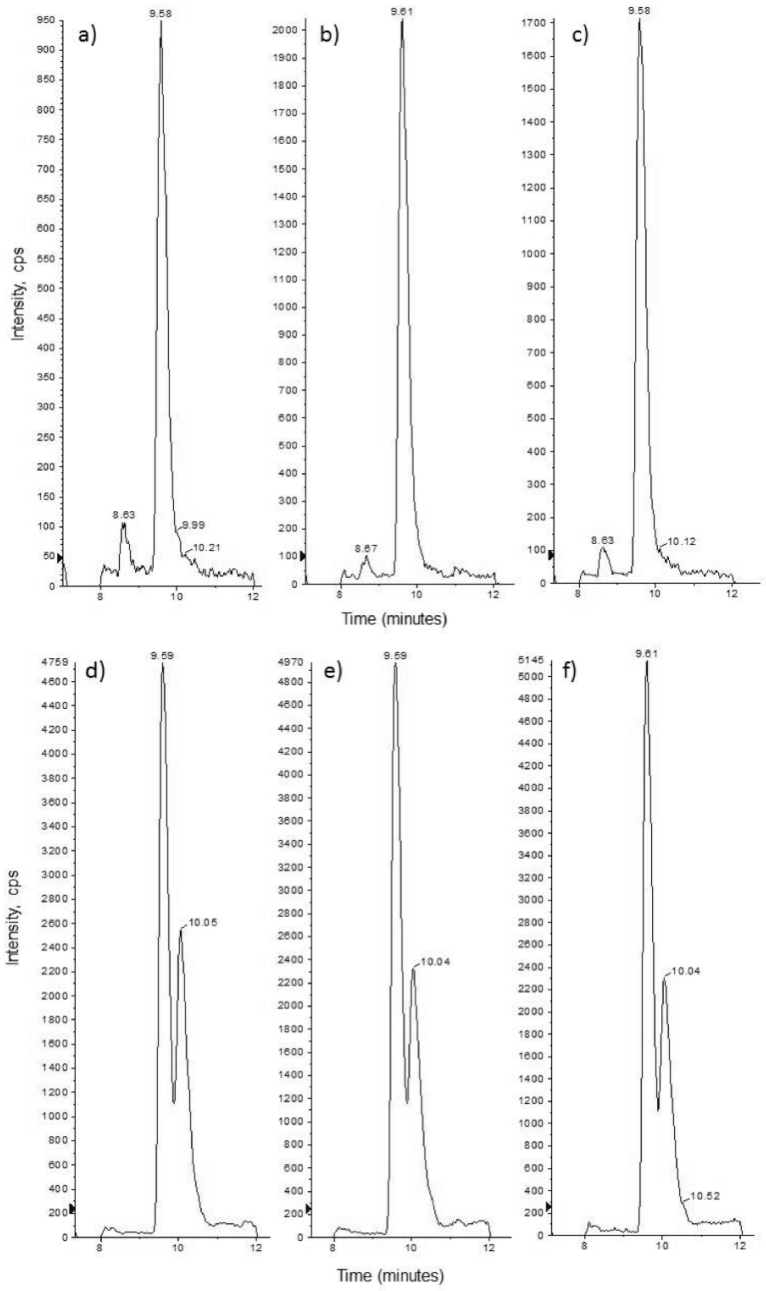

FIGURE 2.4: Extracted ion-chromatograms (XIC) of 2,3-naphthotriazole (NAT). ^{15}N-NAT (m/z 171.1→115.1) XIC is presented in a) $^{15}NO_2^-$ standard in DMEM, b) 20 µM $^{15}N_3$-GTN (vehicle control), and c) 20 µM $^{15}N_3$-GTN (pre-treatment with GTN). These data demonstrate that pre-treatment with GTN resulted in reduced metabolism of $^{15}N_3$-GTN into $^{15}NO_2^-$. ^{14}N-NAT (m/z 170.1→115.1) is presented in d) ^{14}N-nitrite standard in DMEM, e) 20 µM $^{15}N_3$-GTN (Vehicle Control), and f) 20 µM $^{15}N_3$-GTN (pre-treatment with GTN). These data demonstrate that pre-treatment with GTN did not cause a change in $^{14}NO_2^-$ concentration.

Table 2.1: Precision and accuracy of nitrite and nitrate isotopologues in water and DMEM						
Analyte	Isotope	Matrix	Concentration (nM)	Measured Concentration (nM)	Accuracy (%)	Precision (RSD, %)
Nitrite	^{14}N	Water	Blank	91	N/A	8.71
			10	9.22	-7.80	9.43
			100	96.3	-3.70	5.38
			1000	926	-7.40	6.38
		DMEM	Blank	339	N/A	10.3
			10	9.25	-7.50	10.9
			100	101	1.00	4.76
			1000	1060	6.00	9.06
	^{15}N	Water	10	9.49	-5.10	9.17
			100	94.7	-5.30	2.41
			1000	964	-3.60	5.39
		DMEM	10	10.1	1.00	4.42
			100	96	-4.00	3.07
			1000	944	-5.60	6.02
Nitrate	^{14}N	Water	Blank	141	N/A	12.3
			10	9.43	-5.70	6.32
			100	92.7	-7.30	10.4
			1000	841	-15.9	17.6
		DMEM	Blank	467	N/A	13.2
			10	9.31	-6.90	8.59
			100	94.7	-5.30	9.43
			1000	796	-20.4	19.2
	^{15}N	Water	10	9.61	-3.90	7.26
			100	95.3	-4.70	8.51
			1000	884	-11.6	15.6
		DMEM	10	10.1	1.00	5.16
			100	98.9	-1.10	6.48
			1000	821	-17.9	12.4

TABLE 2.1: Precision and accuracy of nitrite and nitrate isotopologues. Three concentrations (10 nM, 100 nM, 1000 nM) of $^{15}NO_2^-$, NO_2^-, $^{15}NO_3^-$, and NO_3^- were spiked into water (n=10) and DMEM (n=10), and the concentration was calculated by comparing to a seven-point concentration curve. Accuracy is determined as the percentage deviation of calculated concentration from the nominal concentrations. Precision is determined as the relative standard deviation (RSD) of the 10 measurements. Blank values for ^{14}N-nitrite and ^{14}N-nitrate in DMEM and water are provided.

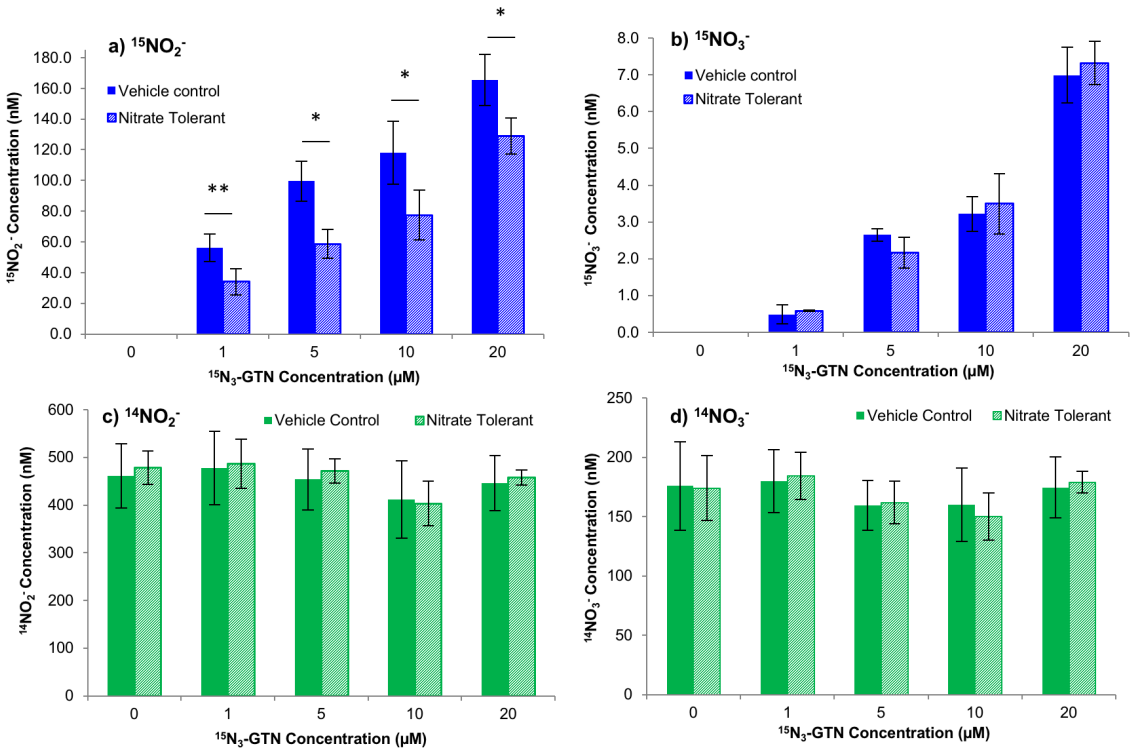

FIGURE 2.5: $^{15}NO_2^-$ and $^{15}NO_3^-$ production from $^{15}N_3$-GTN treatment in EA.hy926 endothelial cells. Cells were pre-treated with 20 μM glyceryl trinitrate (GTN), washed, and then treated with $^{15}N_3$-GTN. Acetonitrile (5 μL) was used as a vehicle control. a) $^{15}NO_2^-$ levels decreased in response to GTN pre-treatment, n=3 ($P<0.05$ at all concentration points). A dose-response curve with $^{15}N_3$-GTN demonstrated linear production of $^{15}NO_2^-$ in nanomolar levels. b) GTN pre-treatment had no significant effect on $^{15}NO_3^-$ levels. A dose-response curve with $^{15}N_3$-GTN demonstrated linear production of $^{15}NO_3^-$ in low nanomolar levels, indicating very low conversion of nitrite into nitrate. The reduction of nitrite to nitrate may occur non-enzymatically. c) $^{14}NO_2^-$ concentration and d) $^{14}NO_3^-$ concentration was not significantly affected ($P>0.05$ at all concentration points). This demonstrates that the pre-treatment was completely washed away and did not compete with ^{15}N-GTN. The high level of $^{14}NO_2^-$ and $^{14}NO_3^-$ is a result of background levels of nitrite and nitrate, potentially from NO synthesis from L-arginine.

Table 2.2: Quantification of background levels of nitrite in water, HEPES, and DMEM	
	Nitrite (nM)
Millipore water[1]	91 ± 13
200 mM HEPES[2]	103 ± 15
DMEM – blank[3]	339 ± 28
DMEM - EA.hy926[4]	461 ± 61
Value are mean ± standard deviation, n=6	

TABLE 2.2: Quantification of background levels of nitrite. Nitrite was measured in 1) reverse osmosis water filtered with Millipore water filter, 2) 200 mM HEPES made from Milli-Q water, 3) phenol red-free Dulbecco's modified Eagle's medium (DMEM) with 1% FBS, and 4) phenol red-free DMEM with 1% FBS that was used to culture 5 x 10^6 EA.hy926 cells in 2 mL medium for 24 hours at 37°C.

2.9. SUPPLEMENTAL INFORMATION

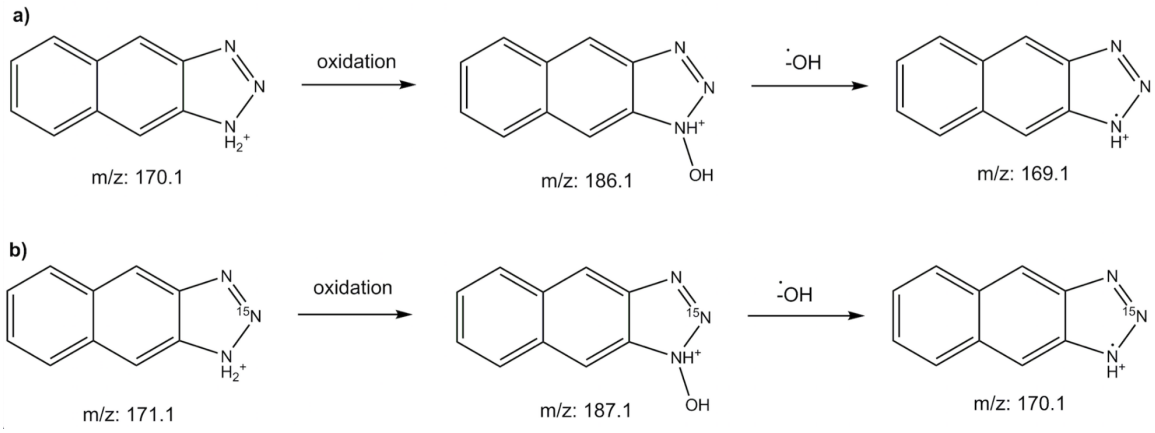

SI FIGURE 2.1: Degradation product of 2,3-naphthotrizaole (NAT). Proposed pathway of degradation of protonated a) ^{14}N-NAT and b) ^{15}N-NAT involves an N-oxide intermediate, and a final mass of 169.1 and 170.1 Da, respectively.

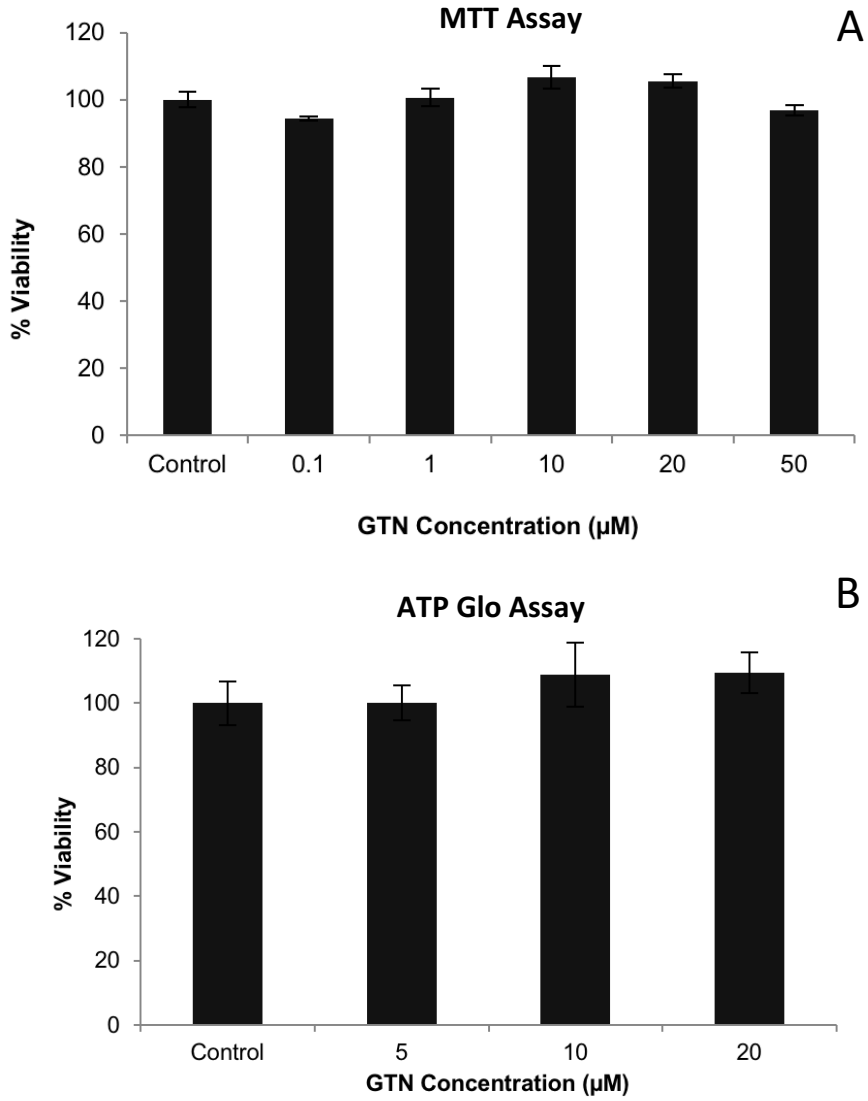

SI FIGURE 2.2: Viability of EA.hy926 cells after glyceryl trinitrate (GTN) treatment. 24-hour treatment with glyceryl trinitrate (GTN)(0.1 – 50 μM) did not significantly alter cell viability (n=5, repeated in triplicate), as evidenced by a MTT assay (A) and ATP-glo Assay (B). Values are mean percent of control ± standard deviation. $P > 0.05$ for all values, indicating no significant differences from control.

CHAPTER 3

ASCORBIC ACID PREVENTS NITROGLYCERIN-INDUCED INACTIVATION OF XANTHINE OXIDASE IN A CELL CULTURE MODEL OF NITRATE TOLERANCE

Elizabeth R. Axton and Jan F. Stevens

Submitted to *Redox Biology*

3.1. ABSTRACT

Glyceryl trinitrate (GTN) is used to treat chest pain resulting from insufficient blood flow (angina). GTN is an organic nitrate prodrug that is metabolized into nitric oxide (NO) to induce vasodilation and improve blood flow. Patients develop tolerance to GTN after several weeks of continuous use, limiting the potential for long-term therapy. The cause of nitrate tolerance is relatively unknown. We developed a cell culture model of nitrate tolerance that utilizes stable isotopes to measure metabolism of $^{15}N_3$-GTN into ^{15}N-nitrite. We performed global metabolomics to identify the mechanism of GTN-induced nitrate tolerance and to elucidate the protective role of vitamin C (ascorbic acid). Metabolomics demonstrated that GTN impaired purine metabolism and depleted intracellular ATP and GTP. GTN inactivated the enzyme xanthine oxidase (XO), an enzyme that is critical for the metabolism of GTN into NO. Ascorbic acid prevented inactivation of XO, resulting in increased NO production from GTN. We conclude that ascorbic acid prevents nitrate tolerance by protecting xanthine oxidase, but not aldehyde dehydrogenase, from GTN-induced inactivation. Ascorbic acid supplementation should be further investigated as a simple and inexpensive strategy to prevent nitrate tolerance.

3.2. INTRODUCTION

Glyceryl trinitrate (GTN), more commonly known as nitroglycerin in the clinic, has been in use since the 1870's. GTN relieves chest pain caused by insufficient blood flow (angina). GTN is a prodrug that is enzymatically bioactivated into nitrite (NO_2^-) and nitric oxide (NO) in endothelial cells. NO diffuses into smooth muscle cells, inducing vasodilation and improving blood flow to relieve chest pain. GTN, and other organic nitrates, are a recommended course of treatment for patients with stable coronary artery disease who are still symptomatic despite treatment with aspirin, beta-adrenergic receptor blocker, ACE-inhibitors/AT-1 receptor blockers, and statins (138). Though GTN is well known to be bioactivated into NO, recent experimental and clinical studies have determined that NO on its own cannot account for all of the vasodilatory effects, suggesting that GTN has additional vasoactive mechanisms (139,140).

Nitrate tolerance. Long-term GTN therapy causes the development of nitrate tolerance, which is defined as the loss of effects, or the need to increase dosages to maintain the effects, of organic nitrates. Patients develop tolerance to GTN after several weeks of continuous use, limiting its efficacy as a long-term treatment. Nitrate tolerance is currently managed by implementing daily 12-hour nitrate-free intervals. Though effective, this strategy leads to increased cardiovascular events during nitrate-free periods, especially in the early morning (16). Some of the systemic changes that occur from nitrate therapy include desensitization of soluble guanylate cyclase (sGC)(141), inactivation of endothelial nitric oxide synthase (eNOS)(29), neurohormonal activation and intravascular volume expansion (termed *pseudotolerance*)(142), and increased vascular superoxide (O_2^-) and peroxynitrite ($ONOO^-$) production (30,143). Superoxide and peroxynitrite are produced as byproducts of GTN bioactivation, and are correlated with the

development of nitrate tolerance (144). Nitrate tolerance and its implications on human health have recently been reviewed (145).

Prevention of nitrate tolerance with ascorbic acid. The efficacy and safety of nitrates could potentially be improved with co-treatment strategies, preventing the need for nitrate-free intervals. Ascorbic acid (vitamin C) is a potent water-soluble antioxidant that also acts as a cofactor for a number of 2-ketoglutarate dependent dioxygenases. Ascorbic acid enhances endothelium-dependent vasodilation and prevents endothelial dysfunction (146,147). Several clinical studies have shown that co-treatments with ascorbic acid prevent the development of nitrate tolerance (41-43). Continuous 3-day transdermal GTN treatment causes a 450% increase in platelet superoxide production in humans, which was reduced to 60% increase upon ascorbic acid co-treatment (148). In addition to its antioxidant and superoxide scavenging properties, ascorbic acid may prevent nitrate tolerance by increasing intracellular glutathione levels (149), increasing intracellular tetrahydrobiopterin to maintain eNOS activity (150), acting as an enzymatic cofactor, or by directly bioactivating GTN into nitrite or NO (151).

Nitrate tolerance has long been regarded as a limitation in nitrate efficacy, but it is now believed to correlate with an onset of potentially harmful vascular abnormalities that increase the risk of adverse cardiovascular outcomes. We performed global metabolomics on a cell culture model of nitrate tolerance as a hypothesis-generating approach to elucidate the mechanism by which ascorbic acid prevents nitrate tolerance. Our results demonstrate that xanthine oxidase (XO) and aldehyde dehydrogenase 2 (ALDH2), both key GTN-bioactivating enzymes (17,25), are inactivated by GTN treatment. We found that ascorbic acid protects XO, but not ALDH, from inactivation and that it restored NO production. Considering that ALDH2 appears to be

irreversibly damaged by GTN, ascorbic acid supplementation could emerge as an important therapeutic strategy to prevent nitrate tolerance by preserving XO activity.

3.3. MATERIALS AND METHODS

Chemicals. All solvents and reagents were commercially available and of analytical grade quality unless otherwise specified. Dulbecco's Modified Eagle Medium (DMEM), fetal bovine serum (FBS), penicillin-streptomycin (PS), 0.25% trypsin-EDTA and Hank's Buffered Salt Solution (HBSS) were procured from Invitrogen (Carlsbad, CA). T75 flasks, culture dishes (100 mm) and other sterile plastic ware were purchased from Corning (Corning, NY). 2,3-diaminonaphthalene (DAN) was procured from TCI America (Portland, OR). $^{15}N_3$-glyceryl trinitrate (^{15}N, 98%) in acetonitrile, sodium ^{15}N-nitrite (^{15}N, 98%), and sodium ^{15}N-nitrate (^{15}N, 98%) were from Cambridge Isotope Laboratories (Tewksbery, MA). Sodium ascorbate, bovine xanthine oxidase, human recombinant mitochondrial aldehyde dehydrogenase (ALDH2), diphenyleneiodonium chloride, allopurinol, disulfiram, L-NAME, and glyceryl trinitrate (GTN) were procured from Sigma Aldrich (St. Louis, MO). LC-MS grade water, methanol, and acetonitrile were purchased from J.T. Baker (Center Valley, PA). Formic acid and ammonium bicarbonate were obtained from Fluka (Buchs, Switzerland).

Cell culture. Porcine renal epithelial cells (LLC-PK1, ATCC, Manassas, VA) were chosen for metabolomics analysis because of their ability to bioactivate GTN and because they have an intact NO-sGC-cGMP pathway (129). Cells were maintained under sterile conditions in 75 cm^2 flasks in DMEM supplemented with 10% FBS and 1% PS, with 5% CO_2 at 37°C. Cells were used for experiments on passages 5 to 8 only.

LLC-PK1 cells were plated in 100 mm culture dishes at a density of 500,000 cells in DMEM with 10% FBS and 1% PS. 24 hours after plating, cells were treated with 100 µM sodium ascorbate. After a 24-hour treatment, the medium was changed and the cells were treated with a second 100 µM dose of sodium ascorbate in DMEM with 1% FBS and 1% PS, and immediately challenged with 1 µM GTN. Treatment groups were 1) vehicle control, 2) GTN, 3) ascorbic acid, and 4) GTN + ascorbic acid. After a 5-hour treatment, cells were either extracted for metabolomics analysis or assayed for nitrate tolerance (Nitrite Assay, cGMP Assay), intracellular ascorbic acid, or intracellular reactive oxygen species (ROS)(DCFDA Assay)(Experiment Design, Figure 3.1).

This ascorbic acid treatment protocol was chosen because it did not alter cell viability or proliferation, it effectively attenuated nitrate tolerance, and is a physiologically relevant dose. Similarly, the 1 µM GTN dose was chosen because it was previously shown to be effective at inducing nitrate tolerance with no effect on cell viability or proliferation in LLC-PK1 cells (19,129), while being a sufficient dose for the nitrite method detection limits (152). A vehicle control of 2.3 µL acetonitrile was chosen to control for the 2.3 µL of acetonitrile added with the GTN treatment. Cell viability assays demonstrate that neither GTN nor ascorbic acid caused any significant changes in cell viability at the concentrations used for metabolomics analysis, as measured by an MTT Assay (SI Figure 3.1).

Nitrate Tolerance Analyses

Pre-treated cells (vehicle, GTN, ASC, or GTN + ASC) were washed once with 3 mL warm HBSS. Cells were challenged with 1 µM $^{15}N_3$-GTN for 30 minutes. 100 µL of the medium was transferred to 1.5 mL Eppendorf tubes and immediately assayed for ^{15}N-nitrite production.

Nitrite LC-MS/MS assay. ^{15}N-nitrite was measured as a biomarker for bioactivation of $^{15}N_3$-GTN. Isotope labeling allows us to distinguish between endogenous nitrite and nitrite produced from GTN bioactivation. 10 µL of 316 µM 2,3-diaminonaphthalene (DAN) in 0.62 M HCl was added to 100 µL of cell culture medium and incubated at 24°C for 60 minutes. The reaction was quenched with 5 µL of 2.8 M NaOH. The samples were centrifuged at 16,000 x g for 1 minute, and the supernatant was transferred to mass spectrometry vials and analyzed for ^{15}N-nitrite with the previously described method with minor modifications (152). The column was switched to a Poroshell 120 HPH-C18 column (2.7 µm, 2.1 x 50 mm, Agilent, Santa Clara, CA), allowing for a reduced run time of 10 minutes.

cGMP ELISA assay. Cyclic guanosine monophosphate (cGMP) was quantified as a marker for NO production. Pre-treated cells were washed twice with HBSS, then incubated with 0.5 mM isobutylmethylxanthine (IBMX). 1 µM GTN was added and incubated for 30 minutes. Medium was aspirated and cells were washed twice with HBSS. 5 mL of 0.1 M HCl was added to each petri dish and incubated for 20 minutes. The cells were scraped and the plate contents were transferred to a 15-mL conical tube and centrifuged at 1,000 x g for 10 minutes. The supernatant was assayed for cGMP according the kit protocol (cGMP ELISA Kit, Cayman Chemical, Ann Arbor, MI). Samples were analyzed on a fluorescence plate reader (Molecular Devices SpectraMax GeminiXS).

Quantification of intracellular ascorbic acid with HPLC/ECD. Ascorbic acid was quantified with paired ion reverse phase HPLC coupled with electrochemical detection, as previously described (153). In short, cells were harvested with trypsin, and the cell pellet was extracted with 10% perchloric acid with 1 mM diethylenetriamine pentaacetic acid (DTPA). The supernatant was diluted 10x with mobile phase and adjusted to pH 5.0 with 2.58 M K_2PO_4 (pH 9.8). Samples were

analyzed with a Waters HPLC equipped with a Supelcosil LC-8 column (25 cm x 4.6 mm (i.d.))(Supelco, St.Louis, MO) and a LC-18 guard column (2 cm x 4.6 mm (i.d.), Supelco). The eluant (40 mM sodium acetate, 7.5% (vol/vol) methanol, 0.54 mM DTPA, 1.5 mM dodecyl-triethylammonium phosphate in purified Milli-Q water (taken to pH 4.75 with glacial acetic acid)) was delivered at 1.0 mL/min. Analysis was performed on a LC 4B amperometric electrochemical detector equipped with a glassy-carbon working electrode and a Ag/AgCl reference electrode (Bioanalytical Systems, West Lafayette, IN). Ascorbic acid was analyzed with an applied potential of +0.5 V with a sensitivity of 50 nA, and eluted as a single peak at 5.8 minutes.

Quantification of intracellular reactive oxygen species (ROS). Intracellular production of ROS was quantified with a 2',7'-dichlorofluorescein diacetate (DCFDA) assay. LLC-PK1 cells were plated in a black 96-well plate (5,000 cells/well). 10 µM H_2DCFDA (ThermoFisher, Waltham, MA) was added to cells in phenol red-free DMEM with 1% FBS and incubated for 20 minutes. The DCFDA medium was aspirated and the cells were washed 3x with DMEM. Phenol red-free and FBS-free DMEM was added to the cells. Intracellular production of DCF was measured with a fluorescence spectrophotometer (Ex/Em = 485/ 530 nm)(Molecular Devices SpectraMax GeminiXS) every 20 minutes for 3 hours. Results were processed with SoftMax Pro 5.4.

Statistical analyses. All analyses with 3 or more treatment groups were analyzed with a either one-way or two-way ANOVA with Bonferroni post-hoc analysis with a p-value of < 0.05 indicating significance. Values of *n* represent independent biological replicates. If needed, data were logarithmically transformed to correct for unequal variance or non-normal distribution. No outliers were excluded from the statistical analyses. All statistical analyses and figures were generated with GraphPad Prism 4.

Metabolomics

Metabolomics sample preparation. Treated cells were washed twice with 3 mL of warm HBSS. 3 mL of warm trypsin (0.25%) was added to each petri dish and incubated for 3 minutes. 3 mL of medium was added, and detached cells were transferred to 15-mL conical centrifuge tubes. Cells were centrifuged at 4°C at 500 x g for 5 minutes. The liquid was aspirated, and the pellets were washed with cold HBSS 3X. 1 mL of ice-cold degassed methanol: acetonitrile: water (2:2:1) was added to each cell pellet and vortexed for 30 seconds. The cells were frozen in liquid N_2 for 60 seconds, then sonicated and allowed to thaw in a water bath for 10 minutes. This freeze-thaw cycle was repeated for a total of 3 times. The cell extracts were incubated at -20°C for 1 hour, then centrifuged at 4°C at 13,000 x g for 15 minutes. The supernatant was transferred to 1.5 mL Eppendorf tubes and evaporated using a freeze dryer (Labconco FreeZone 6 Plus). The cell extracts were re-suspended in 100 µL ice-cold 50% acetonitrile, sonicated at room temperature for 10 minutes, then centrifuged at 4°C at 13,000 x g for 15 minutes. The supernatant was transferred to mass spectrometry vials (Microsolv, Eatontown, NJ) and frozen at -80°C until analysis.

Instrumentation. LC-MS/MS based metabolomics was performed as previously described (154). In short, high-pressure liquid chromatography (HPLC) was performed on a Shimadzu Nexera system (Shimadzu, Columbia, MD) with a phenyl-3 stationary phase column (Inertsil Phenyl-3, 4.6 x 150 mm, GL Sciences, Torrance, CA) coupled to a quadrupole time-of-flight mass spectrometer (AB SCIEX TripleTOF 5600) operated in information dependent MS/MS acquisition mode in both positive and negative ion mode. The flow rate was 0.4 ml/min, and mobile phases consisted of water (A) and methanol (B), both with 0.1% formic acid. The elution gradient was as follows: 0 min, 5% B; 1 min, 5% B; 11 min, 30% B; 23 min, 100% B; 35 min, 100% B; 37 min, 5% B;

and 47 min, 5% B. Samples were randomized, and a pooled QC sample was analyzed every 5 samples. Auto-calibration was performed after every two samples.

Metabolomics data processing. All metabolomics samples were analyzed using PeakView with XIC Manager 1.2.0 (ABSciex, Framingham, MA) for peak picking, retention time correction, and peak alignment. Metabolite identities were assigned by matching accurate mass (error < 10 ppm), retention time (error < 10%), MS/MS fragmentation (library score > 70), and isotope distribution (error < 20%) with an in-house library consisting of IROA standards (IROA Technology, Bolton, MA) and other commercially available standards (650 total). The peak list was exported to MultiQuant 3.0.2 (ABSciex), and used to create a MultiQuant method. All sample chromatograms were integrated to obtain peak area for all of the assigned metabolites.

Statistical analysis of metabolomics data. Annotated metabolites were used for multivariate statistical analysis. Pathway analyses and principal component analysis (PCA) plots were generated with MetaboAnalyst 3.0 (155). The significance of individual metabolites between the four treatment groups was assessed with a Two-way ANOVA followed by Fisher's post-hoc analysis and Holm FDR-correction, with a P-value of < 0.05 indicating significance (n=6/group). If needed, data were logarithmically transformed to correct for unequal variance or non-normal distribution. No outliers were excluded from the statistical analyses. Figures were generated with GraphPad Prism 4 (La Jolla, CA), PowerPoint 2016 (Microsoft, Redmond, WA), and MetaboAnalyst 3.0.

3.4. RESULTS AND DISCUSSION

Nitrate tolerance in LLC-PK1 cells

We induced nitrate tolerance in ascorbic acid-deficient or ascorbic acid-supplemented LLC-PK1 cells with a 5-hour pre-treatment of 1 μM GTN. Pre-treatment with GTN (GTN Tolerant) caused reduced bioactivation of a second challenge with $^{15}N_3$-GTN, as evidenced by quantification of ^{15}N-nitrite ($p < 0.001$). This observed nitrate tolerance was attenuated by co-treatment with ascorbic acid ($p < 0.01$). There was no significant difference in $^{15}N_3$-GTN bioactivation between control cells and cells pre-treated with both GTN and ascorbic acid. In cells that did not receive a pre-treatment with GTN (GTN Naïve), ascorbic acid did not cause a significant increase in $^{15}N_3$-GTN bioactivation (Figure 3.2A).

Cyclic guanosine-3',-5'-monophosphate (cGMP) is released when NO reacts with soluble guanylate cyclase (sGC), and is a key intermediate in NO-induced vasodilation. cGMP was measured as a biomarker of NO production. Pre-treatment with GTN caused impaired bioactivation of GTN into NO ($p < 0.001$), which was attenuated by co-treatment with ascorbic acid ($p < 0.001$)(Figure 3.2B). There was no significant difference in cGMP production between control cells and cells treated with both GTN and ascorbic acid. The cGMP results are supported by studies demonstrating that cGMP can be measured as a marker of nitrate tolerance, and that tolerance can be induced in LLC-PK1 cells with GTN treatment (129,156). These results demonstrate that ascorbic acid increases both nitrite and NO production from GTN in nitrate tolerant cells.

We quantified intracellular ascorbic acid to determine the physiological significance of our ascorbic acid treatment. Intracellular concentration of ascorbic acid in the supplemented cells

was 1.46 ± 0.03 mM. Ascorbic acid was not detected in the non-supplemented cells (lower limit of detection 1 μM). The intracellular concentration exceeds the 100 μM treatment concentration due to active uptake of ascorbic acid. Nitrate tolerant cells had reduced intracellular ascorbic acid compared to cells treated with ascorbic acid alone (1.07 ± 0.06 mM)($p < 0.001$)(Figure 3.2C). This suggests that GTN treatment increases intracellular oxidative stress and depletes ascorbic acid. This observation has been previously reported in guinea pig blood plasma (157). This is a relevant finding because humans, unlike most other animals, are unable to synthesize ascorbic acid and require it in the diet. Therefore, ascorbic acid supplementation may be a strategy to prevent GTN-induced ascorbic acid deficiency.

A 2',7'-dichlorofluorescein diacetate (DCFDA) assay to measure intracellular H_2O_2 demonstrated that GTN caused increased intracellular oxidative stress ($p < 0.01$), which was not attenuated by ascorbic acid supplementation (Figure 3.2D). The increase in oxidative stress can be caused by superoxide (O_2^-) production by XO, mitochondrial dysfunction, or formation of peroxynitrite ($ONOO^-$) from the reaction between NO and O_2^-. These results support the "oxidative stress hypothesis" by Thomas Münzel, which hypothesizes that oxidative stress caused by nitrate treatment leads to enzyme inactivation (30). These results suggest that the protective role of ascorbic acid may not be solely due to its antioxidant capacity.

The nitrite and cGMP assays demonstrate that we induced nitrate tolerance in LLC-PK1 cells, which was attenuated by pre-treatment with ascorbic acid. Quantifying ^{15}N-nitrite (the first intermediate in $^{15}N_3$-GTN bioactivation) and cGMP (biomarker for the bioactive molecule NO) allowed us to measure nitrate tolerance in cells. Using stable isotopes in the GTN bioactivation assay allowed us to distinguish between nitrite released from GTN and nitrite produced

endogenously by eNOS. We performed untargeted metabolomics to gain insight in the cause of nitrate tolerance and the mechanism of ascorbic acid in the prevention of nitrate tolerance.

Untargeted metabolomics of LLC-PK1 cells exposed to GTN

Metabolomics analysis was performed on nitrate tolerant and control LLC-PK1 cells that were ascorbic acid-deficient or ascorbic acid-supplemented. 3,338 monoisotopic features were detected in positive and negative mode, combined. Of these, 653 were significantly changed in at least one of the treatment groups, compared to the others (Two-way ANOVA with Fisher's Post-hoc analysis (n=6/group), $p < 0.05$ after Holm's FDR-correction indicating significance, MetaboAnalyst 3.0). 87 metabolites were assigned using our in-house library, all of which are listed in the Supplementary Information with their molecular formula, accurate mass, ppm error, and retention times (SI Table 3.1). The p-values for all annotated metabolites between all treatment groups are listed (Two-way ANOVA with Fisher's Post-hoc analysis (n=6/group), $p < 0.05$ after Holm's FDR-correction indicating significance, MetaboAnalyst 3.0)(SI Table 3.2).

Pathway Analysis. Principal component analysis (PCA) plots of all annotated metabolites demonstrate separation and clustering of control, GTN, ASC, and GTN + ASC groups (Figure 3.3A). The PCA plots demonstrate that our treatments had a significant effect on the metabolic profile, and that our replicates cluster. MetaboAnalyst was used to generate a pathway analysis with the annotated metabolites (Figure 3.3B). 11 pathways were significantly changed upon GTN treatment compared to control ($p < 0.05$ after Holm FDR correction)(tabulated results and P-values available in SI Table 3.3). Of the significant pathways, most notable were purine metabolism, arginine and ornithine metabolism, glutathione metabolism, cysteine and methionine metabolism, arginine and proline metabolism, arachidonic metabolism and linoleic

acid metabolism. Furthermore, MetaboAnalyst was used to generate a heat map of select metabolites within pathways that are changed among Control, GTN, ASC, and GTN + ASC groups (Figure 3.4). Here, we discuss a few of the significant changes that were measured by untargeted metabolomics and their relevance to the vasoactive mechanisms of GTN and the development of nitrate tolerance.

Glutathione (GSH) and oxidized glutathione (GSSG) metabolism. GSH is elevated with both GTN treatment ($p < 0.01$) and ascorbic acid supplementation ($p < 0.05$). This may be due to an adaptive stress response to the reactive oxygen and nitrogen species generated with GTN treatment. Alternatively, peroxynitrite produced by GTN bioactivation causes S-nitrosylation of glutathione S-transferase (GST)(158), potentially causing reduced conjugation of GSH for detoxification. Ascorbic acid can increase intracellular glutathione through a sparing mechanism. GSSG is generated when GSH reacts with ROS. The ratio of GSH/GSSG is considered a biomarker of oxidative stress. Cells treated with GTN have a significant increase in GSSG ($p < 0.001$), which is prevented by ascorbic acid supplementation ($p < 0.001$). These findings demonstrate that ascorbic acid is having predicted effects on glutathione metabolism in this cell culture model of nitrate tolerance.

GTN impairs L-arginine metabolism. Endothelial nitric oxide synthase (eNOS) metabolizes L-arginine and O_2 into L-citrulline and NO. GTN treatment increases L-arginine ($p < 0.001$) and decreases L-citrulline ($p < 0.01$). This accumulation of L-arginine suggests that eNOS activity is impaired with GTN treatment. In vitro studies have shown that eNOS has higher expression but lower activity after GTN treatment, and is associated with higher superoxide levels (30). eNOS activity may be lower because peroxynitrite, a product of enzymatic GTN bioactivation, can oxidize tetrahydrobiopterin (BH4), an essential cofactor of eNOS activity, into the ineffective

dihydrobiopterin (BH2) through the radical intermediate trihydrobiopterin (BH3)(159). Ascorbic acid can recycle BH3 back into BH4, effectively restoring eNOS activity (160). Citrulline is significantly increased with ascorbic acid treatment ($p < 0.001$), suggesting that ascorbic acid is increasing eNOS activity.

Urea cycle, amino acids, and polyamines. Accumulation of L-arginine has significant downstream metabolic effects. Ornithine levels were higher in GTN-treated cells compared to the controls ($p < 0.001$). Increased ornithine, a member of the urea cycle, results in changes in amino acid metabolism, TCA cycle, glycolysis, and gluconeogenesis. We observed that increased ornithine parallels increased proline and glutamate, which are products of ornithine. Glutamate is an amino acid that can feed into the TCA cycle via reversible transamination or glutamate dehydrogenase. The polyamines spermine and spermidine are also increased with GTN treatment ($p < 0.05$, $p < 0.05$). Polyamines control cell growth and differentiation and are important modulators of ion channels such as NMDA (N-methyl D-aspartate receptor) and AMPA (α-amino-3-hydroxy-5-methyl-4-isoxazolepropionic acid receptor). Although eNOS activity has already been implicated in the development of nitrate tolerance, this is the first report of downstream metabolic effects on the urea cycle, polyamine synthesis, and glutamate and proline metabolism.

GTN treatment impairs purine metabolism and energy production. Fatty acids (oleic acid, linoleic acid, arachidonic acid, myristic acid, palmitic acid), glycolytic intermediates (glucose, fructose 1,6-bisphosphate) and TCA cycle intermediates (citrate, isocitrate, malate) were increased with GTN treatment. Several purines were significantly increased in GTN-treated cells (Figure 3.5A). This pattern is observed in guanine, guanosine, and guanosine monophosphate (GMP) and well

as in adenine, adenosine, and adenosine monophosphate (AMP). The only purines that were not significantly increased with GTN treatment were inosine and inosine monophosphate (IMP).

Interestingly, we observed that increased AMP and GMP do not correlate to increased ADP/ATP or GDP/GTP. An increase in the relative ratio of AMP, ADP, and ATP, otherwise known as the adenylate energy charge, indicates significant mitochondrial dysfunction potentially due to the increase in oxidative stress resulting from GTN treatment. A decrease in cellular ATP and GTP levels will have profound effects on energy metabolism. Here, we explore several mechanisms for the impairment of purine metabolism and cellular energy status.

Depletion of ADP and ATP indicates mitochondrial dysfunction. ALDH2, a mitochondrial GTN-bioactivating enzyme, can release peroxynitrite when exposed to GTN (161). High levels of nitrate lead to mitochondrial uncoupling, perhaps mediated by ALDH2 activity (162). In addition, nitric oxide modulates cytochrome c oxidase (Complex IV of mitochondrial respiration) via S-nitrosylation (163). Together, these findings indicate that GTN, or products thereof, are causing mitochondrial dysfunction and reduced ATP production. Interestingly, we observed that ascorbic acid co-treatment restored ATP and ADP production, as well as GDP and GTP (Figure 3.5 B-C). One possible explanation is that ascorbic acid maintains ALDH2 activity to prevent it from producing peroxynitrite. This would reduce mitochondrial oxidative stress and maintain cellular ATP production. Ascorbic acid has previously been shown to detoxify and eliminate 4-hydroxy-2(*E*)-nonenal (HNE) to prevent mitochondrial dysfunction in human monocytic THP-1 cells (164).

Ascorbic acid prevents xanthine oxidase inactivation. XO oxidizes hypoxanthine and xanthine into uric acid, which are the final steps in purine metabolism in humans. In GTN-treated cells,

hypoxanthine is increased ($p < 0.001$) and uric acid is decreased ($p < 0.05$)(Figure 3.5 D-E). These results suggest that xanthine oxidase activity is impaired with GTN treatment. Co-treatment with ascorbic acid prevents this effect, resulting in increased metabolism of hypoxanthine to uric acid and restoring purine metabolism. Since both hypoxanthine and xanthine are oxidized at the molybdenum site of XO, this suggests that ascorbic acid may act through the molybdenum site to increase XO activity. Inactivation of xanthine oxidase could cause the increased levels of purines, including AMP and GMP. The nucleotide salvage pathways hypoxanthine/guanine phosphoribosyl transferase (HPGRT) and adenine phosphoribosyl transferase (APRT) can recover the bases hypoxanthine, adenine, and guanine back into their corresponding nucleotide monophosphates. Therefore, XO inactivation and disruption of the final step of purine metabolism could lead to accumulation of purines and nucleotide monophosphates.

An alternate explanation for the increase in purines is that decreased ATP would lead to increase of adenylate kinase (ADK, myokinase) activity, disproportioning 2 ADP to produce ATP + AMP. Increased activity of ADK would lead to depletion of ADP and an increase in ATP and AMP. With increased nucleotide monophospates we would also expect to see an increase in the corresponding bases (hypoxanthine, adenine, guanine). Interestingly, ascorbic acid deficiency has been previously shown to activate the purine nucleotide cycle in zebrafish by increasing AMP deaminase (AMPD) activity (154). The absence of a significant change in IMP and inosine with treatment suggests low AMPD activity, with most of the AMP either being metabolized into adenosine and adenine, or being utilized for ATP production. Ascorbic acid deficiency has previously been shown to decrease the adenylate charge in zebrafish (154) and in chick cartilage cells (165). We demonstrate here that GTN-induced decrease of the adenylate energy charge is prevented by ascorbic acid co-treatment.

Our metabolomics results suggest both GTN-induced mitochondrial dysfunction and disrupted purine metabolism. Both of these dramatic metabolic changes were prevented with ascorbic acid co-treatment. These metabolic effects can be attributed to impaired XO and ALDH2 activity, both GTN-bioactivating enzymes that are known to be inactivated with continuous GTN treatment.

Enzymatic Bioactivation of GTN

The precise mechanism of GTN bioactivation has yet to be elucidated. It is commonly believed that ALDH2 bioactivates GTN into nitrite in endothelial cells, which is then reduced to NO (17). NO diffuses into the smooth muscle cells, and through a cascade of signaling events activates soluble guanylyl cyclase (sGC) to produce cyclic guanosine-3',-5'-monophosphate (cGMP) to induce vasodilation. Another enzyme that has been shown to bioactivate both inorganic and organic nitrates into NO is XO (24-26,33), however the physiological significance has yet to be demonstrated. Although XO is inactivated by continuous GTN treatment, it is not yet known if XO is an important GTN bioactivating enzyme in vivo. It is believed that XO is a low-affinity pathway of GTN bioactivation that may be more significant in certain disease states and under low oxygen ischemic conditions (29).

To validate our metabolomics results, we incubated commercially available bovine XO and human recombinant ALDH2 with $^{15}N_3$-GTN (0.5 – 20 μM). The enzymes were incubated in HEPES buffer (pH 7.4) for 30 minutes at 37°C. ALDH2 was incubated with 100 μM NAD+ and XO was incubated with 100 μM xanthine. Samples were assayed for ^{15}N-nitrite to measure $^{15}N_3$-GTN bioactivation. We determined that both XO and ALDH2 can bioactivate GTN into nitrite with a linear dose-response (Figure 3.6 A-B). Ascorbic acid (100 μM) increased GTN bioactivation by

XO, but not ALDH2. XO and ALDH2 were incubated with $^{15}N_3$-GTN (20 μM) and sodium ascorbate (10 - 1000 μM) to characterize the dose-response of ascorbic acid. Ascorbic acid increased GTN bioactivation by XO at concentrations 50 μM and greater ($p < 0.01$), but did not have an effect on ALDH2 at any concentration (Figure 3.6 C-D). The effect of ascorbic acid on XO-mediated GTN bioactivation is physiologically relevant given that intracellular ascorbic acid was 1.46 ± 0.03 mM in LLC-PK1 cells.

ALDH2 is widely regarded as the primary GTN-bioactivating enzyme in vivo. However, our metabolomics results suggested a role of XO in the development of nitrate tolerance. Of particular importance, the protective role of ascorbic acid may be mediated through XO. We chose to use chemical inhibitors of both XO and ALDH2 to determine relative role of these enzymes in GTN bioactivation in LLC-PK1 cells. To determine the specificity of the inhibitors, we first incubated bovine XO and human ALDH2 with the inhibitors allopurinol (inhibitor of molybdenum site of XO), disulfiram (ALDH2 inhibitor), diphenyleneiodonium (FAD-site inhibitor of flavoenzymes), and L-N^G-Nitroarginine methyl ester (L-NAME, inhibitor of eNOS). This approach was chosen because knockouts and knockdowns of XOR in LLC-PK1 cells were not viable, which was not unexpected given that mouse knockouts of XOR are lethal (166).

Inhibition of bovine XO with the inhibitors allopurinol and DPI significantly decreased GTN bioactivation ($p < 0.001$). Interestingly, disulfiram decreased GTN bioactivation by XO ($p < 0.05$), demonstrating off-target effects. ALDH2 was inhibited by disulfiram ($p < 0.001$). L-NAME did not have a significant effect on ALDH2 or XO (SI Figure 3.3). These results demonstrate that we have two inhibitors for XO - allopurinol is a specific molybdenum-site inhibitor, whereas DPI is a non-specific FAD-site inhibitor. Disulfiram is an inhibitor of ALDH2, but may have off-target effects.

We then used the chemical inhibitors of XO and ALDH2 to test the role of XO and ALDH2 on GTN bioactivation in LLC-PK1 cells. It should be noted that with a single dose of the inhibitors, we were not attempting to characterize enzyme kinetics, but testing for presence or absence of XO and ALDH2 activity in the LLC-PK1 cells. Both ^{15}N-nitrite production and cGMP production were reduced upon treatment with XO inhibitors – most remarkably by DPI ($p < 0.01$, $p < 0.001$). Allopurinol decreased both ^{15}N-nitrite production ($p < 0.01$) and cGMP production ($p < 0.001$). This is expected because allopurinol is an inhibitor of the molybdenum site of XO, and prevents both the reduction of nitrite into NO and the oxidation of hypoxanthine and xanthine. Disulfiram caused a minor but significant decrease in both GTN bioactivation and cGMP production ($p < 0.01$, $p < 0.05$). Together, these results demonstrate that both XO and ALDH2 bioactivate GTN in LLC-PK1 cells.

We measured XO and ALDH2 enzyme activity in LLC-PK1 cells. LLC-PK1 cells were supplemented with 100 µM ascorbic acid for 24 hours, then subjected to a 5-hour 1 µM GTN treatment following the same protocol performed for the metabolomics analysis. XO activity was measured with a commercially available assay (Xanthine Oxidase Activity Assay Kit, ABcam, Cambridge, UK), which measured XO oxidation of xanthine, thereby converting O_2 to H_2O_2 which reacts stoichiometrically with an OxiRed Probe (Ex/Em=535/587 nm). ALDH2 was measured with a commercially available assay (ALDH2 Activity Assay Kit, Abcam, Cambridge, UK) which uses immunocapture to isolate ALDH2 in a microplate and measures the acetaldehyde-dependent conversion of NAD+ into NADH, which reacts with a reporter dye (absorbance 450 nm).

LLC-PK1 cells express active XO and ALDH2. XO was inactivated by GTN ($p < 0.01$), which was attenuated by ascorbic acid co-treatment ($p < 0.001$). Ascorbic acid increased XO activity in both GTN naïve and GTN tolerant cells ($p < 0.001$). ALDH2 activity was reduced by GTN treatment ($p <$

0.001), however ascorbic acid did not alter ALDH2 activity. We predict that the reduction in XO and ALDH2 activity by GTN are physiologically significant, as evidenced by the metabolic changes in purine metabolism and mitochondrial function. Furthermore, inactivation of XO by oxidative species is permanent and activity can only be recovered by de novo protein synthesis (167). These results demonstrate that both XO and ALDH2 are inactivated by GTN treatment, however ascorbic acid supplementation protects only XO from inactivation (Figure 3.8).

Our results demonstrate that both ALDH2 and XO are involved in GTN bioactivation. ALDH2 is a high-affinity pathway of GTN bioactivation into nitrite (17), however, when it is inactivated and intracellular oxidative stress levels rise, XO could become the predominant GTN-bioactivating enzyme as a second line of defense. Given that XO is necessary to convert nitrite into NO, preserving XO activity is paramount to preventing nitrate tolerance.

3.5. CONCLUSION

In addition to preserving XO activity for GTN bioactivation, supplementation with ascorbic acid should be re-investigated as a potential means of preventing GTN toxicity because it increases intracellular glutathione, restores cellular energy metabolism, and prevents disruption of purine metabolism. Ascorbic acid supplementation, a simple and inexpensive treatment, could prevent toxicity from organic nitrate therapy and allow for long-term use in the clinic. Supplementation with ascorbic acid should be beneficial because patients with angina, and subjects at risk to develop myocardial infarction, have lower plasma and tissue ascorbic acid concentrations compared to healthy subjects (168,169). In addition, in both our cell culture experiments and previous guinea pig studies, GTN treatment reduced ascorbic acid levels. Therefore, ascorbic acid supplements may be effective because they counteract GTN-induced ascorbic acid

deficiency. Our findings suggest that an adequate vitamin C status prevents nitrate tolerance by preserving XO activity.

3.6. ACKNOWLEDGMENTS

This work was supported in part by National Institute of Health Grants T32 ES007060 and S10RR027878. The authors would like to acknowledge Jeffrey Morré, Eleonso Cristobal, Mary Fantacone, Dr. Jaewoo Choi, and Dr. Cristobal Miranda for their technical assistance.

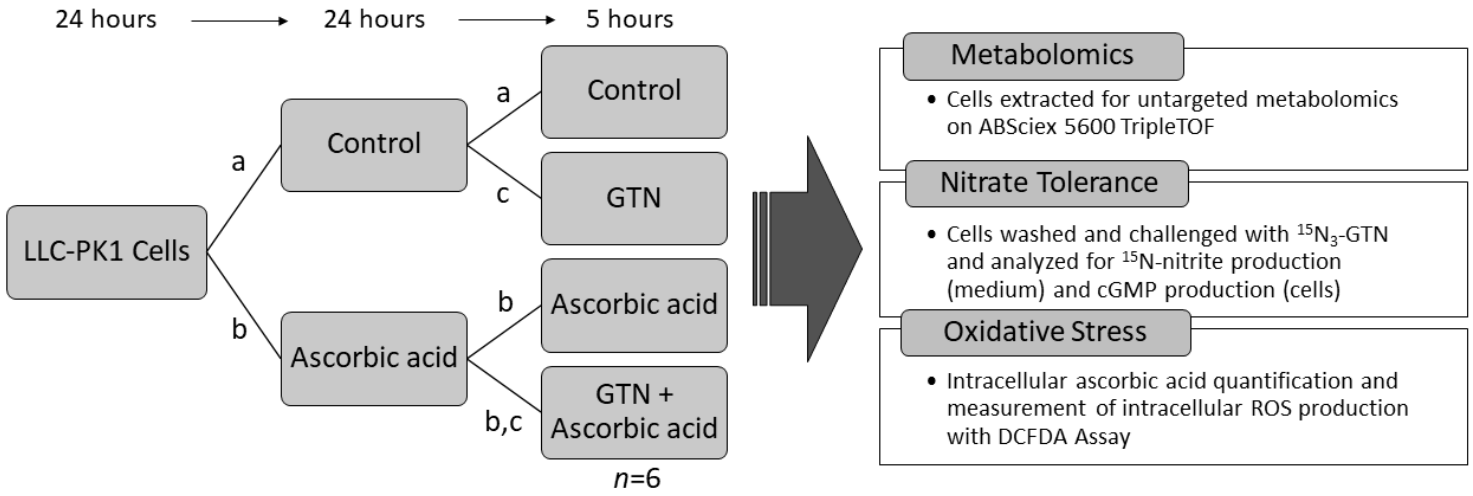

FIGURE 3.1: Experimental design. LLC-PK1 cells were plated at a density of 5.0 x 10^7 cells per 100 mm cell culture dish. 24 hours later, they were treated with a) vehicle control, or b) 100 µM sodium ascorbate. After 24 hours, cells were treated with a) vehicle control, b) 100 µM sodium ascorbate, or c) 1 µM glyceryl trinitrate (GTN). After 5 hours, the cells (n=6) were analyzed for metabolomics, nitrate tolerance, intracellular ascorbic acid, or intracellular reactive oxygen species (ROS).

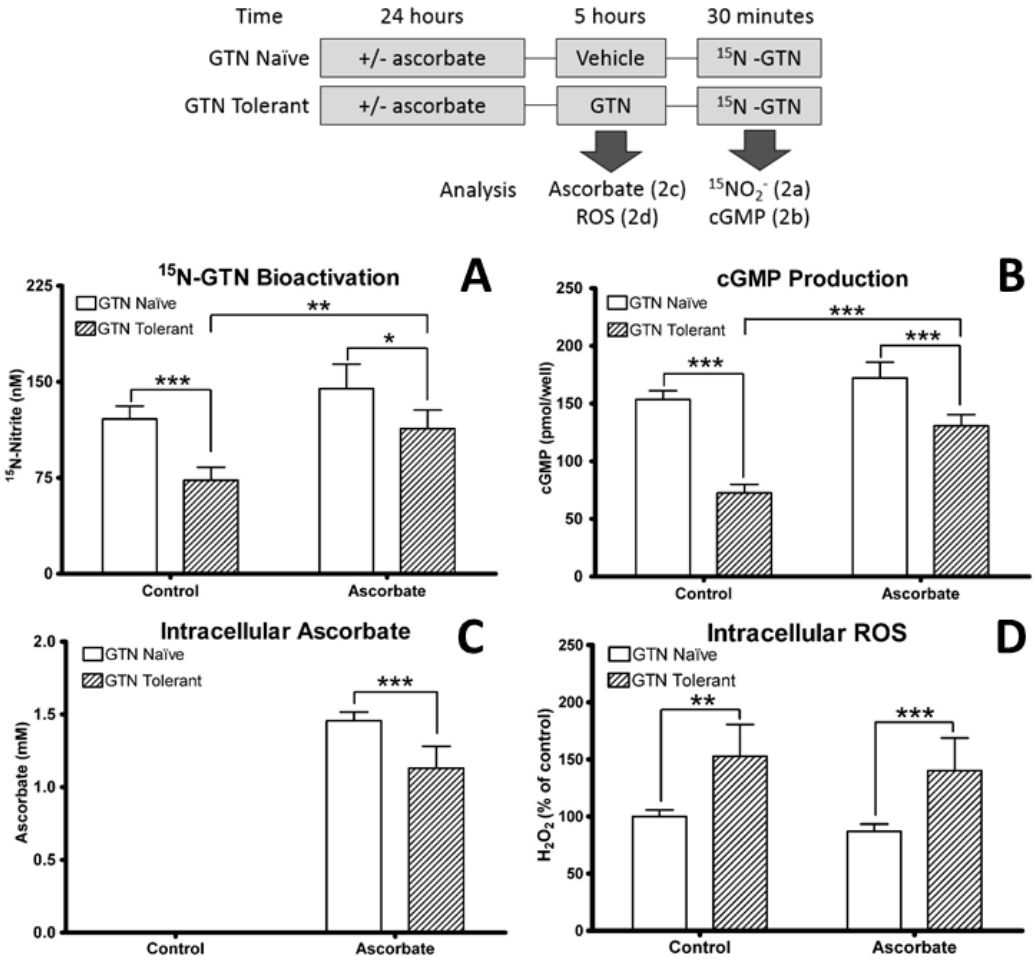

FIGURE 3.2: Nitrate tolerance in LLC-PK1 cells. Cells were pre-treated with vehicle control (GTN Naïve) or GTN (GTN Tolerant). A) Pre-treatment with GTN caused reduced metabolism of $^{15}N_3$-GTN into ^{15}N-nitrite ($p < 0.001$), which was attenuated by ascorbic acid ($p < 0.01$). B) cGMP production was reduced by GTN ($p < 0.001$), and attenuated with ascorbic acid ($p < 0.001$). C) Non-supplemented cells had no detectable ascorbic acid. Ascorbic acid-treated cells had 1.46 ± 0.03 mM intracellular ascorbic acid. GTN decreased ascorbic acid ($p < 0.001$). D) GTN increased H_2O_2 in both control ($p < 0.01$) and ascorbic acid-treated cells ($p < 0.001$). Two-way ANOVA with Bonferroni post-hoc analysis, $p < 0.05$ indicating significance (n=6/group), GraphPad Prism 4. * $p < 0.05$, ** $p < 0.01$, *** $p < 0.001$.

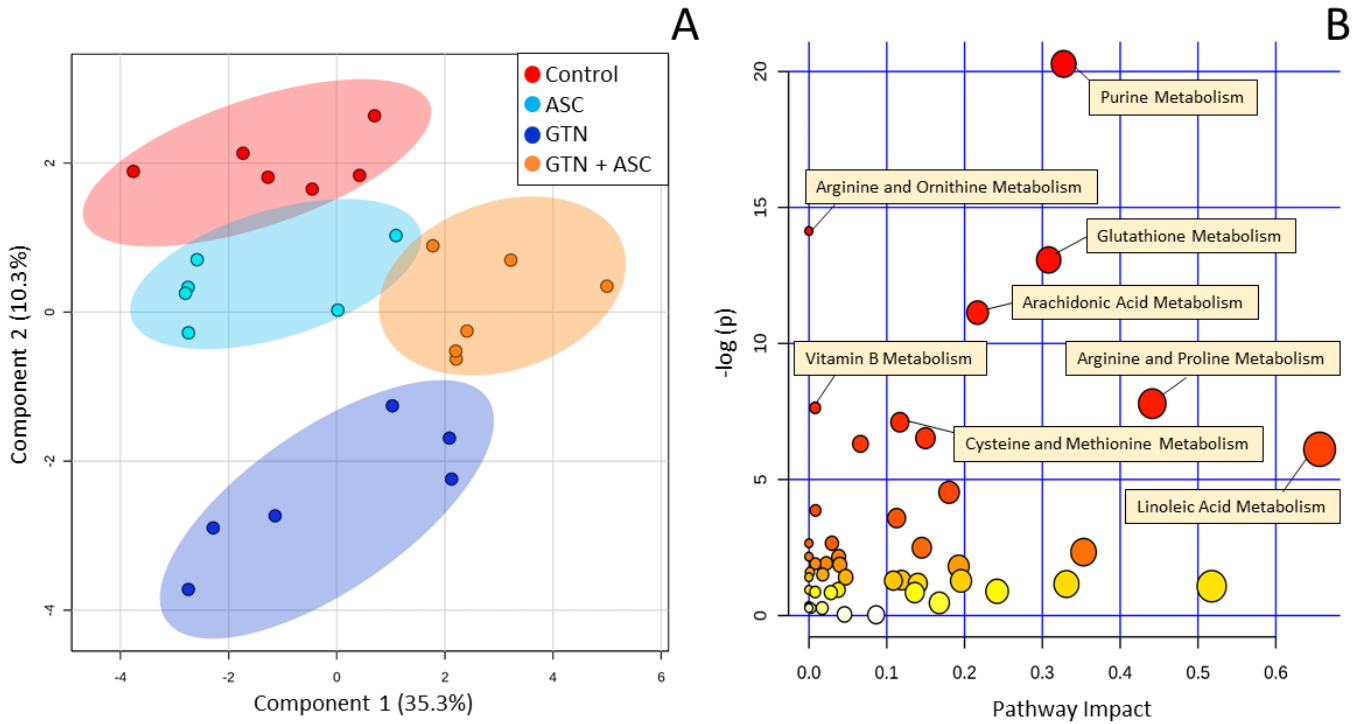

FIGURE 3.3: Multivariate analysis of nitrate tolerant LLC-PK1 cells A) Principal Component Analysis (PCA) score plot, and B) Pathway Analysis. Analyses are based on all annotated metabolites (n=6/group)(log transformation, pareto scaling) . Pathway analysis tabulated results are in SI Table 3. Plots generated with MetaboAnalyst 3.0.

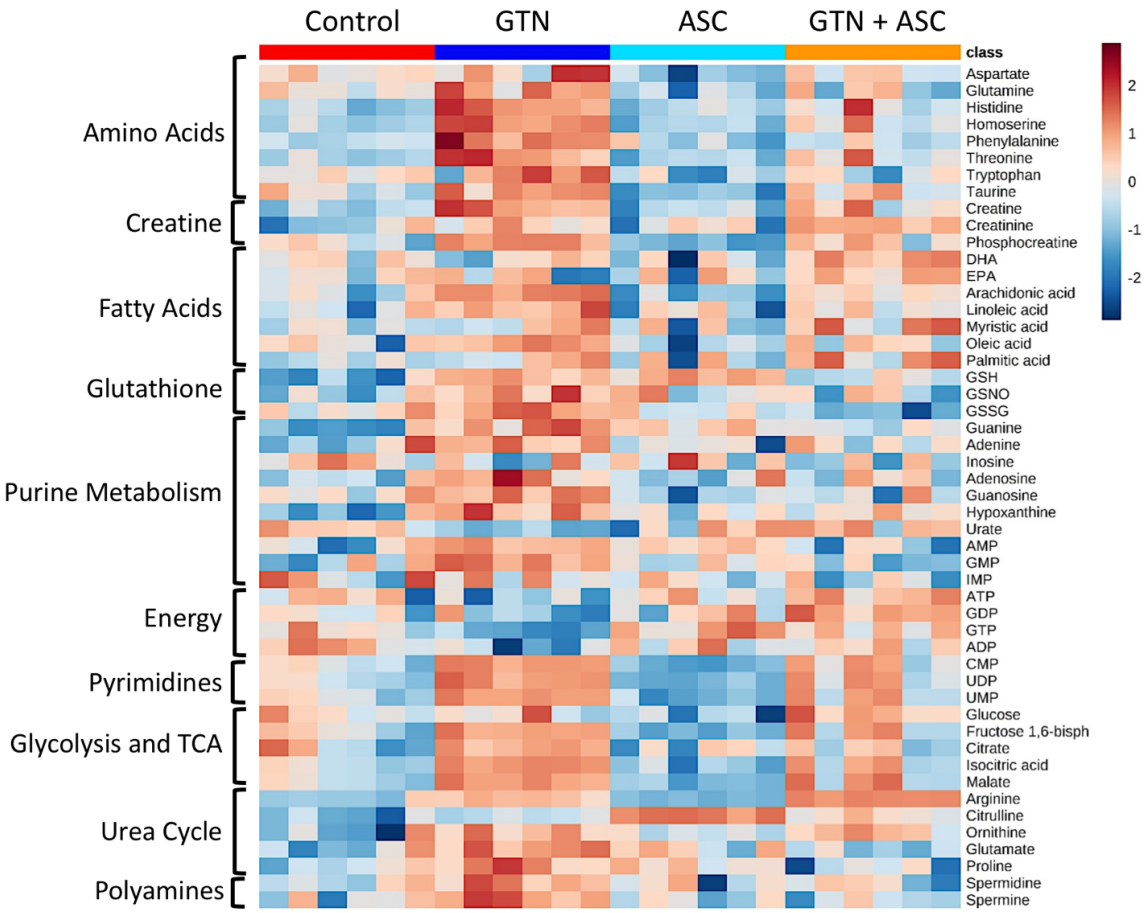

FIGURE 3.4: Heat map of metabolites in LLC-PK1 cells. The metabolites were chosen based on top p-values and physiological significance. Colors indicate z-score (standard deviation from the mean). The heat map was generated with MetaboAnalyst 3.0 using normalized data (log transformation, pareto scaling) using Euclidean distance measure (n=6/group).

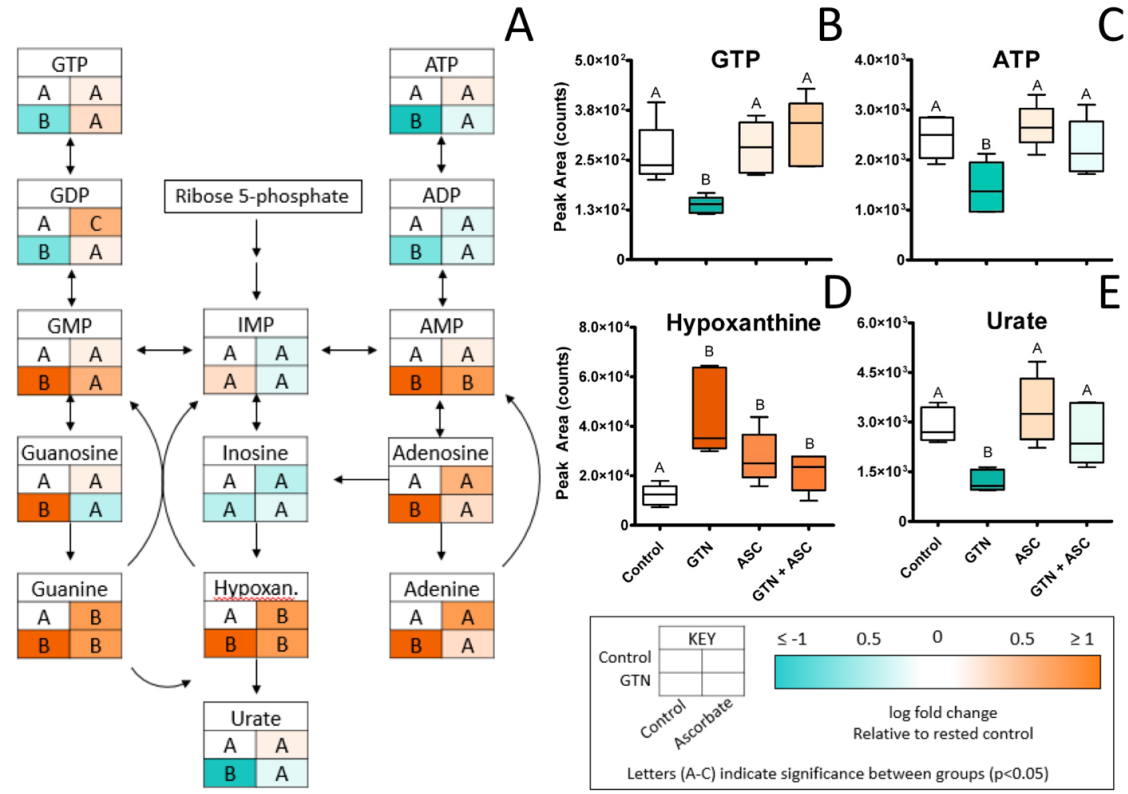

FIGURE 3.5: GTN disrupts purine metabolism. A) GTN treatment increases the purines GMP, guanosine, guanine, AMP, adenosine, and adenine yet decreases nucleotide diphosphates and triphosphates. B) GTP and C) ATP are decreased with GTN treatment, which was prevented by ascorbic acid. D) Hypoxanthine was significantly increased with GTN treatment. E) Uric acid was significantly decreased with GTN treatment, which was prevented with ascorbic acid co-treatment. Two-way ANOVA with Fisher's post-hoc analysis and FDR correction, $p < 0.05$ indicating significance (n=6/group), GraphPad Prism 4. P-values for all annotated metabolites are located in SI Table 2.

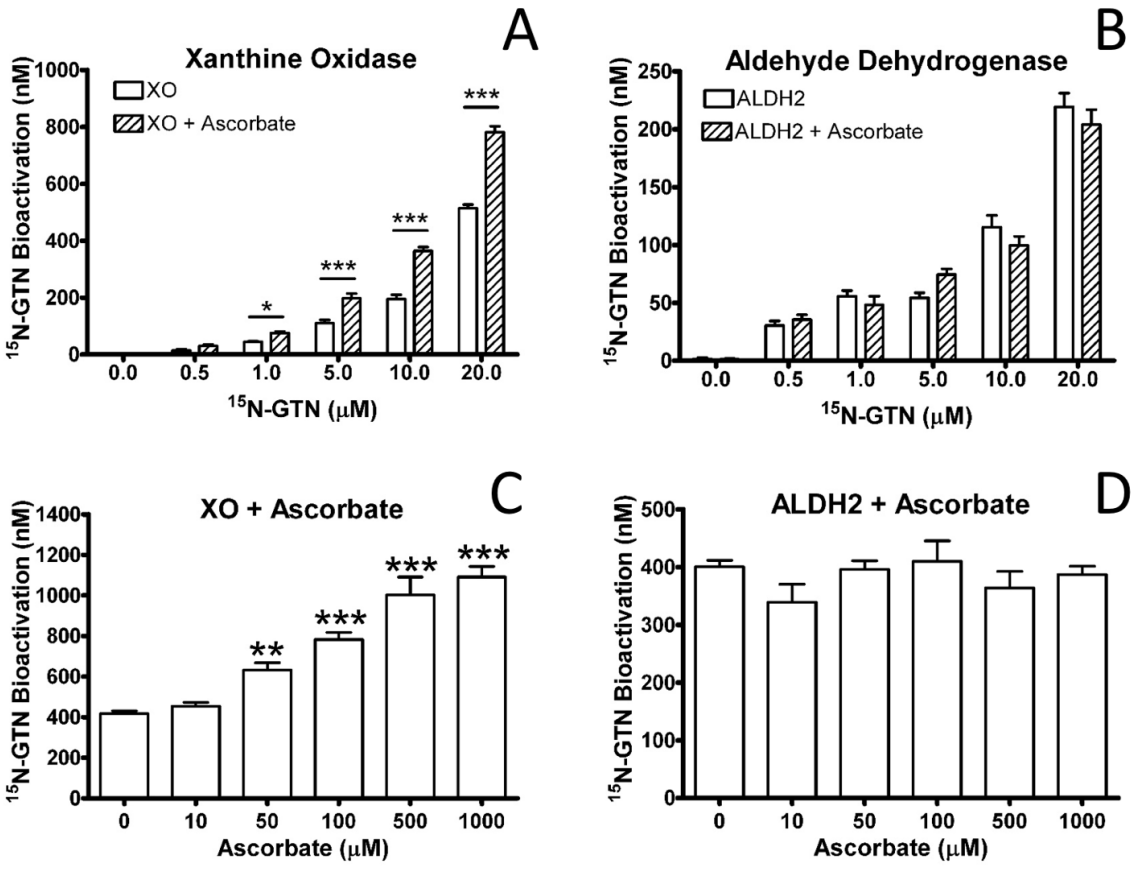

FIGURE 3.6: Xanthine oxidase (XO) and mitochondrial aldehyde dehydrogenase (ALDH2) assays. Enzymes were incubated for 30 minutes at 37°C with 100 μM xanthine (XO) or 100 μM NAD+ (ALDH2). A, B) XO and ALDH2 bioactivated $^{15}N_3$-GTN (0.5-20 μM) into ^{15}N-nitrite with a linear dose-dependent response ($R^2 > 0.99$, $p < 0.001$ with Linear Fit). 100 μM sodium ascorbate increased activity of XO, but not ALDH2. C, D) XO and ALDH2 were incubated with $^{15}N_3$-GTN (20 μM) and sodium ascorbate (10 – 1000 μM). Ascorbic acid increased GTN bioactivation by XO at all concentrations above 10 μM ($p < 0.05$), yet did not change GTN bioactivation by ALDH2 at any concentration. Two-way ANOVA with Bonferroni post-hoc analysis, $p < 0.05$ indicating significance (n=3/group), GraphPad Prism 4. * $p < 0.05$, ** $p < 0.01$, *** $p < 0.001$.

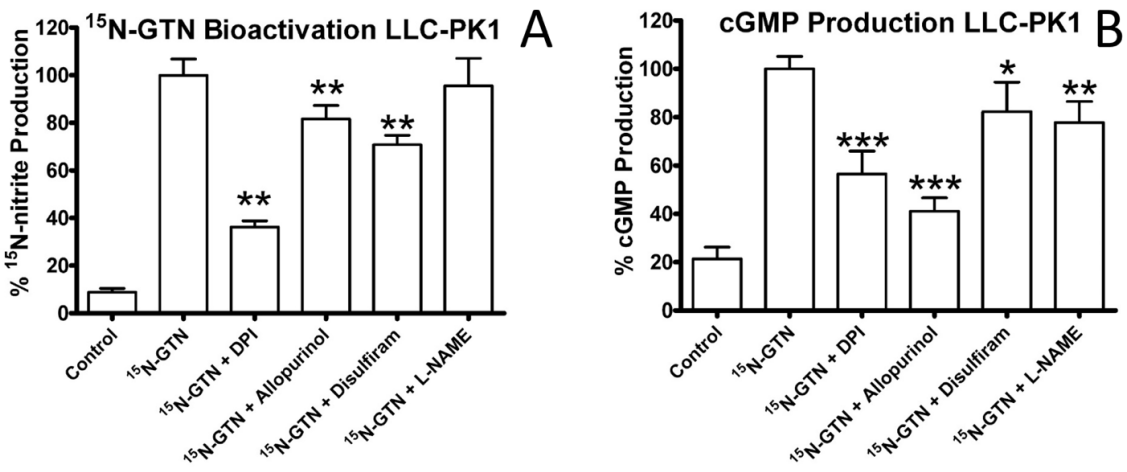

FIGURE 3.7: Inhibition of XO and ALDH2 in LLC-PK1 cells. LLC-PK1 cells were incubated with ^{15}N-GTN (1 µM) in the presence/absence of allopurinol, diphenylene iodonium (DPI), disulfiram, and L-N^{G}-Nitroarginine methyl ester (L-NAME)(100 µM). A) GTN bioactivation was inhibited by DPI ($p<0.01$), allopurinol ($p<0.01$), and disulfiram ($p<0.01$). B) cGMP production was inhibited by DPI ($p<0.001$), allopurinol ($p<0.001$), disulfiram ($p<0.05$), and L-NAME ($p<0.01$). One-way ANOVA with Bonferroni post-hoc analysis, $p<0.05$ indicating significance (n=6/group), GraphPad Prism 4. * $p < 0.05$, ** $p < 0.01$, *** $p < 0.001$.

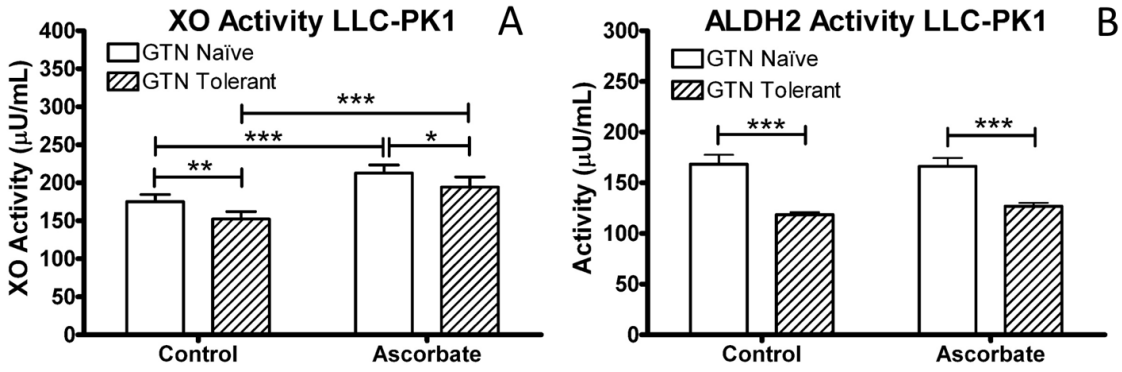

FIGURE 3.8: XO and ALDH2 activity in LLC-PK1 cells. Cells were incubated in the presence or absence of sodium ascorbate (100 μM), then treated with 1 μM GTN. Cells were analyzed for XO (xanthine conversion to H_2O_2) or ALDH2 (acetaldehyde conversion to NADH) activity. A) GTN decreased XO activity ($p < 0.05$), and ascorbic acid increased XO activity ($p < 0.001$). The GTN with ascorbic acid group had significantly higher XO activity compared to control, demonstrating that ascorbic acid prevented GTN-induced XO inactivation ($p < 0.001$). B) GTN decreased ALDH2 activity ($p < 0.001$). Ascorbic acid did not change ALDH2 activity. Two-way ANOVA with Bonferroni post-hoc analysis, $p < 0.05$ indicating significance (n=6/group), GraphPad Prism 4. * $p < 0.05$, ** $p < 0.01$, *** $p < 0.001$.

3.8. SUPPLEMENTAL INFORMATION

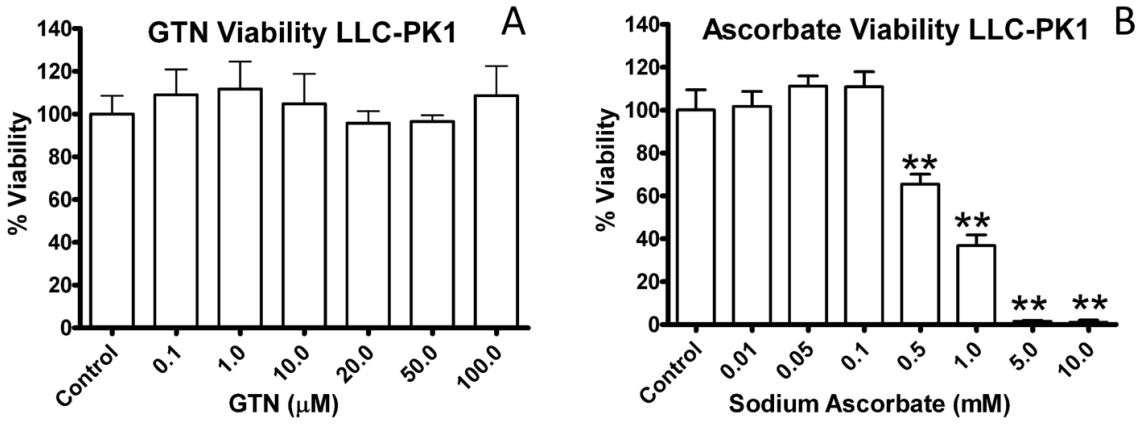

SI FIGURE 3.1: MTT Assay of LLC-PK1 cells. A) GTN did not cause any change in viability at any concentration. B) sodium ascorbate reduced cell viability 0.5 mM and higher ($P<0.01$). One-way ANOVA with Bonferroni post-hoc analysis, $P<0.05$ indicating significance (n=5/group), GraphPad Prism 4. * $p < 0.05$, ** $p < 0.01$, *** $p < 0.001$.

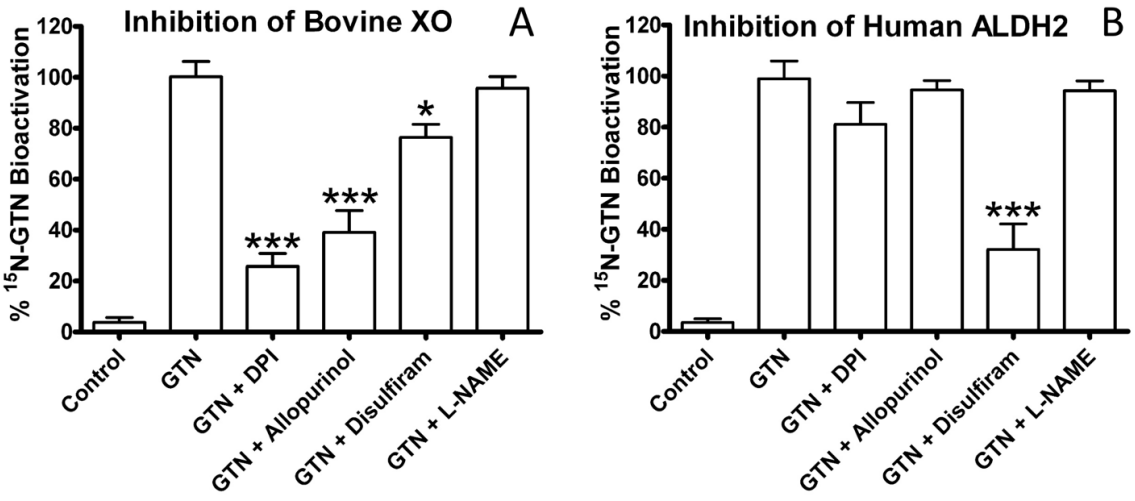

SI FIGURE 3.2: Inhibitors of bovine XO and human ALDH2. XO and ALDH2 were incubated with $^{15}N_3$-GTN (20 μM) and allopurinol, diphenylene iodonium (DPI), disulfiram, and L-N^G-nitroarginine methyl ester (L-NAME)(100 μM). XO was inhibited by DPI ($p<0.001$), allopurinol ($p<0.001$), and disulfiram ($p<0.05$). ALDH2 was inhibited by disulfiram ($p<0.001$). One-way ANOVA with Bonferroni post-hoc analysis, $p < 0.05$ indicating significance (n=3/group), GraphPad Prism 4. * $p < 0.05$, ** $p < 0.01$, *** $p < 0.001$.

SI TABLE 3.1: Annotated Metabolites in LLC-PK1 cells							
Analyte	Ion Mode	Formula	Accurate Mass (m/z)	Error (ppm)	RT (min)	MS/MS Match	Isotope Match
5-Aminopentanoate	[M+H]+	C5H11NO2	118.0857	-4.7	5.43	Yes	Yes
5'-methylthioadenosine	[M+H]+	C11H15N5O3S	298.0965	-1.0	16.32	Yes	Yes
Adenine	[M+H]+	C5H5N5	136.0619	1.4	7.79	Yes	Yes
Adenosine	[M+H]+	C10H13N5O4	268.1037	-1.3	9.28	Yes	Yes
ADP	[M+H]+	C10H15N5O10P2	428.0364	-0.6	4.86	Yes	Yes
Linoleic Acid	[M-H]-	C18H32O2	279.2334	1.6	25.67	Yes	Yes
Allantoin	[M+H]+	C4H6N4O3	159.0501	-5.3	5.05	Yes	Yes
Aminoadipate	[M+H]+	C6H11NO4	162.0756	-2.9	4.93	NA	Yes
AMP	[M+H]+	C10H14N5O7P	348.0690	-3.8	4.83	NA	Yes
Arachidonic Acid	[M-H]-	C20H32O2	303.2338	2.7	25.9	Yes	Yes
Arginine	[M+H]+	C6H14N4O2	175.1180	-5.3	4.44	Yes	Yes
Asparagine	[M+H]+	C4H8N2O3	133.0603	-3.7	4.70	NA	Yes
Aspartate	[M+H]+	C4H7NO4	134.0438	-7.3	4.57	NA	Yes
ATP	[M-H]-	C10H16N5O13P3	508.0030	0.9	5.36	Yes	Yes
Betaine	[M+H]+	C5H11NO2	118.0856	-5.6	6.50	Yes	Yes
Carnitine	[M+H]+	C7H15NO3	162.1118	-4.5	6.05	Yes	Yes
Chenodeoxycholate	[M+H]+	C24H40O4	393.2980	-5.0	26.45	Yes	Yes
Citrate	[M+H]+	C6H8O7	193.0335	-3.9	5.32	Yes	Yes
Citrulline	[M+H]+	C6H13N3O3	176.1023	-3.7	4.79	NA	Yes
CMP	[M+H]+	C9H14N3O8P	324.0598	-0.5	4.81	NA	Yes
Creatine	[M+H]+	C4H9N3O2	132.0763	-3.7	5.35	Yes	Yes
Creatinine	[M+H]+	C4H7N3O	114.0658	-3.6	5.88	NA	Yes
Desmosterol	[M+H]+	C27H44O	385.3458	-1.9	25.99	Yes	Yes
DHA	[M-H]-	C22H32O2	327.2339	2.9	26.11	Yes	Yes
Elaidic Acid	[M-H]-	C18H34O2	281.2492	2.1	25.80	Yes	Yes
EPA	[M-H]-	C20H30O2	301.2179	2.3	25.80	Yes	Yes
Erucic Acid	[M-H]-	C22H42O2	337.3108	-1.1	26.39	Yes	Yes
Fructose 1,6-BP	[M+H]+	C6H14O12P2	338.9913	2.4	7.44	Yes	Yes
GDP	[M-H]-	C10H15N5O11P2	442.0167	-0.1	4.78	NA	Yes
Gluconic Acid	[M-H]-	C6H12O7	195.0515	2.6	4.71	Yes	Yes
Glucose	[M-H]-	C6H12O6	179.0571	5.2	4.75	Yes	Yes
Glutamate	[M+H]+	C5H9NO4	148.0596	-5.3	4.68	Yes	Yes
Glutamine	[M+H]+	C5H10N2O3	147.0757	-5.2	4.66	Yes	Yes
GMP	[M+H]+	C10H14N5O8P	364.0655	0.5	5.35	NA	Yes
GSH	[M-H]-	C10H17N3O6S	306.0768	0.9	5.93	Yes	Yes
GSNO	[M-H]-	C10H16N4O7S	335.0659	-5.7	6.88	NA	Yes

GSSG	[M-H]-	C20H32N6O12S2	611.1458	1.8	5.79	Yes	Yes
GTP	[M+H]+	C10H16N5O14P3	523.9969	-1.9	5.45	Yes	Yes
Guanine	[M+H]+	C5H5N5O	150.0429	1.3	7.42	NA	Yes
Guanosine	[M+H]+	C10H13N5O5	284.0978	-3.9	7.42	NA	Yes
Histidine	[M-H]-	C6H9N3O2	154.0626	1.3	4.56	NA	Yes
Homoserine	[M+H]+	C4H9NO3	120.0650	-4.5	4.57	Yes	Yes
Hypoxanthine	[M+H]+	C5H4N4O	137.0451	-5.3	8.35	Yes	Yes
IMP	[M+H]+	C10H13N4O8P	349.0544	1.1	4.94	Yes	Yes
Inosine	[M-H]-	C10H12N4O5	267.0739	1.7	7.42	Yes	Yes
Isocitric Acid	[M+H]+	C6H8O7	193.0335	-3.9	5.32	Yes	Yes
Isoleucine	[M+H]+	C6H13NO2	132.1010	-7	6.63	Yes	Yes
Lauric acid	[M-H]-	C12H24O2	199.1710	3.2	24.61	Yes	Yes
Lauroylcarnitine	[M+H]+	C19H37NO4	344.2799	1.0	23.03	Yes	Yes
Leucine	[M+H]+	C6H13NO2	132.1010	-7	6.63	Yes	Yes
Lysine	[M+H]+	C6H14N2O2	147.1123	-3.8	4.16	Yes	Yes
Malate	[M-H]-	C4H6O5	133.0143	1.1	6.57	Yes	Yes
Methionine	[M+H]+	C5H11NO2S	150.0578	-4.3	6.14	Yes	Yes
Myristic Acid	[M-H]-	C14H28O2	227.2030	5.8	25.17	Yes	Yes
N-acetyl-L-aspartate	[M-H]-	C6H9NO5	173.0576	4.5	6.10	NA	Yes
N-acetyl-L-leucine	[M+H]+	C8H15NO3	174.1114	-6	17.23	Yes	Yes
N-acetyl-L-phenylalanine	[M+H]+	C11H13NO3	208.0961	-3.3	19.22	Yes	Yes
Nicotinamide	[M+H]+	C6H6N2O	123.0547	-4.5	10.00	NA	Yes
N-methyl-D-aspartate	[M+H]+	C5H9NO4	148.0597	-5.3	4.67	NA	Yes
N-methyl-L-glutarate	[M+H]+	C6H11NO4	162.0753	-5	5.88	NA	Yes
Norvaline	[M+H]+	C5H11NO2	118.0857	-4.8	6.49	Yes	Yes
Oleic Acid	[M+H]+	C18H34O2	283.2634	1	25.8	Yes	Yes
Ornithine	[M-H]-	C5H12N2O2	131.0831	2.4	4.80	NA	Yes
Palmitate	[M+H]+	C16H32O2	257.2468	-2.6	25.59	Yes	Yes
Pantothenic Acid	[M+H]+	C9H17NO5	220.1171	-3.7	10.58	Yes	Yes
Phenylalanine	[M+H]+	C9H11NO2	166.0855	-4.3	9.80	Yes	Yes
Phosphocholine	[M+H]+	C5H14NO4P	184.0727	-3.3	5.32	Yes	Yes
Phosphocreatine	[M+H]+	C4H10N3O5P	212.0425	-2.7	4.98	Yes	Yes
Proline	[M+H]+	C5H9NO2	116.0700	-4.8	5.40	Yes	Yes
Riboflavin	[M-H]-	C17H20N4O6	375.1288	-5.8	19.11	Yes	Yes
Ribose 5-phosphate	[M-H]-	230.01916	229.0102	-5.1	4.88	Yes	Yes
Spermidine	[M+H]+	C7H19N3	146.1646	-4.1	3.48	Yes	Yes
Spermine	[M+H]+	C10H26N4	203.2226	-2.0	3.22	Yes	Yes
Sphinganine	[M+H]+	C18H39NO2	302.3053	-0.1	23.25	Yes	Yes
Sphingomyelin	[M+H]+	C41H83N2O6P	731.6067	0.8	27.45	Yes	Yes
Succinate	[M-H]-	C4H6O3	101.0244	0.4	4.76	Yes	Yes

Taurine	[M+H]+	C2H7NO3S	126.0211	-6.3	4.57	Yes	Yes
Threonine	[M+H]+	C4H9NO3	120.0650	-4.5	4.65	Yes	Yes
Tryptophan	[M+H]+	C11H12N2O2	205.0964	-3.7	12.04	Yes	Yes
Tyrosine	[M+H]+	C9H11NO3	182.0803	-4.8	6.33	Yes	Yes
UDP	[M-H]-	C9H14N2O12P2	402.9956	1.7	41.24	Yes	Yes
UMP	[M-H]-	C9H13N2O9P	323.0295	2.9	40.52	Yes	Yes
Uracil	[M+H]+	C4H4N2O2	113.0339	-5.6	6.70	Yes	Yes
Urate	[M+H]+	C5H4N4O3	169.0351	2.3	6.82	NA	Yes
Valine	[M+H]+	C5H11NO2	118.0857	-4.7	5.43	Yes	Yes

SI Table 3.1: Table of annotated metabolites in LLC-PK1 cells. 87 metabolites were annotated. Identifiers (accurate mass, ppm error, retention time (RT), and isotope and MS/MS matching) were acquired using MasterView with the retention-time matched IROA library. NA – not acquired, or unknown. Metabolites were excluded if they did not have either MS/MS fragmentation or retention time matching.

SI TABLE 3.2: Significance of Annotated Metabolites in LLC-PK1 Cells						
Analyte	Control vs. GTN	Control vs. ASC	Control vs. GTN + ASC	ASC vs. GTN + ASC	GTN vs. GTN + ASC	ASC vs. GTN
5-Aminopentanoate	0.00713	0.26689	0.45036	0.57447	0.03341	0.27703
5'-methylthioadenosine	0.00949	0.72252	0.39114	0.36421	0.00236	0.04884
Adenine	0.00056	0.13297	0.69543	0.38171	0.00898	0.03766
Adenosine	0.00206	0.09207	0.43565	0.50795	0.03730	0.11493
ADP	0.00510	0.24025	0.32546	0.93970	0.03546	0.03941
Linoleic Acid	0.00195	0.23021	0.84111	0.18186	0.00178	0.01421
Allantoin	0.16672	0.12527	0.37776	0.40640	0.73210	0.47102
Aminoadipate	0.90174	0.64142	0.00382	0.00219	0.04038	0.63884
AMP	0.00737	0.85435	0.02824	0.04293	0.06261	0.01170
Arachidonic Acid	0.00035	0.03410	0.12640	0.00147	0.00003	0.00152
Arginine	4.79E-08	0.00662	4.06E-12	9.72E-12	0.00011	7.97E-08
Asparagine	0.38049	0.99966	0.02507	0.08099	0.13818	0.50225
Aspartate	0.21944	0.51321	0.01264	0.00852	0.36924	0.14235
ATP	0.00324	0.40088	0.34508	0.12100	0.01492	0.00253
Betaine	0.00587	0.13425	0.39462	0.28325	0.18590	0.60593
Carnitine	0.25221	0.33354	0.68062	0.25092	0.18275	0.79641
Chenodeoxycholate	0.00122	0.74851	0.07892	0.52252	0.21099	0.20575
Citrate	0.63394	0.75825	0.35616	0.47457	0.59865	0.84686
Citrulline	0.01266	0.00003	0.00120	0.00019	0.01231	0.00000
CMP	0.69336	0.56979	0.00076	0.00176	0.04810	0.46451
Creatine	0.32447	0.32791	0.35540	0.03120	0.03135	0.95823
Creatinine	0.00258	0.71462	0.56638	0.55417	0.07260	0.16198
Desmosterol	0.00110	0.51124	0.02249	0.57237	0.14794	0.27311
DHA	0.48437	0.08181	0.58223	0.03184	0.20015	0.10269
Elaidic Acid	0.49112	0.02002	0.62812	0.02159	0.29249	0.04279
EPA	0.03633	0.05971	0.80729	0.17656	0.11073	0.68438
Erucic Acid	0.68017	0.09047	0.83844	0.06721	0.54108	0.16507
Fructose 1,6-BP	0.31561	0.71450	0.00160	0.00414	0.08230	0.25413
GDP	0.00079	0.04436	0.65159	0.08237	0.01876	0.00008
Gluconic Acid	0.92835	0.17030	0.15797	0.00956	0.18477	0.14772
Glucose	0.75931	0.21242	0.09326	0.04947	0.06673	0.13034
Glutamate	0.00048	0.18316	0.91377	0.14047	0.00006	0.01560
Glutamine	0.69657	0.59991	0.02928	0.13798	0.08684	0.88270
GMP	0.00195	0.95196	0.23120	0.25869	0.00270	0.00227
GSH	0.00002	0.00708	0.00002	0.00516	0.69126	0.00571
GSNO	0.00373	0.34710	0.14107	0.67855	0.10709	0.06642

GSSG	0.00128	0.00528	0.47030	0.01887	0.00111	0.00012
GTP	0.00021	0.81260	0.14108	0.20259	0.00002	0.00011
Guanine	0.00001	0.00030	0.00001	0.04352	0.06521	0.00486
Guanosine	0.00163	0.80737	0.15780	0.43612	0.00061	0.02355
Histidine	0.39349	0.43910	0.61010	0.08983	0.08734	0.95683
Homoserine	0.38818	0.42991	0.25258	0.02138	0.04026	0.89133
Hypoxanthine	0.00009	0.00178	0.00523	0.41930	0.01542	0.06964
IMP	0.27353	0.75252	0.85845	0.82750	0.14514	0.16839
Inosine	0.03589	0.05265	0.40932	0.26939	0.21266	0.93681
Isocitric Acid	0.94576	0.47555	0.03872	0.01846	0.04368	0.53395
Isoleucine	0.15349	0.93902	0.69256	0.67892	0.12584	0.25667
Lauric acid	0.17288	0.14039	0.88241	0.06272	0.08234	0.63138
Lauroylcarnitine	0.00049	0.68868	0.38733	0.42037	0.01097	0.03450
Leucine	0.15349	0.93902	0.69256	0.67892	0.12584	0.25667
Lysine	0.74420	0.97204	0.09731	0.19176	0.30052	0.80609
Malate	0.87567	0.35555	0.01185	0.00621	0.04821	0.34401
Methionine	0.00586	0.25728	0.78903	0.26321	0.01807	0.20977
Myristic Acid	0.10752	0.06196	0.84479	0.11374	0.16875	0.60142
N-acetyl-L-aspartate	0.47514	0.99570	0.02304	0.05373	0.14187	0.55007
N-acetyl-L-leucine	0.71097	0.28301	0.28762	0.05479	0.35800	0.04931
N-acetyl-L-phenylalanine	0.30142	0.24878	0.76023	0.18942	0.21280	0.75231
Nicotinamide	0.01407	0.01564	0.00076	0.27193	0.35970	0.90129
N-methyl-D-aspartate	0.86549	0.60035	0.00470	0.00196	0.04650	0.57122
N-methyl-L-glutarate	0.90174	0.64142	0.00382	0.00219	0.04038	0.63884
Norvaline	0.15593	0.51753	0.31148	0.28325	0.18590	0.60593
Oleic Acid	0.01416	0.22068	0.63161	0.05621	0.00116	0.05759
Ornithine	0.00087	0.05005	0.00216	0.01787	0.36645	0.00454
Palmitate	0.06996	0.03478	0.80682	0.13248	0.22873	0.52001
Pantothenic Acid	0.89937	0.77709	0.12715	0.21471	0.37732	0.84594
Phenylalanine	0.94265	0.17107	0.42768	0.30835	0.37985	0.14500
Phosphocholine	0.95745	0.75757	0.00081	0.00184	0.01931	0.78530
Phosphocreatine	0.39325	0.90730	0.00036	0.00210	0.04427	0.41365
Proline	0.00155	0.01737	0.71474	0.06075	0.00767	0.12112
Riboflavin	0.08254	0.19301	0.03177	0.18976	0.70310	0.50733
Ribose 5-phosphate	0.40891	0.36305	0.30336	0.78567	0.94113	0.87172
Spermidine	0.00165	0.75862	0.90914	0.85401	0.01581	0.03507
Spermine	0.01991	0.61182	0.60495	0.98293	0.00153	0.00187
Sphinganine	0.77414	0.83676	0.33902	0.50107	0.44929	0.96769
Sphingomyelin	0.00142	0.25663	0.19602	0.87432	0.05713	0.18790
Succinate	0.22080	0.38299	0.65791	0.21751	0.11257	0.77730

Taurine	0.31351	0.80054	0.00634	0.00499	0.02479	0.19162
Threonine	0.38818	0.42991	0.25258	0.02138	0.04026	0.89133
Tryptophan	0.03478	0.56911	0.62268	0.93210	0.02718	0.03037
Tyrosine	0.70243	0.46088	0.20278	0.08393	0.10553	0.58930
UDP	0.92179	0.39485	0.00670	0.00134	0.02952	0.41272
UMP	0.72006	0.50274	0.00940	0.00436	0.03834	0.35629
Uracil	0.00396	0.85465	0.91401	0.83314	0.09017	0.18990
Urate	0.00002	0.75617	0.20985	0.39344	0.12381	0.00379
Valine	0.17752	0.49812	0.24889	0.17778	0.08213	0.64240

SI TABLE 3.2: Significance of annotated metabolites in LLC-PK1 cells. The significance of the annotated metabolites was assessed with a Two-way ANOVA with Fisher's post-hoc analysis (n=6/group). Holm's FDR-correction was performed to account for the false discovery rate. FDR-corrected P-values are listed between all groups for all annotated metabolites.

SI TABLE 3.3: Pathway Analysis Results LLC-PK1 Cells Exposed to GTN				
Pathway	Impact	p-value	Total Compounds	Hits
Purine metabolism	0.33	2.51E-09	92	15
D-Arginine and D-ornithine metabolism	0.00	7.24E-07	8	2
Glutathione metabolism	0.31	2.10E-06	38	5
Arachidonic acid metabolism	0.23	0.00021	62	3
Sphingolipid metabolism	0.15	0.00147	25	2
Linoleic acid metabolism	0.66	0.00222	15	1
Arginine and proline metabolism	0.46	0.01166	77	13
Primary bile acid biosynthesis	0.01	0.02091	47	2
Histidine metabolism	0.21	0.02752	44	3
beta-Alanine metabolism	0.07	0.03971	28	7
Pantothenate and CoA biosynthesis	0.18	0.04224	27	4

SI Table 3.3: Pathway analysis results LLC-PK1 cells exposed to GTN. 11 pathways were significantly changed (FDR-corrected p-value < 0.05) between control and GTN-treated cells (MetaboAnalyst 3.0, Pathway Analysis).

CHAPTER 4

NITRATE IMPROVES EXERCISE PERFORMANCE BY STIMULATING GLYCOLYSIS IN ZEBRAFISH (*DANIO RERIO*)

Elizabeth R. Axton*, Laura M. Beaver*, Lindsey St. Mary, Lisa Truong, Christiana Logan, Sean Spagnoli, Mary Catherine Prater, Rosa Moon Keller, Manuel Garcia-Jaramillo, Sean Newsom, Matt Robinson, Robert Tanguay, Jan F. Stevens and Norman Hord

Manuscript in preparation

4.1. ABSTRACT

Inorganic nitrate improves exercise performance by reducing the oxygen cost of exercise. Nitrate is reduced into nitrite and NO in vivo, which is favored under acidic and hypoxic conditions. Although previous research has suggested that nitrate consumption improves mitochondrial efficiency and stimulates mitochondrial biogenesis, we have an incomplete understanding of the mechanism for nitrate-induced improvement in exercise performance. We hypothesized that nitrate reduces oxygen consumption by stimulating changes in utilization of metabolic fuels for energy production. To test this hypothesis, we utilized the zebrafish (*Danio rerio)* model and treated with sodium nitrate (606.9 mg/L) or control water for 21 days. Nitrate treatment significantly increased both blood and whole-body levels of nitrate and nitrite, demonstrating that nitrate was taken up and reduced into nitrite. Nitrate reduced the oxygen cost of exercise during a vigorous 2-hour submaximal graded exercise test. There were no significant differences in mitochondrial function between control and nitrate-treated zebrafish, but nitrate treatment increased resting ADP, ATP, and cyclic AMP levels. Metabolomics analysis of whole fish illustrated that nitrate stimulated glycolysis and ketone body metabolism. Both eNOS and XOR substrate utilization were altered with both nitrate treatment and exercise. We conclude that nitrate reduces the oxygen cost of exercise by stimulating glycolysis, thereby producing more ATP while consuming less oxygen.

4.2. INTRODUCTION

Exercise performance requires substantial muscular, cardiovascular, and metabolic adaptations. Nutrition is a fundamental component of any exercise regimen because it provides the essential macronutrients (carbohydrates, protein, lipids) and micronutrients (vitamins, minerals) that are needed for optimal performance. Humans are exposed to inorganic nitrate (NO_3^-) through consumption of vegetables, most notably beets and leafy greens (45). Nitrate consumption reduces the oxygen cost of exercise and improves exercise performance in humans (62,87,170,171). These findings contradict the basic tenet of exercise that oxygen consumption during submaximal exercise is fixed, and is not altered by age, health, fitness status, nutrition, or pharmacological interventions (67). For these reasons, nitrate-containing foods and dietary supplements are increasing in popularity among both recreational and elite athletes alike (4).

The beneficial effects of nitrate are dependent on its reduction into nitrite and nitric oxide (NO)(52-54). Humans concentrate nitrate in the salivary glands, which is then reduced to nitrite by sublingual bacteria. Nitrite is swallowed and then reduced to NO and other nitrogen oxides in the acidic environment of the stomach (46,47). Nitrite acts as a bioavailable reservoir for NO, with its reduction to NO favored in acidic and hypoxic conditions (172,173). NO is a potent signaling molecule that is well-known to regulate vascular tone and blood pressure by stimulating cGMP-dependent vasodilation (1). Previous research has suggested that nitrate consumption improves mitochondrial efficiency and may stimulate mitochondrial biogenesis (84,174). 90% of total oxygen consumption comes from the mitochondrial electron transport chain, and is ultimately responsible for virtually all cellular energy production (175). This suggests that nitrate increases skeletal muscle contractile efficiency, thereby increasing the total work output while maintaining the same energy cost. We have an incomplete understanding of

how nitrate reduces the oxygen cost of exercise and improves exercise performance. We hypothesized that nitrate reduces oxygen consumption by stimulating changes in utilization of metabolic fuels for energy production.

We tested the hypothesis in zebrafish (*Danio rerio*), which is a premier model for development and toxicology (176). Zebrafish are small, complex vertebrates with rapid development and a short life cycle (177). It is estimated that 99% of embryonic-essential fish genes are homologous in humans (178,179). Zebrafish are a suitable model for exercise performance (180-182), and reduce nitrite into NO similar to humans (183). The zebrafish model allows for multiple assays to be performed in parallel, a controlled diet and environment, high statistical power, and is ideal for molecular mechanism discovery. With the understanding that adaptation to exercise requires intricate coordination of multiple organ systems, we chose a zebrafish model because their relatively small size allows for the assessment of whole-body metabolism. We treated adult zebrafish with nitrate for 21 days, then measured oxygen consumption during a vigorous 2-hour graded exercise test. As predicted, nitrate reduced oxygen consumption in zebrafish during exercise. Metabolomics analysis was performed on whole zebrafish to assess treatment-induced metabolic changes during rest or directly following exercise.

The results of this study demonstrate that changes in oxygen consumption in zebrafish were associated with differential use of fatty acids, ketones, and glycolytic intermediates. Furthermore, we demonstrate that these effects are independent of changes in mitochondrial function.

4.3. MATERIALS AND METHODS

Fish Husbandry. Wild type zebrafish (5D) were raised and maintained at the Sinnhuber Aquatic Research Laboratory (SARL) at Oregon State University on standard lab diet (Gemma Micro Skretting, Tooele, France) in accordance with protocols approved by the Oregon State University Institutional Animal Care and Use Committee (IACUC). At approximately 9 months of age, fish were transferred to clean enclosures of 3 male and 3 female fish and housed in 4 liters of water. The fish were randomized into two treatment groups of either 1) control (no treatment) or 2) sodium nitrate-exposed fish (606.9 mg $NaNO_3$/L) resulting in a total of 126 animals. The nitrate dose represents concentrations achievable by dietary means; regular consumption of high nitrate-containing vegetables, including spinach, can achieve these consumption levels. Sodium nitrate has been shown to be toxic in zebrafish at higher concentration than we propose to use here. In these studies, the concentrations we used produced no significant toxic effect (184,185).

Unless otherwise indicated, chemicals came from Sigma-Aldrich (St. Louis, MO). For stable isotope work at 18 days into the treatment a subset of the fish were switched to 100% $Na^{15}NO_3$ (Cambridge Isotope Laboratories, Tewksbury, MA) for 3 days of treatment prior to collection. To maintain low ammonia levels and consistent treatments, the fish water and treatment exposure were replaced every 36 hours throughout the duration of the experiment. The fish water consisted of reverse osmosis (RO) water with Instant Ocean® at 1.4 g of salt / gallon of water (Instant Ocean® Spectrum Brands, Blacksburg, VA) with a conductivity between 500-600 µS. Throughout treatment, the fish water was monitored for pH (6.8-7), total ammonia levels (0-2.0 ppm), and temperature (27-29 °C). Fish were fed a standard lab diet (Gemma Micro. Skretting)

at a volume of ~3% body weight/day, given over 2 feedings per day. Fish were treated for up to 28 days.

For sample collections fish were euthanized with an overdose of the anesthesia drug tricaine mesylate, and all efforts were made to minimize suffering. Fish were then dried, weighed, and measured for standard length. Fish were then snap frozen, dissected for muscle, or whole blood was collected as previously described (186).

Pathology. To examine fish for possible pathological changes associated with treatment, the fish were humanely euthanized on days 21-25, the tails were removed, and the abdominal cavity was opened with scissors to allow fixative into the body. The fish were fixed in Dietrich's solution (30% ethanol, 10% formalin, and 2% Glacial acetic acid and 58% water) at a concentration of 15 mL / fish on a rocking table for 2 weeks (187). The fish were then decalcified in Dietrich's with 5% trichloroacetic acid solution overnight with rocking. Finally, the fish were rinsed in 70% ethanol three times, and remained in ethanol for preservation as previously described(188). Fish were submitted to Oregon State University Veterinary Diagnostic Laboratory, where they were paraffin embedded, sectioned, and stained with Hematoxylin and eosin and screened for changes in pathology.

Zebrafish Free Swim Behavior. Locomotor activity was monitored in 1.8 L tanks (30 cm L × 10 cm W × 15 cm H) at 14 – 17 days of treatment. The swimming behavior was captured using Q-See cameras and Noldus (Leesburg, Virginia) Media Recorder software (189). The Noldus EthoVision software was used to analyze videos and track fish movement. After an initial 21 minute acclimation period, seven minutes of data were collected for 41-48 fish (of both genders) per treatment group. Data analyzed include the average distance, and average velocity for each fish

as calculated from the seven different 1 min time bins. A one-way ANOVA with Tukey post-tests was used to determine statistical significance ($p < 0.05$ indication significance).

Zebrafish Oxygen Consumption with Exercise. Fish were exercised in an AutoResp swim tunnel where oxygen consumption rate was measured using a Fibox fiber optic oxygen probe, and an oxy4 sensor (Loligo Systems, Denmark) as previously described with small modifications (190). Briefly six animals per group were weighed prior to the experiment and then placed in the large swim tunnel in a 2.5 L tank with an oxygen sensor connected to the AutoResp software. Oxygen consumption rate (O_2 mg/kg/hr) was measured every 10 min, consisting of a 240s flush period, in which water was renewed in the swim tunnel with a flush pump, then the pump was turned off to create a closed system during a 60s wait period, and a 300s measure period, as described in (190). The zebrafish were given a 50-min free swim at a water flow of 5 cm / sec (108 rpm) before swimming against increasing water current at speeds of 10, 20, 30, and 40 cm / sec (300-901 rpm), where each speed was held for a 20-minute duration. The fish were then returned to the 5 cm / sec current for 20 minutes, and then directly humanely euthanized and snap frozen for metabolomics analysis, or placed back in their tank for later use. The AutoResp software was used to calculate oxygen consumption rates from the slope of oxygen depletion. Five experiments were run for each treatment group both pre- and post-treatment (on days 21-25 of treatment), with all data points included in analysis having an R^2 value of 0.8 or higher (191-193). A repeat measures in time (mixed effects) ANOVA with Tukey post-hoc analysis was used to determine if there was a significant effect of treatment, and compare oxygen consumption pre- and post-treatment, respectively.

Mitochondrial analysis. For analysis of muscle mitochondria, the epaxial and hypaxial muscles were collected on days 21-25 of treatment. Tissue was dissected from the fish, weighed, placed

in ice-cold mitochondrial homogenation buffer (100 mM KCl, 50 mM Tris base, 5 mM $MgCl_2$, 1.8 mM ATP, 1 mM EDTA, pH 7.2) and promptly processed to isolate mitochondria as previously described (194). Mitochondrial oxygen and H_2O_2 fluxes were measured using the OROBOROS O2K-Fluorometer based on the Oxygraph-2k for high resolution respirometry and the O2k-Fluo LED2-Module for the detection of H2O2 by Amplex® UltraRed (195).

Protein was harvested from muscle using a hand held-pestle (Thermo Scientific, Waltham, MA, USA), and radioimmunoprecipitation assay (RIPA) protein lysis buffer (Thermo Fisher) with protease inhibitor cocktail (Thermo Scientific). Equal amounts of protein were separated on NuPage Bis-Tris SDS-PAGE gels with recommended buffers (Thermos Fisher) and blotted to a nitrocellulose membrane (BioRad). Membranes were blocked and probed for the indicated proteins using the antibodies anti- citrate synthase (ab96600), ATP5A (ab110273) and β-actin (ab8226) (Abcam, Cambridge, MA), followed by goat anti-rabbit, or goat anti-mouse secondary antibodies (Santa Cruz Biotechnology) and standard conditions. Membranes were incubated in SuperSignal West Femto Reagent (Thermo Scientific) and developed on the AlphaInnotech FluorChem 8900 system for visualization (San Jose, CA, USA). Densitometric analyses were performed on using ImageJ software (National Institute of Health, Bethesda, MD). For each membrane, the relative densitometric value of each replicate for a given probe was normalized to the corresponding relative level of the normalizing protein (β-actin).

Nitrate and nitrite quantification in water, blood, and whole zebrafish

Water and zebrafish blood. Water was collected as 1 mL samples, taken from five tanks for each treatment group. Water condition was either fresh water, taken directly following a water change, or water taken 36 hours since water change and designated as used. To assess nitrate

and nitrite content of fish water 1 mL of water was mixed with 250 µL of a stop solution (containing potassium ferricyanide, N-ethylmaleimide, NP-40) to prevent oxidation as previously described (196). Water was collected during the first week of the experiment, but was also confirmed to have similar values in an independent water collection 20 days into the experiment (data not shown). As zebrafish are small and have very little blood, the collection volumes of blood were modified to 2 µl of whole blood mixed with 18 µl ice-cold RO water for determination of nitrate blood concentrations. Likewise, to determine nitrite blood concentrations 16 µl of whole blood was mixed with 4 µl of stop solution. All samples were snap frozen and water and blood nitrate and nitrite concentrations were determined by ozone chemiluminescence using standard protocols and a Sievers Nitric Oxide Analyzer (NOA) as previously described (196).

Whole zebrafish. Whole, frozen zebrafish (n=9/group, n=54 total) were ground in liquid N_2 using a mortar and pestle. A mixture of 80:20 methanol:water at -80 °C was used as the extraction solvent (100 mg fish powder/100 µL solvent). Fish powder was homogenized with a bullet blender using zirconium oxide beads (0.5 mm diameter, ceria stabilized)(Next Advance, Averill Park, NY), Extracts were chilled at -20° C for 1 hour. The supernatant was clarified by centrifugation at 13,000 x g for 10 minutes. The supernatant was split into three 1.5 mL Eppendorf tubes: 100 µL was aliquoted for nitrate and nitrite isotope dilution analysis by mass spectrometry, 200 µL was aliquoted for metabolomics analysis, and the remainder (variable volume) was reserved. The supernatant was evaporated (FreeZone Plus 6, Labconco, Kansas City, MO).

Nitrite reacts with 2,3-diaminonaphthalene (DAN) under acidic conditions to produce 2,3-naphthotriazole (NAT). Freeze-dried zebrafish extracts were re-suspended in 250 µL MilliQ

water. Extracts were sonicated for 5 minutes, then clarified by centrifugation at 13,000 x g for 10 minutes. 100 µL (x2) of the supernatant was aliquoted into 1.5 mL Eppendorf tubes. One aliquot was reduced with nitrate reductase to convert nitrate into nitrite (152). Both aliquots were derivatized with 10 µL of 316 µM DAN (TCI Chemicals, Portland, OR) in 0.62M HCl for 60 minutes at 24°C. The reaction was quenched with 5 µL of 2.8 M NaOH. The samples were centrifuged at 13,000 x g for 1 minute, and the supernatant was removed to mass spectrometry vials (Microsolv, Eatontown, NJ). The samples were analyzed for 2,3-naphthotraizole (NAT) with the previously described method with minor modifications (152). The column was switched to a Poroshell 120 HPH-C18 (2.7 µm, 2.1 x 50 mm, Agilent, Santa Clara, CA), allowing for a reduced run time of 10 minutes.

Metabolomics Analysis

Sample preparation. Freeze-dried extracts were re-suspended in 100 µL 50:50 methanol:water at -80 °C. Extracts were sonicated for 5 minutes, then clarified by centrifugation at 13,000 x g for 10 minutes. Supernatant was transferred to glass mass spectrometry vials. LC-MS/MS based metabolomics was performed as previously described (154). High-pressure liquid chromatography (HPLC) was performed on a Shimadzu Nexera system (Shimadzu, Columbia, MD) with a phenyl-3 stationary phase column (Inertsil Phenyl-3, 4.6 x 150 mm, GL Sciences, Torrance, CA) coupled to a quadrupole time-of-flight mass spectrometer (AB SCIEX TripleTOF 5600). The flow rate was 0.4 ml/min, and mobile phases were composed of water (A) and methanol (B), both with 0.1% formic acid. All samples were analyzed in TOF scan mode in both positive and negative ion mode. MS/MS analysis (IDA and SWATH) was performed separately on quality control (QC) samples. Samples were randomized, and a pooled QC sample was analyzed every 10 samples. Auto-calibration was performed after every two samples.

Metabolomics data processing. The raw data was analyzed using PeakView with XIC Manager 1.2.0 (ABSciex, Framingham, MA) for peak picking, retention time correction, and peak alignment. Metabolite identities were assigned by matching accurate mass (error < 10 ppm), retention time (error < 10%), MS/MS fragmentation (library score > 70), and isotope distribution (error < 20%) with an in-house library consisting of IROA standards (IROA Technology, Bolton, MA) and other commercially available standards (650 total). Additional features were assigned by querying online databases (Metlin, HMDB). The peak list was exported to MultiQuant 3.0.2 to integrate chromatograms to obtain peak area for all of the assigned metabolites.

Statistical analysis of metabolomics data. Annotated metabolites were used for multivariate statistical analysis. Pathway analysis, principal component analysis (PCA), and heat map plots were generated with MetaboAnalyst 3.0 (155). The significance of individual metabolites between the treatment groups was assessed with a Two-way ANOVA followed by Fisher's post-hoc analysis and Holm FDR-correction, with a P-value of < 0.05 indicating significance (n=9/group). If needed, data were logarithmically transformed to correct for unequal variance or non-normal distribution. No outliers were excluded from the statistical analyses. Figures were generated with GraphPad Prism 4 (La Jolla, CA), PowerPoint 2016 (Microsoft, Redmond, WA), and MetaboAnalyst 3.0.

4.4. RESULTS

Adult zebrafish were treated with control water or sodium nitrate (606.9 mg/L) for a duration of 21-28 days (Figure 4.1). There were no significant differences in fish length or weight of fish treated with nitrate compared to control water (SI Figure 4.1 A-B). Pathological examination did not reveal any negative health outcomes in either control or nitrate-treated fish. Glutathione

(GSH) and oxidized glutathione (GSSG), markers of oxidative stress, were not significantly changed by the treatments (SI Figure 4.1 C-D). Together, these results demonstrate no indication of toxicity with nitrate treatment.

Nitrate and nitrite concentration in water and blood. Nitrate treatment increased nitrate concentration in the water, and there was no difference in nitrate content between fresh and used water. Nitrite concentration was negligible in water recently treated with nitrate, however nitrite increased in the 36 hours between water changes, likely due to excretion of nitrite (Figure 4.2A). A maximum of 0.5 mg nitrite/L was measured in the water, which is not predicted to have a toxic effect given that Voslarova et al. did not observe toxic effects of nitrite until 130 mg nitrite/L (185). Ammonia levels increased across 36 hours, however did not reach toxic levels (< 2.0 ppm). Control zebrafish had 227 ± 17.8 µmol/L nitrate and 4.42 ± 1.02 µmol/L nitrite in the blood. Zebrafish treated with nitrate had increased blood nitrate and nitrite at 1040 ± 169 µmol/L and 8.63 ± 1.97 µmol/L, respectively (Figure 4.2B).

Whole-body nitrate and nitrite. Nitrate and nitrite concentration in the control zebrafish was 5.06 ± 0.47 µmol/g and 0.52 ± 0.02 µmol/g ground tissue, respectively. Nitrate treatment increased whole-body nitrate concentration to 12.0 ± 0.70 µmol/g, and nitrite concentration to 1.89 ± 0.06 µmol/g (Figure 4.2C). We also assessed the proportion of the nitrate and nitrite that was derived from exogenous sources (the treatment in water) versus endogenous source (produced from NO synthase) by introducing ^{15}N-labeled nitrate for the final 3 days in a subset of fish. ^{15}N-nitrate treatment resulted in 88 ± 1.7% percent enrichment of nitrate, and 44 ± 7.8% enrichment of nitrite. The percent enrichment results demonstrate that nitrate was metabolized into nitrite, and that a significant percentage of the total nitrate and nitrite in whole zebrafish can be derived from exogenous sources (Figure 4.2D).

Exercise performance. Oxygen consumption during exercise was measured both before and after a 21-day nitrate treatment. In control zebrafish, there was not a statistically significant difference in oxygen consumption before and after treatment. Oxygen consumption during exercise was decreased with nitrate treatment ($p < 0.05$, Mixed Effects ANOVA with Tukey post-hoc analysis)(Figure 4.3A). Voluntary swimming behavior was also assessed in zebrafish. There were no statistically significant differences in the total distance or swimming velocity of zebrafish treated with nitrate as compared to the controls (Figure 4.3B). Furthermore, after exercising, whole-body nitrite was depleted in zebrafish treated with nitrate ($p < 0.01$, Two-way ANOVA with Tukey post-hoc analysis)(Figure 4.3C). There was no difference in whole-body nitrate concentration between rested and exercised zebrafish.

Mitochondria. Functional analysis was performed on mitochondria isolated from zebrafish muscle. There were no significant differences between mitochondrial function between control and nitrate-treated zebrafish (SI Figure 4.2A). There were no treatment-induced changes in mitochondrial protein content, as evidenced by Western Blot analysis of ATP synthase (ATP5A) and citrate synthase (SI Figure 4.2B). We performed global metabolomics to determine the biochemical origin of the changes in oxygen consumption with exercise.

Metabolomics Results

Overview. 10,183 unique monoisotopic features were detected in positive and negative mode combined. Of these features, 386 were significantly changed among at least one treatment group compared to the others (Two-way ANOVA with Fisher's post-hoc and Holm FDR-correction, $p < 0.05$ indicating significance, n=9/group). 192 metabolites were annotated using a combination of an in-house library and Metlin database (SI Table 4.1). FDR-corrected P-values

for all metabolites between all treatment groups are listed in SI Table 4.2 (Two-way ANOVA with Fisher's post-hoc and Holm FDR-correction, $p < 0.05$ indicating significance, n=9/group).

Pathway Analysis. Principal component analysis (PCA) demonstrates spatial clustering and separation between treatment groups. Pathway analysis was performed on log-transformed data with MetaboAnalyst using the zebrafish (*Danio rerio*) library. Tabulated pathway analysis results are listed (SI Table 4.3). The most physiologically significant pathways that were altered with nitrate treatment were metabolites associated with the tricarboxylic acid (TCA) cycle, pyruvate metabolism, glycolysis and gluconeogenesis, pentose phosphate pathway, synthesis and degradation of ketone bodies, and purine metabolism (Figure 4.4B). Significantly changed pathways between rested and exercised fish have a high similarity to those that were altered with nitrate treatment (SI Table 4.3). Here, we examine the treatment-specific changes to several metabolic pathways to elucidate the biochemical cause of the nitrate-induced decrease in oxygen consumption during exercise.

Metabolites related to NO homeostasis. Nitric oxide synthase (NOS) catalyzes the conversion of L-arginine and O_2 to L-citrulline and NO. This is the primary pathway of endogenous NO production in humans and zebrafish. L-arginine is elevated in zebrafish that are exposed to nitrate, and is also accumulated after exercise. L-citrulline is decreased in zebrafish that were treated with nitrate after exercise. Furthermore, L-arginine is metabolized into L-ornithine by arginase (ARG). L-ornithine, a member of the urea cycle, is increased with exercise and with nitrate treatment (Figure 4.5). Xanthine oxidoreductase (XOR) catalyzes the conversion of nitrate and nitrite into NO, and is involved in purine metabolism in both humans and zebrafish. At rest, hypoxanthine is accumulated in fish treated with nitrate, which is correlated to a decrease in urate production. After exercise, hypoxanthine is decreased in nitrate-treated

animals with a subsequent increase in urate production. These results demonstrate that both NOS and XOR substrate utilization are altered with both nitrate treatment and exercise.

Purine metabolism. Ribose 5-phosphate from the pentose phosphate pathway is used to generate inosine monophosphate (IMP), which can be interconverted to either guanosine monophosphate (GMP), or adenosine monophosphate (AMP). AMP is a byproduct of ATP synthesis, but can also be used to regenerate adenosine diphosphate (ADP) and adenosine triphosphate (ATP). Cyclic AMP (cAMP) is generated upon hydrolysis of ATP. ATP, ADP, and cAMP are significantly increased in rested zebrafish treated with nitrate. ATP, ADP, and cAMP are utilized with exercise in fish treated with nitrate. Most other purines (GMP, IMP, guanine, inosine, adenine, and adenosine) are not significantly changed with either exercise or nitrate treatment (Figure 4.6). cGMP was not detectable in our data set. Given that we did not measure any differences in mitochondrial function, we hypothesized that the increase in ATP levels may be due to changes in the use of metabolic fuels for ATP production.

Fuel preference caused by nitrate treatment. Glycolysis metabolizes glucose into pyruvate, while simultaneously producing ATP and NADH. Pyruvate is converted to acetyl-CoA or lactate. The pentose phosphate pathway uses glucose 6-phosphate generated by glycolysis, and converts it to ribose 5-phosphate and other pentose sugars, generating NADPH reducing equivalents. Ribose 5-phosphate is used for purine metabolism and nucleotide synthesis. Fatty acids are generated from the hydrolysis of triglycerides, which undergo multiple steps to create $FADH_2$ reducing equivalents and acetyl-CoA. Acetyl-CoA from both glycolysis and fatty acid β-oxidation enters the TCA cycle, which produces both NADH and succinate. During exercise or fasting conditions, excess acetyl-CoA can be converted to ketone bodies (acetoacetate, β-hydroxybutyrate) in the liver, which can be exported to provide energy for other organs,

including skeletal muscle. Ultimately, $FADH_2$, NADH, and succinate enter the electron transport chain, providing reducing equivalents for the production of ATP while consuming oxygen. Reducing substrates (NADH, $FADH_2$, NAPDH) and phosphocreatine were detected in the metabolomics data set, however are not presented here due to high variability.

During rested conditions, nitrate treatment increased levels of glycolytic intermediates (fructose 1,6-bisphosphate, bisphosphoglycerate, 3-phosphoglycerate, phosphoenolpyruvate, pyruvate), TCA cycle intermediates (citrate, succinate, fumarate, malate, oxaloacetate), lactate, and ketone bodies (acetoacetate, β-hydroxybutyrate)(Figure 4.7). There was no difference in glucose levels with any treatment. In the pentose phosphate pathway, 6-phosphogluconolactone is increased with nitrate, yet there was no difference in ribose 5-phosphate generated. The increase in glycolytic and TCA cycle intermediates and ketone bodies correlates to the higher levels of ADP and ATP found with nitrate treatment (Figure 4.6).

After exercise, control zebrafish had several increased glycolytic intermediates (fructose 1,6-bisphosphate, phosphoenolpyruvate), TCA cycle intermediates (citrate, succinate, fumarate, malate, oxaloacetate), and ketone bodies (acetoacetate, β-hydroxybutyrate)(Figure 4.7). Fish that were treated with nitrate had depleted glycolytic and TCA cycle intermediates, compared to their rested counterparts. Notably, glucose was not depleted with exercise. These results demonstrate that although nitrate increases resting levels of glycolytic and TCA cycle intermediates, these metabolites are generally utilized during exercise and used to produce reducing equivalents for ATP production.

Fatty acids and acyl carnitines. Lipolysis is stimulated by exercise, resulting in increased fatty acid levels. Fatty acids are bound to coenzyme A (CoA), and transported into the mitochondrial

matrix by carnitine palmitoyltransferase 1 (CPT1) by forming acyl carnitines. The resulting acyl-CoA undergo β-oxidation, producing $FADH_2$, NADH and acetyl-CoA. Exercise increased both fatty acids and acyl carnitines, which was stimulated in nitrate-treated zebrafish (Figures 4.8 and 4.9). The increase in fatty acids and acyl carnitines correlated to an increase in acetyl-CoA with nitrate treatment following exercise.

4.5. DISCUSSION

We demonstrate here that nitrate treatment reduces the oxygen cost of exercise in zebrafish. Importantly, we did not detect any changes in intrinsic characteristics of the mitochondria, and nitrate treatment did not stimulate an increase in the number of mitochondria in the muscle. Here, we explore the metabolomics results to elucidate a biochemical mechanism for the nitrate-induced changes in oxygen consumption during exercise.

We measured significant changes in metabolites related to NO production by both NOS and XOR. These results suggest that NO homeostasis is altered during exercise. Exercise stimulates NO production (197-199), partially through increased eNOS expression and activity (197,200). XOR, an enzyme that reduces nitrite to NO, has increased activity and expression after strenuous exercise in humans (201). In addition to changes in metabolites related to XOR and eNOS metabolism, we found depleted nitrite levels following exercise. We hypothesize that increased XOR activity with exercise caused increased metabolism of nitrite into NO. Our results, among results from other researchers, suggest that nitrate and nitrite act as a reservoir for NO that is utilized during exercise (202,203).

At rest, nitrate-treated zebrafish had increased glycolytic and TCA cycle intermediates, correlating to an increase in ATP production. Glucose transport across cell membranes by GLUT-

4 is an important regulatory step for glucose utilization in skeletal muscle, heart, and adipose tissue. NO donors facilitate glucose transport in skeletal muscle via GLUT-4 (200,204,205), and by inducing vasodilation and blood flow to increase the delivery of glucose to the muscle (206,207). Importantly, NO has previously been shown to increase glycolysis in response to NO-induced inhibition of mitochondrial respiration (208), mediated by cGMP and AMP-activated protein kinase (AMPK)(209-211). After exercise, nitrate-treated zebrafish have decreased glycolytic and TCA cycle intermediates, compared to their rested counterparts. Although low levels of nitrate over a 3-week exposure resulted in higher resting glycolytic and TCA cycle intermediates, the increased energy demand during a 2-hour bout of exercise was associated with utilization of these energy stores. Interestingly, despite the decrease in glycolytic intermediates, there was no change in glucose levels.

During exercise, fatty acids and acyl carnitine levels rise. We demonstrate that nitrate stimulates fatty acid oxidation with exercise, which has previously been demonstrated in skeletal muscle (212,213). The excess acetyl-CoA is shunted towards the production of ketone bodies (acetoacetate and β-hydroxybutyrate). Ketone bodies were high in nitrate-treated fish during rest and after exercise, whereas control fish only had increased ketone bodies after exercise. We demonstrate here that nitrate has a ketogenic effect: the increased ketones bodies can be utilized in extrahepatic organs for energy production, sparing whole-body glucose levels (214,215). This increase in ketone body metabolism partially substitutes glycolysis, thereby maintaining glucose levels. Furthermore, administration of ketone bodies stimulates NO production (216), suggesting a positive feedback loop.

Finally, we observe that the effects of nitrate approximate that of an exercise mimetic. Nitrate has previously been demonstrated to mimic exercise by stimulating PGC1a-induced fiber-type

transformation, altering the ratio of glycolytic and oxidative type fibers (217). Our metabolomics analysis revealed striking similarity between the metabolic profile after exercise, compared to a 3-week treatment with nitrate. This is evidenced by the similarity in the pathways that were altered with nitrate treatment and with exercise (SI Table 4.3). Notably, we observed that although ketone bodies are usually produced under fasting or exercise conditions, they are increased with nitrate treatment. This pattern is also observed throughout glycolysis and the TCA cycle. This suggests that despite not having increased swimming activity in the weeks leading up to the oxygen consumption assay, zebrafish have physiological and metabolic adaptations that increase exercise performance.

4.6. CONCLUSION

The strength of this metabolomics analysis is that we measured the whole-body metabolic outcome of the diverse mechanisms of nitrate. Instead of focusing on a single target or organ system, we have a snapshot of how nitrate alters whole-body energy metabolism. However, this approach limits the possibility organ-specific interpretations. In addition, our treatments were delivered in the water, as compared to the diet. Given these considerations, we demonstrate that nitrate treatment stimulates both glycolysis and ketogenesis in zebrafish, independently of changes in mitochondrial function or protein content. Increased flux through glycolysis will result in more ATP production while consuming less oxygen. We conclude that alterations in the relative contribution of metabolic fuels for ATP production is responsible for the decrease in oxygen consumption during exercise. Importantly, we demonstrate that because of the cooperation of increased glycolysis and ketone body metabolism, measuring glucose and lactate as single endpoints of energy metabolism is not sufficient.

4.7. ACKNOWLEDGMENTS

The authors would like to acknowledge the Sinhuber Aquatic Research Laboratory (SARL)(Carrie L. Barton, Abraham Garcia, Eric Johnson, Kim Hayward), Oregon State University (OSU) Mass Spectrometry Center (Claudia Maier, Jeffrey Morre), The Linus Pauling Institute Oxidative and Nitrative Stress Lab (ONSL)(Jaewoo Choi). We acknowledge the Celia Strickland and G. Kenneth Austin III Endowment, the Linus Pauling Institute, and the College of Pharmacy for funding.

4.8. FIGURES

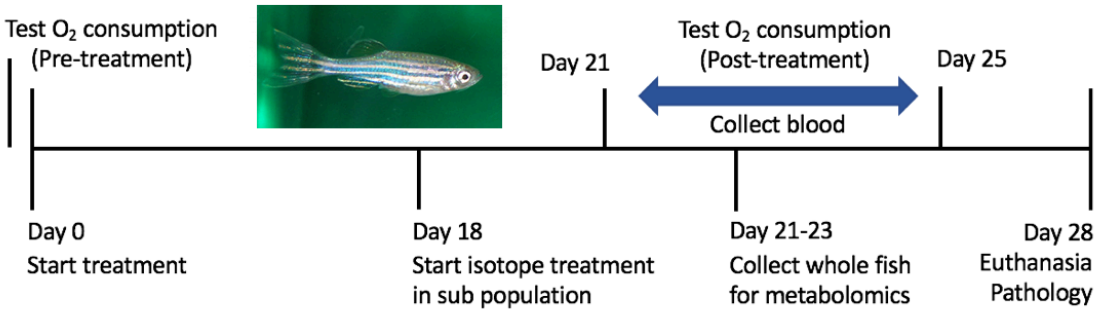

FIGURE 4.1: Zebrafish study design. Adult zebrafish were treated with control water or sodium nitrate for a duration of 21-28 days (n=126 total). A subset of the zebrafish were switched to ^{15}N-nitrate for the final 3 days of the treatment. Water and zebrafish (blood and whole-body) were collected for determination of nitrate and nitrite concentration. Oxygen consumption during an exercise test was assessed before and after treatment, and whole fish were collected for metabolomics analysis. At the study termination (28 days) all remaining zebrafish were euthanized, with a subset sent for pathological examination.

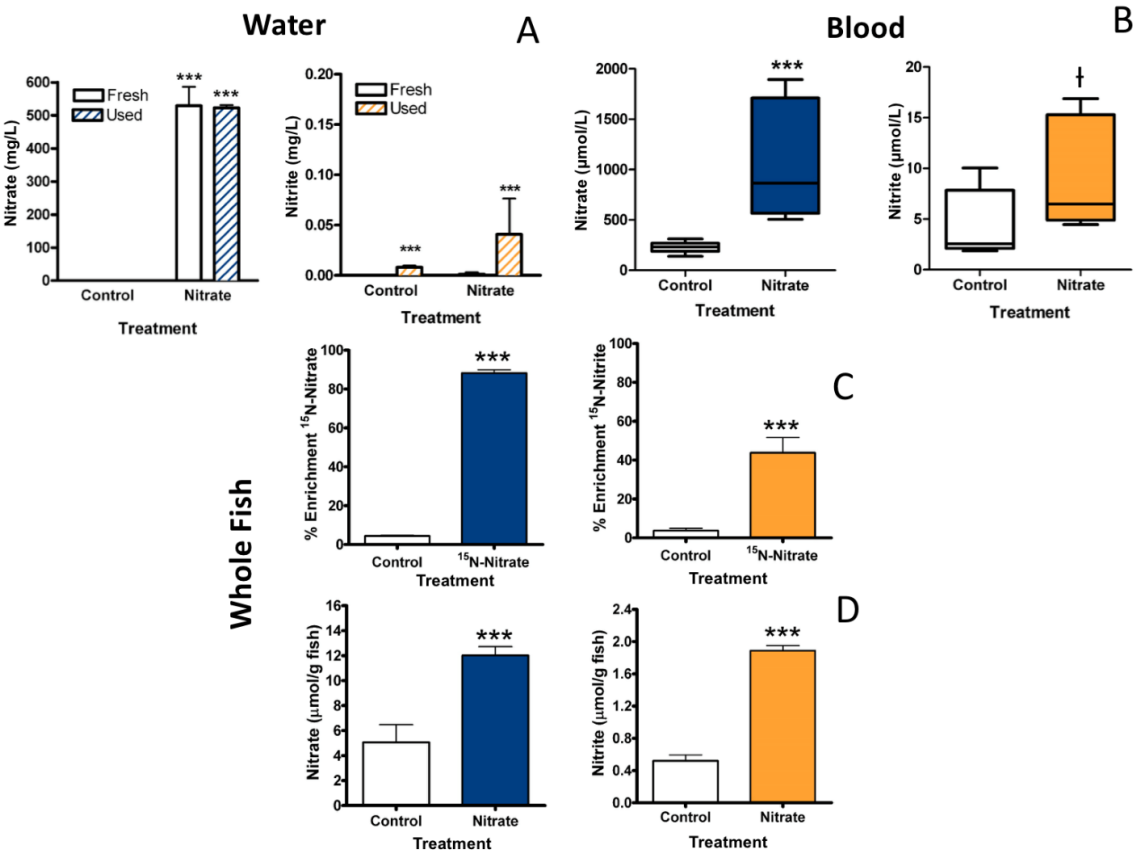

FIGURE 4.2: Water, blood and whole-body nitrate and nitrite concentrations. Nitrate and nitrite concentration in the water (Two-way ANOVA with Tukey post-hoc analysis, $p < 0.05$ indicating significance, n=5/group)(A). Nitrate and nitrite concentration in the blood (n=7-10) (B) and in the whole fish (n=9)(C). Isotope enrichment of nitrate and nitrite in fish treated with 100 % ^{15}N-nitrate (n=9) (D). Student's t-test with $p < 0.05$ indicating significance. Statistics are figures were generated with GraphPad Prism 4. * $p < 0.05$, ** $p < 0.01$, *** $p < 0.001$.

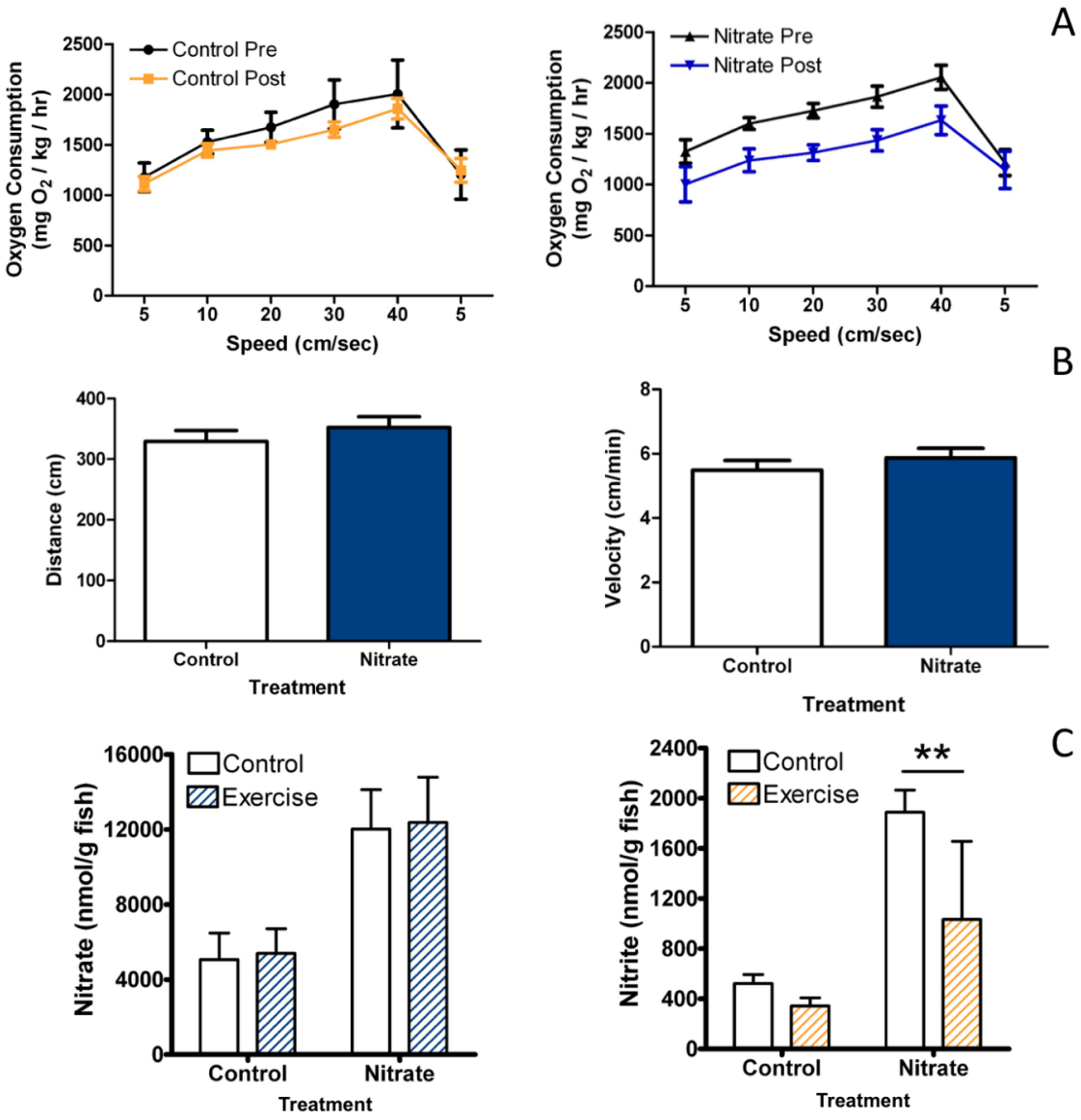

FIGURE 4.3: Swim performance, oxygen consumption and whole-body nitrate and nitrite concentrations after exercise. Zebrafish were subjected to a 2-hour graded swim test before and after treatment. Control fish did not have a difference in oxygen consumption, whereas nitrate-treated fish had reduced oxygen consumption after the 3-week treatment (Mixed effects ANOVA with Tukey post-hoc analysis, $p < 0.05$ indicating significance, n=5/group)(A). Voluntary swimming behavior (distance, velocity) was not changed with nitrate treatment (Student's t-test with $p < 0.05$ indicating significance, n=41-48/group)(B). Whole-body nitrite was decreased after exercise in nitrate-treated fish ($p < 0.01$), whereas there was no change in whole-body nitrate with exercise (Two-way ANOVA with Tukey post-hoc analysis, $p < 0.05$ indicating significance, n=9/group)(C). Statistics and figures were generated with GraphPad Prism 4. * $p < 0.05$, ** $p < 0.01$, *** $p < 0.001$.

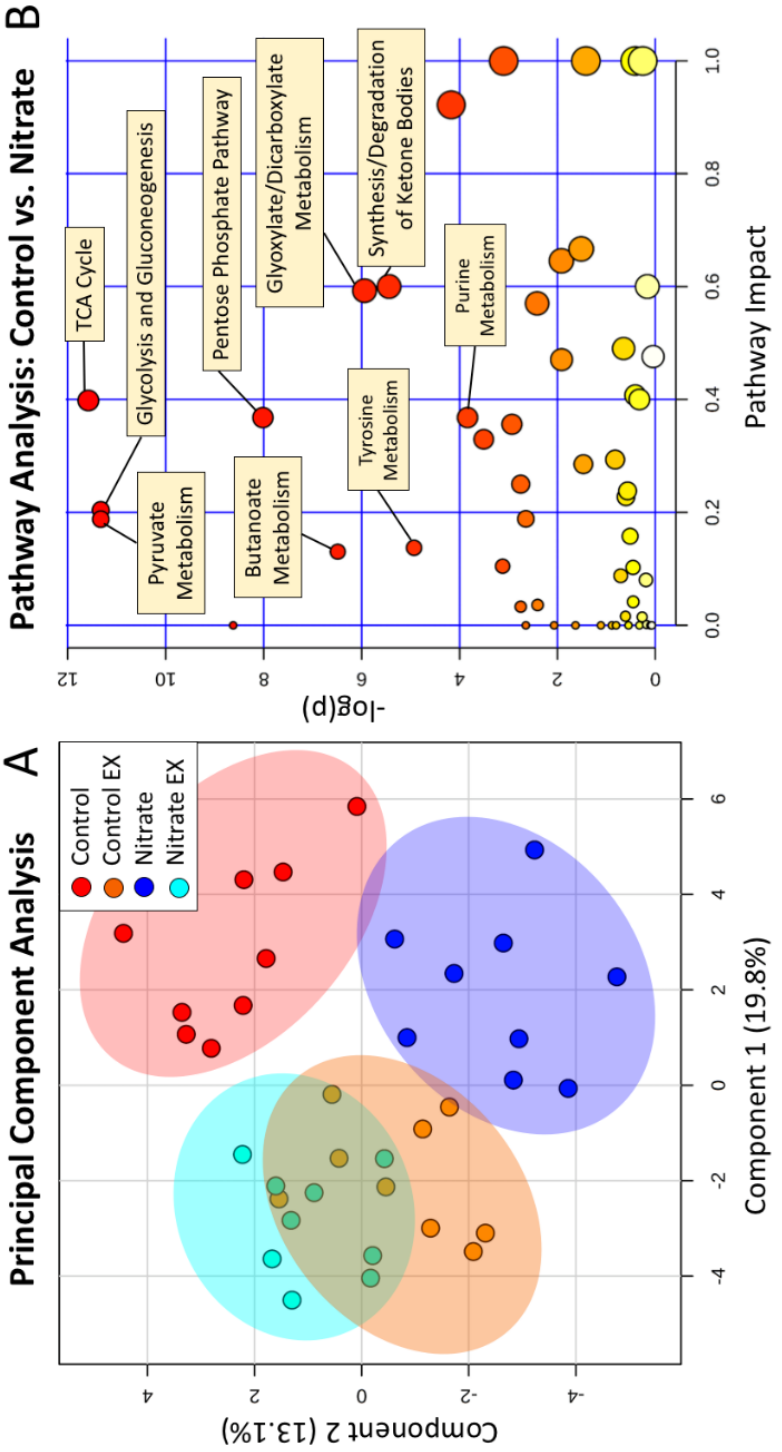

FIGURE 4.4: Metabolomics pathway analysis in zebrafish. Principal component analysis (PCA) of all treatment groups (A). Pathway analysis comparing control and nitrate treatment groups (B). Figure were generated with MetaboAnalyst 3.0 using log-transformed peak intensities of all annotated metabolites detected in positive and negative ion mode (n=9/group).

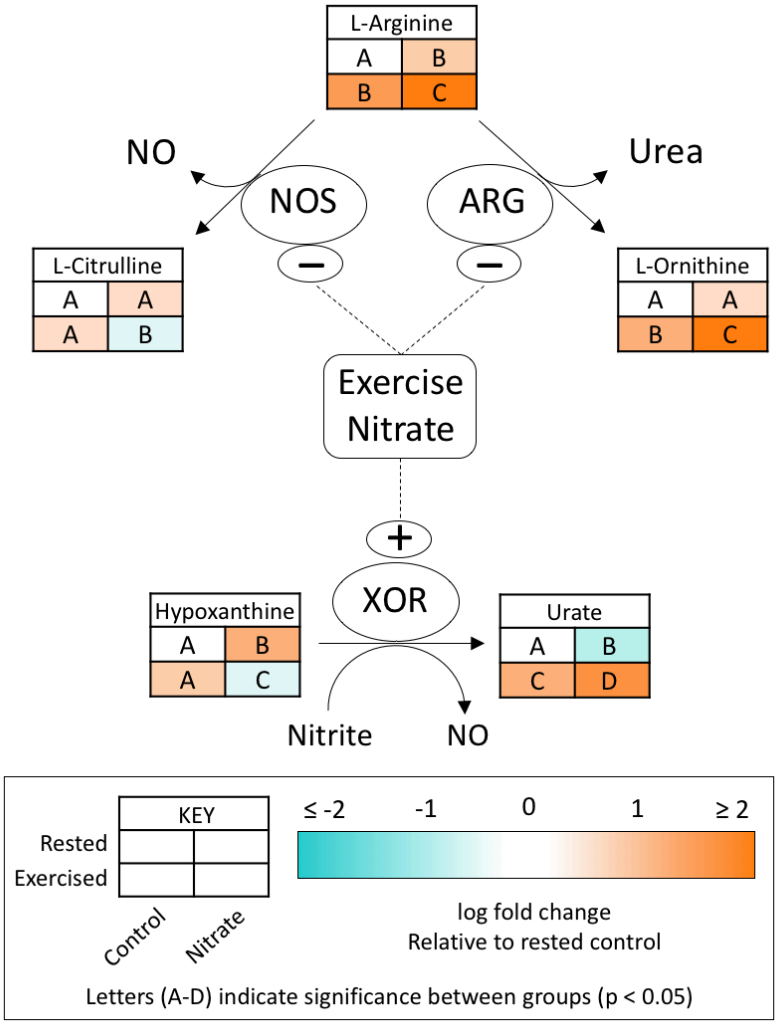

FIGURE 4.5: Metabolites related to NO homeostasis in zebrafish. Relative levels of metabolites metabolized by nitric oxide synthase (NOS), arginase (ARG) and xanthine oxidoreductase (XOR). Color is based upon log-fold change values, compared to the rested control. Log-fold change and p-values between all groups were generated with MetaboAnalyst 3.0 (Two-way ANOVA with Fisher's post-hoc and Holm FDR-correction, $p < 0.05$ indicating significance, n=9/group).

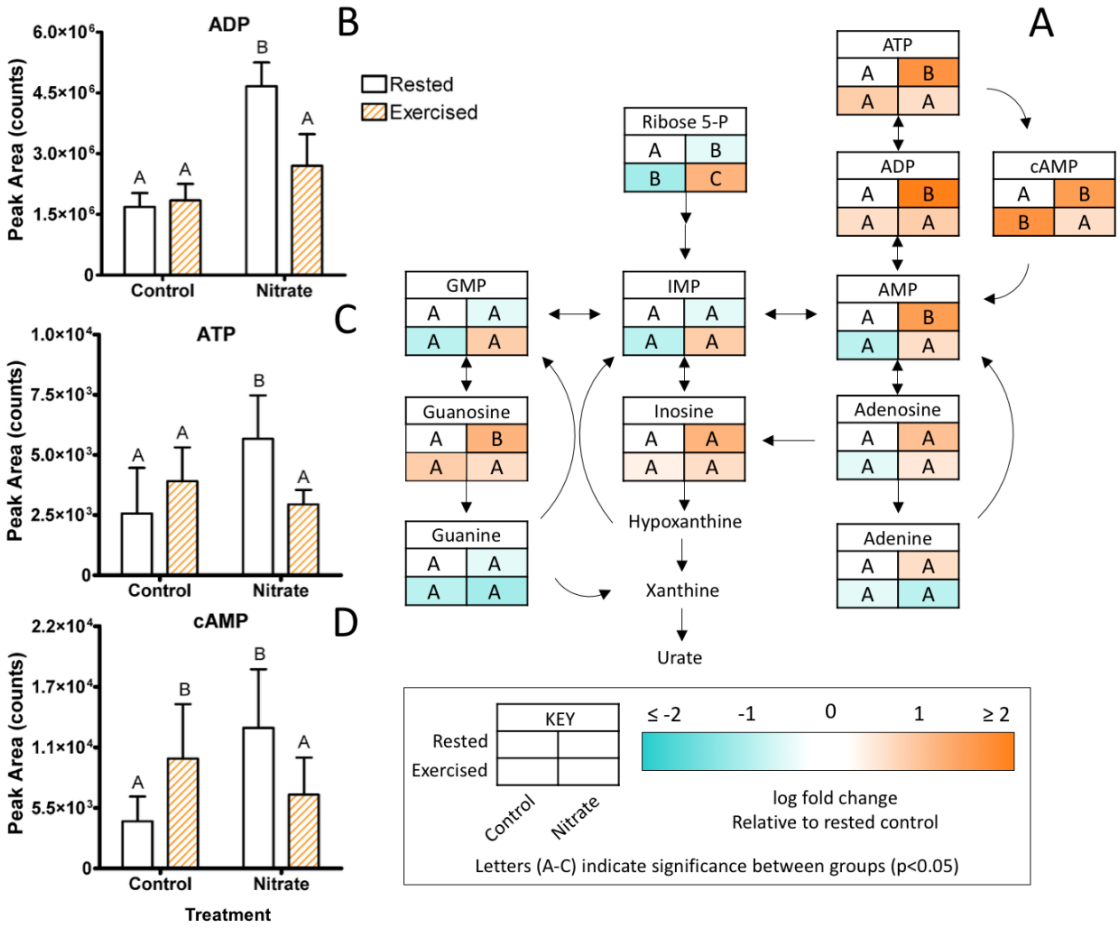

FIGURE 4.6: Purine metabolism in zebrafish. Relative levels of metabolites involved in purine metabolism and nucleotide synthesis are altered by nitrate (A). Adenosine triphosphate (ATP)(B), adenosine diphosphate (ADP)(C), and cyclic adenosine monophosphate (cAMP)(D) are increased with nitrate treatment. Color is based upon log-fold change values, compared to the rested control. Log-fold change and p-values between all groups were generated with MetaboAnalyst 3.0 (Two-way ANOVA with Fisher's post-hoc and Holm FDR-correction, $p < 0.05$ indicating significance, n=9/group). Bar graphs were generated with GraphPad Prism 4.

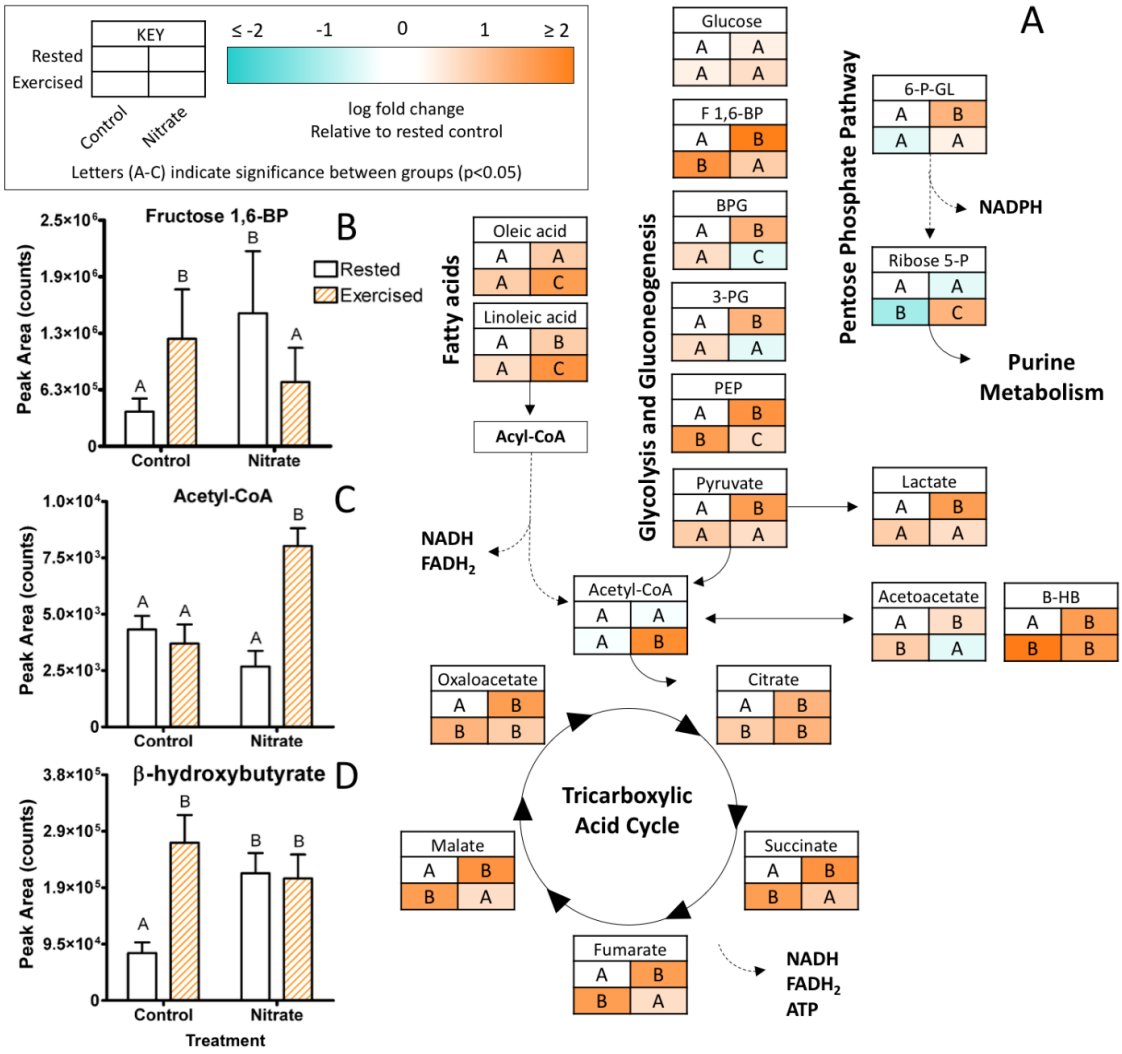

FIGURE 4.7: Energy substrate utilization in zebrafish. Glycolysis, the TCA cycle, the pentose phosphate pathway, fatty acids, and ketone bodies are altered with nitrate treatment or exercise (A). Representative bar graphs demonstrate relative levels of fructose 1,6-bisphosphate (B), acetyl-CoA (C), and β-hydroxybutyrate (D). Color is based upon log-fold change values, compared to the rested control. Log-fold change and p-values between all groups were generated with MetaboAnalyst 3.0 (Two-way ANOVA with Fisher's post-hoc and Holm FDR-correction, $p < 0.05$ indicating significance, n=9/group). Bar graphs were generated with GraphPad Prism 4.

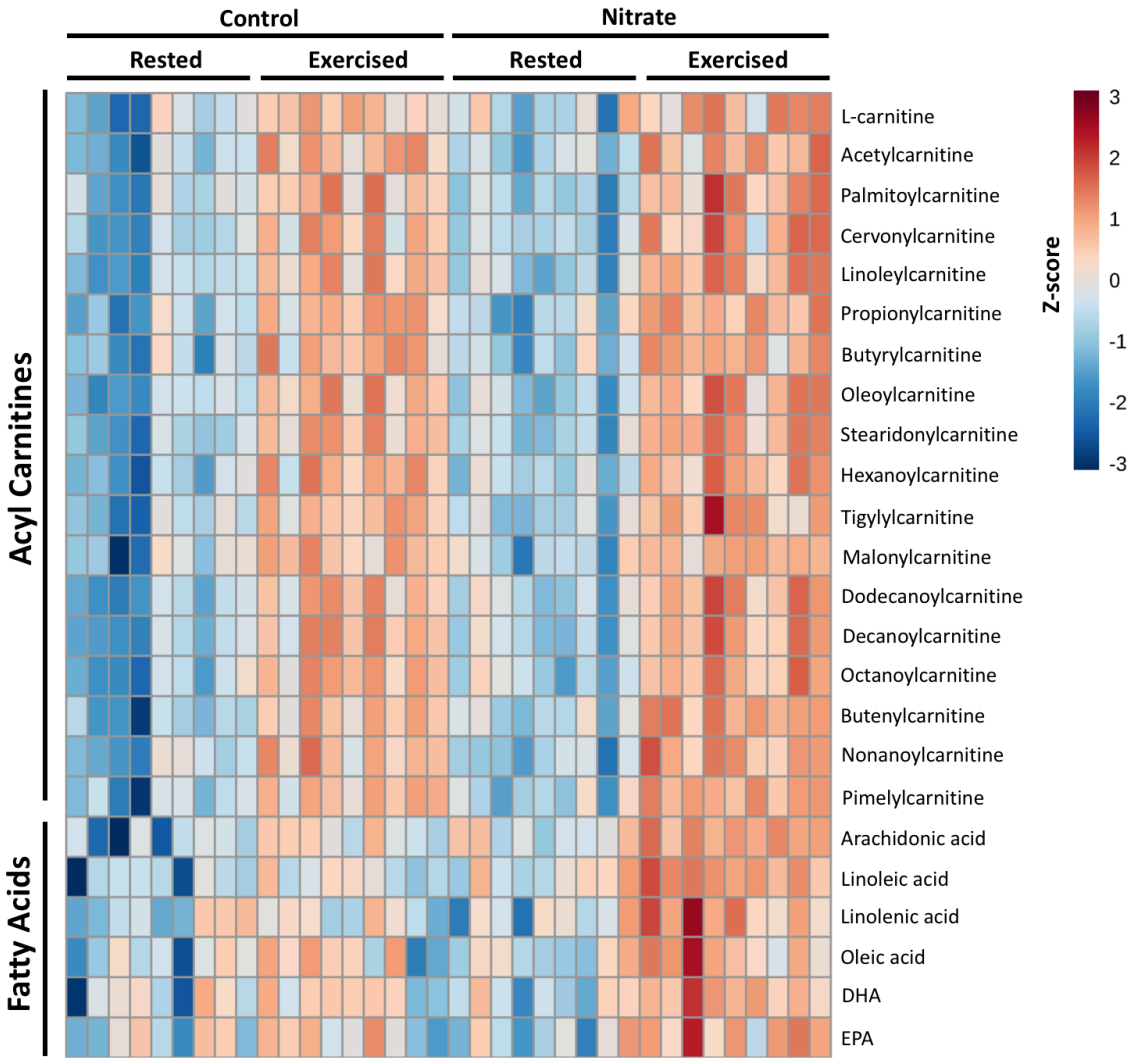

FIGURE 4.8: Heatmap of Fatty acids and acyl carnitines in zebrafish. Heat map was generated with all detected acyl carnitines and fatty acids using MetaboAnalyst 3.0 on log-transformed peak intensities, using Euclidian distance measure, autoscale features, and no clustering algorithms (n=9/group). Color is based upon z-score (distance from the mean).

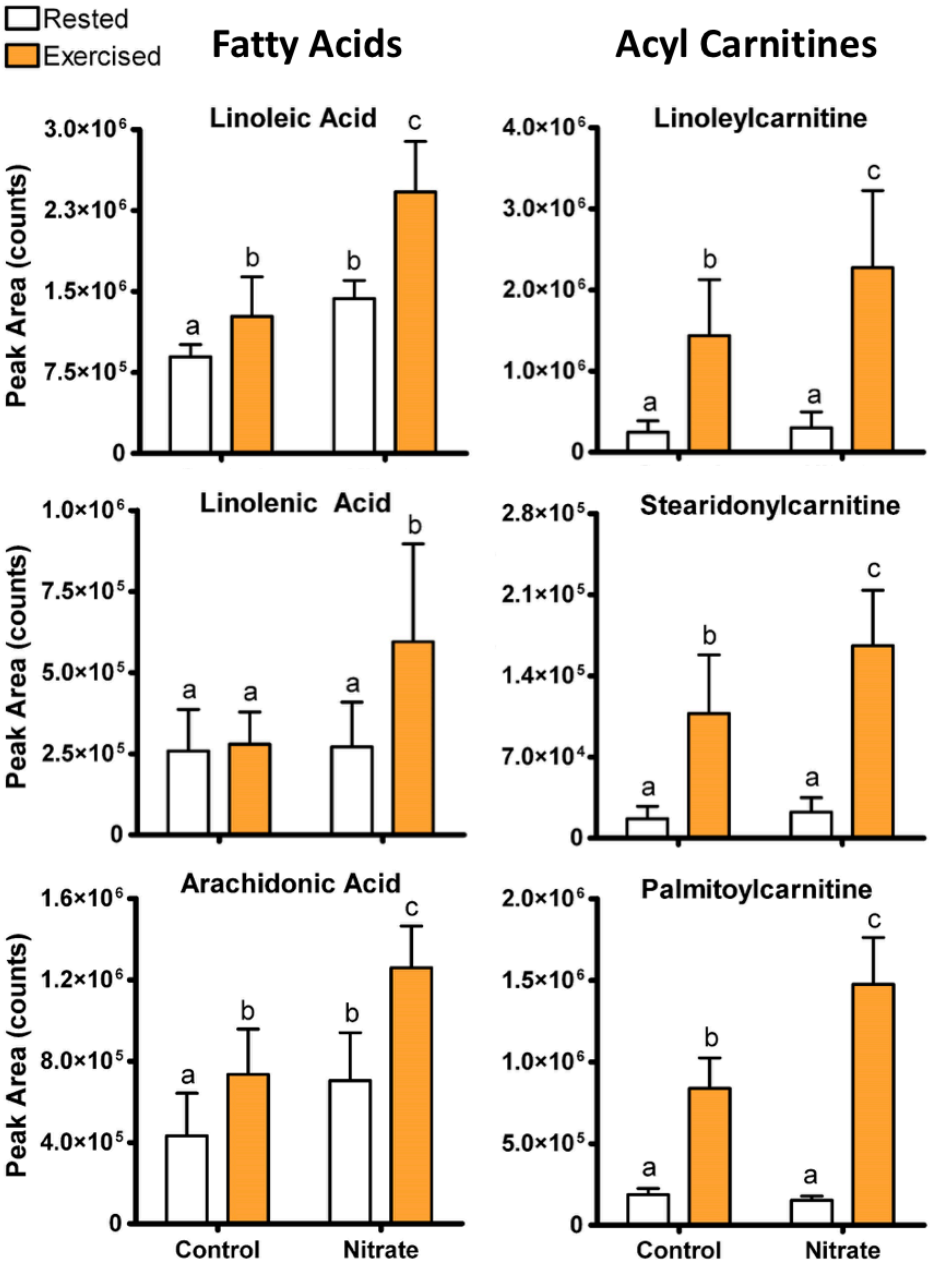

FIGURE 4.9: Fatty acids and acyl carnitine bar plots. Representative fatty acids and acyl carnitines in zebrafish are shown. Two-way ANOVA with Fisher's post-hoc and Holm FDR-correction, $p < 0.05$ indicating significance, n=9/group. Figures generated with GraphPad Prism 4.

4.9. SUPPLEMENTAL INFORMATION

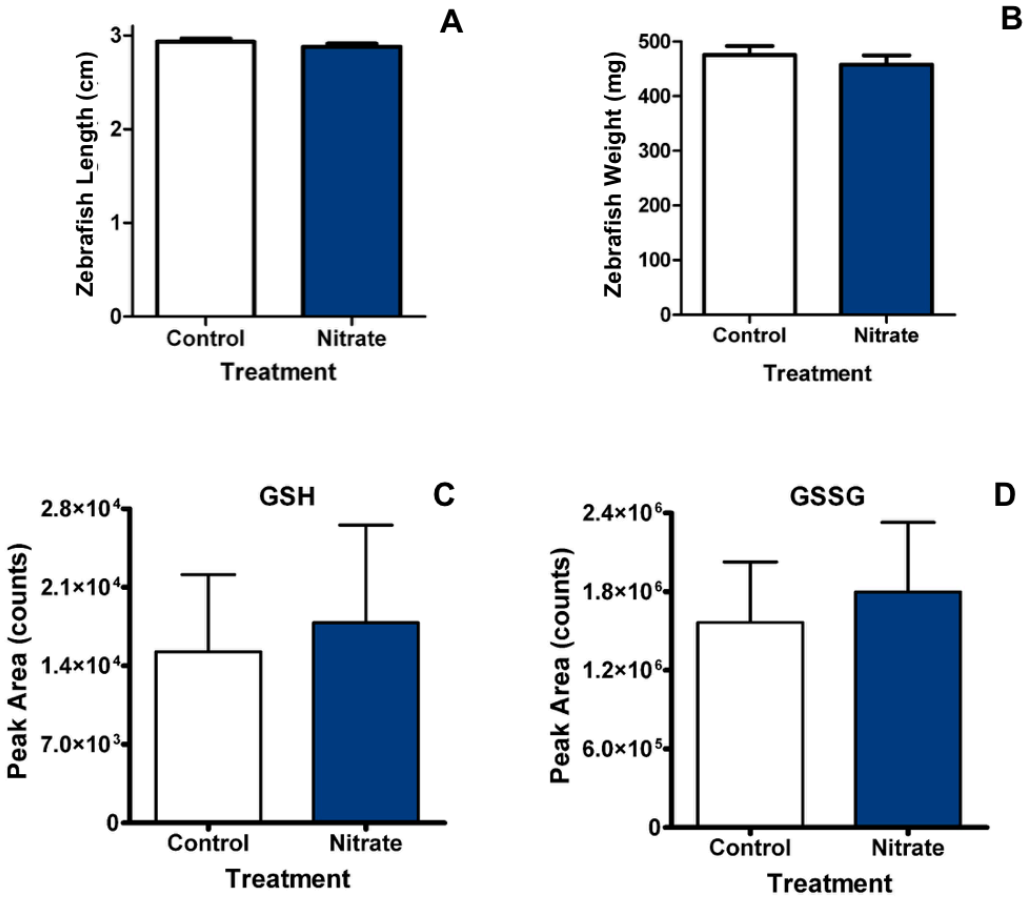

SI FIGURE 4.1: Health effects of nitrate treatment in zebrafish. There were no treatment-specific effects on fish length (n=12)(A), weight (n=18)(B), glutathione (GSH)(C), or oxidized glutathione (GSSG)(n=9)(D). Student's t-test with $p < 0.05$ indicating significance, GraphPad Prism 4.

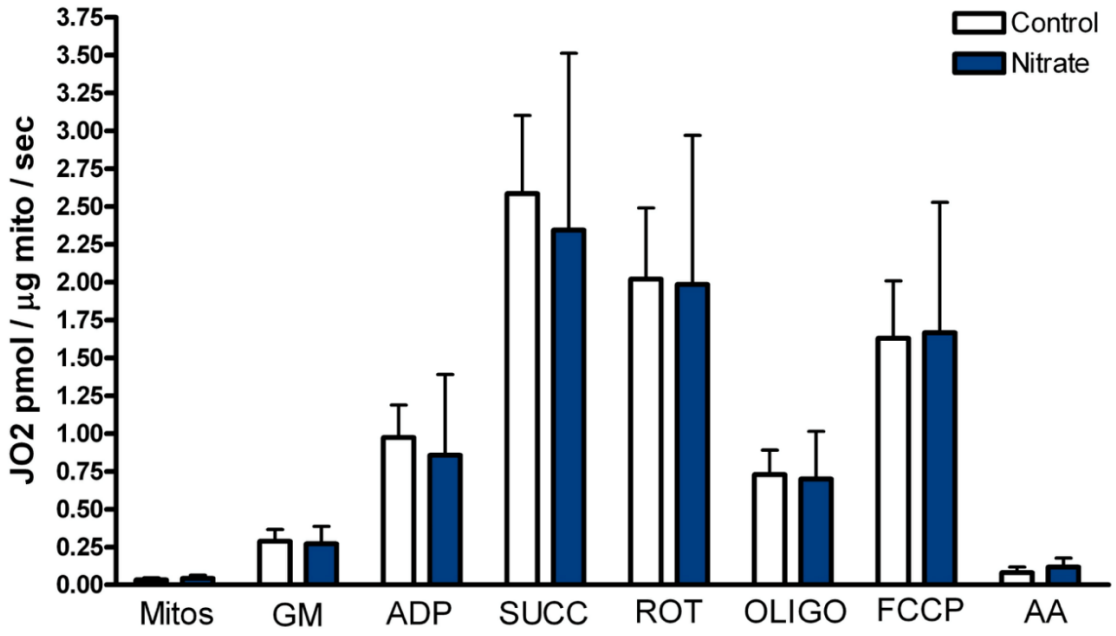

SI FIGURE 4.2: Assessment of mitochondrial function in zebrafish. Mitochondrial function was assessed with OROBOROS. There were no differences in oxidative phosphorylation, proton leak, or residual oxygen consumption. Addition of glutamate and malate (GM) measures proton leak through complex I. Adeonsine diphosphate (ADP) measures oxidative phosphorylation through complex I. Succinate (SUCC) measures oxidative phosphorylation through both complex I and II. Rotenone (ROT) measures oxidative phosphorylation through complex II. Oligomycin (OLIGO) measures proton leak through complex II. Carbonyl cyanide 4-(trifluoromethoxy)phenylhydrazone (FCCP) measures the electron transport system through complex II. Antimycin A (AA) measures residual oxygen consumption. One-way ANOVA with Tukey post-hoc analysis (n=8/group), GraphPad Prism 4.

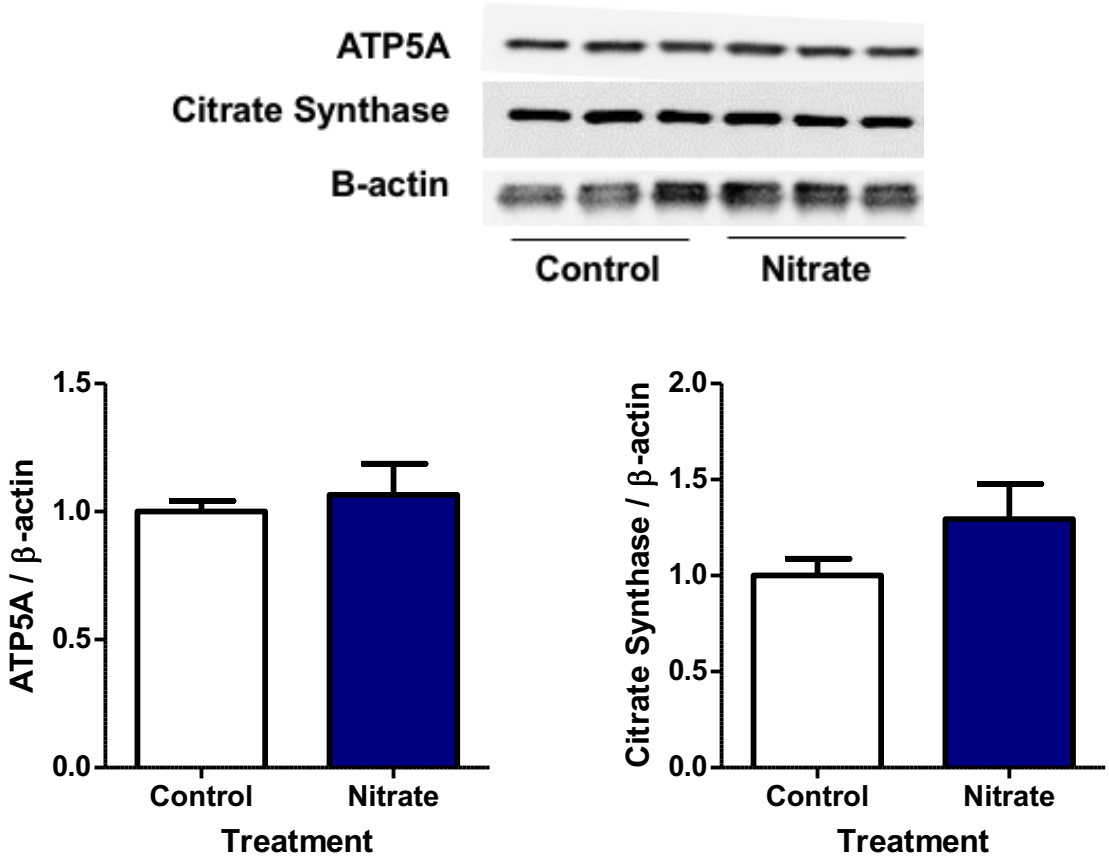

SI FIGURE 4.3: Mitochondrial protein in zebrafish skeletal muscle. Western blot analysis of ATP synthase (ATP5A) and citrate synthase demonstrate no significant differences in mitochondrial protein content in zebrafish skeletal muscle between treatments. Student's t-test (n=6/group) with $p < 0.05$ indicating significance. GraphPad Prism 4.

SI TABLE 4.1: Annotated Metabolites in Zebrafish							
Analyte	Ion Mode	Molecular Formula	m/z	Error (ppm)	RT (min)	MS/MS Match	Library
1-Aminocyclopropane-1-carboxylate	[M+H]+	C4H7NO2	102.0545	-4.7	4.7	Y	IROA
2-Aminobenzoic acid	[M+H]+	C7H7NO2	138.0537	-4.2	17.7	NA	IROA
2-Hexenoylcarnitine	[M+H]+	C13H23NO4	258.1696	-1.5	16.8	Y	IROA
3-Aminoisobutanoic acid	[M+H]+	C4H9NO2	104.0704	-2.4	4.9	Y	IROA
3-Dehydroxycarnitine	[M-H]-	C7H15NO2	144.1028	-1.5	8.9	Y	IROA
3-hydroxybutyrate	[M-H]-	C4H8O3	103.0409	8.2	7.9	Y	IROA
3-Hydroxyphenylacetate	[M-H]-	C8H8O3	151.0407	4.4	16.4	NA	IROA
3-Nitrotyrosine	[M+H]+	C9H10N2O5	227.0647	-5.0	9.1	NA	IROA
3-phosphoglycerate	[M+H]+	C3H7O7P	186.9996	-3.1	4.5	Y	IROA
4-Hydroxy-L-proline	[M+H]+	C5H9NO3	132.0648	-5.4	4.8	NA	IROA
4-Pyridoxic acid	[M-H]-	C8H9NO4	182.0460	0.4	10.1	Y	IROA
5-Aminolevulinic acid	[M+H]+	C5H9NO3	132.0648	-5.4	4.8	Y	IROA
5-Aminopentanoic acid	[M+H]+	C5H11NO2	118.0860	-1.9	5.4	Y	IROA
5-Hydroxylysine	[M+H]+	C6H14N2O3	163.1072	-3.3	4.2	Y	IROA
5'-Methylthioadenosine	[M+H]+	C11H15N5O3S	298.0966	-0.8	16.1	Y	IROA
6-phosphogluconate	[M-H]-	C6H13O10P	275.0213	4.4	25.5	Y	IROA
6-phosphogluconolactone	[M+H]+	C6H11O9P	257.0065	-1.1	4.3	Y	IROA
AC 14:0	[M+H]+	C21H41NO4	372.3103	-1.4	23.7	Y	Metlin
AC 14:1	[M+H]+	C21H39NO4	370.2945	-2.0	23.5	Y	Metlin
AC 14:2	[M+H]+	C21H37NO4	368.2789	-1.8	23.3	Y	Metlin
AC 15:0	[M+H]+	C22H43NO4	386.3259	-1.4	23.9	Y	Metlin
AC 16:2	[M+H]+	C23H41NO4	396.3096	-3.0	23.8	Y	Metlin
AC 16:3	[M+H]+	C23H39NO4	394.2942	-2.4	23.6	Y	Metlin
AC 17:0	[M+H]+	C24H47NO4	414.3559	-4.7	24.3	Y	Metlin
AC 18:0-OH	[M+H]+	C25H49NO5	444.3674	-2.1	24.0	Y	Metlin
AC 18:1	[M+H]+	C25H47NO4	426.3567	-2.5	24.4	Y	Metlin
AC 18:1-OH	[M+H]+	C25H47NO5	442.3517	-2.2	23.9	Y	Metlin
AC 18:3	[M+H]+	C25H43NO4	422.3255	-2.4	24.1	Y	Metlin
AC 20:1	[M+H]+	C27H51NO4	454.3878	-2.8	24.7	Y	Metlin
AC 20:2	[M+H]+	C27H49NO4	452.3726	-1.8	24.6	Y	Metlin
AC 20:3	[M+H]+	C27H47NO4	450.3560	-4.0	24.5	Y	Metlin
AC 20:4	[M+H]+	C27H45NO4	448.3403	-4.1	24.4	Y	Metlin
AC4:1-OH	[M+H]+	C11H21NO5	248.1485	-3.2	8.7	Y	Metlin
Acetoacetate	[M+H]+	C4H6O3	103.0386	-4.1	6.0	Y	Metlin

Adenine	[M+H]+	C5H5N5	136.0613	-3.7	7.8	Y	IROA
Adenosine	[M+H]+	C10H13N5O4	268.1038	-1.0	9.2	Y	IROA
Adenylosuccinate	[M+H]+	C14H18N5O11P	462.0666	-0.5	7.4	Y	Metlin
ADP	[M+H]+	C10H15N5O10P2	428.0364	-0.6	4.9	Y	IROA
ADP-glucose	[M+H]+	C16H25N5O15P2	590.0856	-6.6	4.9	Y	IROA
Alanine	[M+H]+	C3H7NO2	90.0549	-0.1	5.3	Y	IROA
Allantoin	[M+H]+	C4H6N4O3	159.0504	-5.8	5.1	Y	IROA
Allothreonine	[M+H]+	C4H9NO3	120.0649	-5.1	4.7	Y	IROA
Aminoadipic acid	[M+H]+	C6H11NO4	162.0754	-4.1	4.9	Y	IROA
AMP	[M+H]+	C10H14N5O7P	348.0704	0.2	5.5	Y	IROA
Arachidonic acid	[M-H]-	C20H32O2	303.2326	-1.2	25.9	Y	Metlin
Arachidyl carnitine	[M+H]+	C27H53NO4	456.4034	-2.8	24.8	Y	Metlin
Arginine	[M+H]+	C6H14N4O2	175.1183	-4.0	4.5	Y	IROA
Argininosuccinate	[M+H]+	C10H18N4O6	291.1295	-1.4	4.6	Y	Metlin
Ascorbic acid	[M-H]-	C6H8O6	175.0249	0.4	7.3	Y	IROA
Asparagine	[M+H]+	C4H8N2O3	133.0599	-6.5	4.6	Y	IROA
Aspartic acid	[M-H]-	C4H7NO4	132.0306	2.6	4.5	Y	IROA
ATP	[M+H]+	C10H16N5O13P3	508.0013	-3.4	5.1	Y	IROA
Azelaic acid	[M+H]+	C9H16O4	189.1112	-4.7	20.3	NA	IROA
Betaine	[M+H]+	C5H11NO2	118.0860	-2.4	6.7	Y	IROA
Biliverdin	[M+H]+	C33H34N4O6	583.2554	0.4	25.3	NA	IROA
Bisphosphoglycerate	[M+H]+	C3H8O10P2	264.9512	-3.1	4.1	Y	IROA
Butenylcarnitine	[M+H]+	C11H19NO4	230.1386	-0.5	12.5	Y	Metlin
Butyrylcarnitine	[M+H]+	C11H21NO4	232.1541	-0.9	13.4	Y	Metlin
cAMP	[M+H]+	C10H12N5O6P	330.0597	-0.4	8.7	Y	IROA
Carnitine	[M+H]+	C7H15NO3	162.1119	-3.3	6.2	Y	IROA
Cervonyl carnitine	[M+H]+	C29H45NO4	472.3412	-2.0	24.6	Y	Metlin
cGMP	[M+H]+	C10H12N5O7P	346.0524	-6.7	5.9	Y	IROA
cis-4-Hydroxy-D-proline	[M+H]+	C5H9NO3	132.0648	-5.4	4.8	NA	IROA
cis-Aconitic acid	[M-H]-	C6H6O6	173.0092	0.2	6.7	Y	IROA
Citrate	[M-H]-	C6H8O7	191.0197	0.1	5.8	Y	IROA
Citrulline	[M+H]+	C6H13N3O3	176.1026	-1.8	4.8	Y	IROA
Creatine	[M+H]+	C4H9N3O2	132.0764	-3.0	5.3	Y	IROA
Cystathionine	[M+H]+	C7H14N2O4S	223.0746	-0.5	4.5	Y	IROA
Cytidine	[M+H]+	C9H13N3O5	244.0924	-1.6	5.2	Y	IROA
Cytosine	[M+H]+	C4H5N3O	112.0499	-5.6	5.2	Y	IROA
Decanoylcarnitine	[M+H]+	C17H33NO4	316.2479	-1.2	22.1	Y	Metlin
Dehydroascorbate	[M+H]+	C6H6O6	175.0238	0.5	6.6	NA	IROA

deoxyAMP	[M+H]+	C10H14N5O6P	332.0747	-2.2	7.3	NA	IROA
Deoxyuridine	[M-H]-	C9H12N2O5	227.0670	-1.5	8.6	NA	IROA
DHA	[M-H]-	C22H32O2	327.2329	-0.2	26.1	Y	Metlin
Dodecanoic acid	[M-H]-	C12H24O2	199.1701	-1.5	24.5	Y	IROA
Dodecanoylcarnitine	[M+H]+	C19H37NO4	344.2789	-1.8	23.0	Y	Metlin
Elaidic acid	[M+H]+	C18H34O2	283.2630	-0.6	25.7	NA	IROA
EPA	[M-H]-	C20H30O2	301.2169	-1.3	25.8	Y	Metlin
Erythrose 4-phosphate	[M+H]+	C4H9O7P	199.0014	0.5	5.1	Y	IROA
Ethylmalonic acid	[M-H]-	C5H8O4	131.0352	1.3	10.2	Y	IROA
FAD	[M+H]+	C27H33N9O15P2	786.1637	-0.9	16.0	Y	IROA
Fructose 1,6-BP	[M+H]+	C6H14O12P2	341.0033	-0.1	4.0	Y	IROA
Fumarate	[M-H]-	C4H4O4	115.0038	1.2	6.5	Y	IROA
GABA	[M-H]-	C4H9NO2	102.0563	2.5	4.7	Y	IROA
GDP-glucose	[M+H]+	C10H15N5O11P2	442.0169	-0.3	4.9	Y	IROA
Gluconic acid	[M-H]-	C6H12O7	195.0507	-1.6	4.7	Y	IROA
Glucose	[M-H]-	C6H12O6	179.0561	0.0	4.8	Y	IROA
Glucose 6-phosphate	[M-H]-	C6H13O9P	259.0225	0.1	4.3	Y	IROA
Glutamic acid	[M+H]+	C5H9NO4	148.0600	-3.1	4.7	Y	IROA
Glutamine	[M+H]+	C5H10N2O3	147.0758	-4.4	4.7	Y	IROA
Glutaric acid	[M+H]+	C5H8O4	133.0490	-4.2	8.3	Y	IROA
Glyceric acid	[M-H]-	C3H6O4	105.0195	1.8	5.1	Y	IROA
Glycine	[M+H]+	C2H5NO2	76.0393	-0.3	4.5	NA	IROA
GMP	[M-H]-	C10H14N5O8P	362.0506	-0.4	5.3	Y	IROA
GSH	[M+H]+	C10H17N3O6S	308.0911	0.0	5.1	Y	IROA
GSSG	[M+H]+	C20H32N6O12S2	611.1450	0.5	5.4	Y	IROA
Guanine	[M+H]+	C5H5N5O	152.0563	-2.9	7.9	Y	IROA
Guanosine	[M+H]+	C10H13N5O5	284.0991	0.4	7.9	Y	IROA
Heptadecanoic acid	[M+H]+	C17H34O2	271.2631	-0.4	25.4	Y	IROA
Hexanoylcarnitine	[M+H]+	C13H25NO4	260.1852	-1.9	18.2	Y	Metlin
Hippuric acid	[M+H]+	C9H9NO3	180.0648	-4.2	18.2	Y	IROA
Histidine	[M+H]+	C6H9N3O2	156.0763	-3.2	4.5	Y	IROA
Homoserine	[M+H]+	C4H9NO3	120.0649	-5.1	4.7	Y	IROA
Hypotaurine	[M+H]+	C2H7NO2S	110.0260	-9.2	4.7	NA	IROA
Hypoxanthine	[M+H]+	C5H4N4O	137.0455	-2.3	8.1	Y	IROA
IMP	[M+H]+	C10H13N4O8P	349.0544	0.0	5.4	Y	IROA
Indoleacetic acid	[M+H]+	C10H9NO2	176.0699	-4.1	19.8	Y	IROA
Inosine	[M+H]+	C10H12N4O5	269.0879	-0.4	8.1	Y	IROA
Kynurenine	[M+H]+	C10H12N2O3	209.0917	-1.7	11.9	NA	IROA

L-Acetylcarnitine	[M+H]+	C9H17NO4	204.1223	-3.7	8.8	Y	Metlin
Lactate	[M+H]+	C3H6O3	91.0389	-1.3	6.1	Y	IROA
Leucine	[M+H]+	C6H13NO2	132.1013	-4.8	6.9	Y	IROA
Linoleic acid	[M-H]-	C18H32O2	279.2332	0.7	25.7	Y	Metlin
Linolenic acid	[M-H]-	C18H30O2	277.2173	-0.1	25.6	Y	Metlin
Linoleyl carnitine	[M+H]+	C25H45NO4	424.3413	-2.0	24.2	Y	Metlin
Lumichrome	[M+H]+	C12H10N4O2	243.0872	-1.8	22.1	NA	IROA
Lysine	[M+H]+	C6H14N2O2	147.1125	-1.8	4.2	NA	IROA
Malate	[M+H]+	C4H6O5	135.0292	3.1	7.9	Y	IROA
Malonic acid	[M-H]-	C3H4O4	103.0046	4.0	5.3	NA	IROA
Malonylcarnitine	[M+H]+	C10H17NO6	248.1135	2.6	4.9	Y	Metlin
Mandelic acid	[M-H]-	C8H8O3	151.0402	0.9	14.7	Y	IROA
Methionine	[M+H]+	C5H11NO2S	150.0575	-5.3	6.2	Y	IROA
Methyl beta-D-glucopyranoside	[M+H]+	C7H14O6	195.0873	5.2	5.2	Y	IROA
Methylmalonic acid	[M-H]-	C4H6O4	117.0184	-8.3	20.5	NA	IROA
Myoinositol	[M-H]-	C6H12O6	179.0561	0.0	4.8	Y	IROA
N-Acetylglutamic acid	[M-H]-	C7H11NO5	188.0564	-0.2	7.6	Y	IROA
N-Acetyl-L-alanine	[M-H]-	C5H9NO3	130.0514	3.2	6.5	Y	IROA
N-Acetyl-L-aspartic acid	[M-H]-	C6H9NO5	174.0410	0.9	6.5	Y	IROA
N-Acetyl-L-methionine	[M-H]-	C7H13NO3S	190.0544	0.4	14.6	Y	IROA
N-Acetyl-L-phenylalanine	[M-H]-	C11H13NO3	206.0823	-0.1	19.7	Y	IROA
N-Acetylserine	[M-H]-	C5H9NO4	146.0457	-1.3	5.2	Y	IROA
N-Acetylserotonin	[M+H]+	C12H14N2O2	219.1123	-2.4	18.4	NA	IROA
NAD	[M+H]+	C21H27N7O14P2	664.1157	-1.0	6.6	Y	IROA
NADP	[M+H]+	C21H28N7O17P3	744.0821	-0.8	5.1	Y	IROA
Niacinamide	[M+H]+	C6H6N2O	123.0548	-4.1	9.9	Y	IROA
Nicotinamide mononucleotide	[M-H]-	C11H15N2O8P	333.0505	3.4	5.4	Y	IROA
Nicotinic acid	[M+H]+	C6H5NO2	124.0380	-1.4	9.1	Y	IROA
N-Methyl-D-aspartic acid	[M-H]-	C5H9NO4	146.0460	0.9	4.7	Y	IROA
N-Methyl-L-glutarate	[M+H]+	C6H11NO4	162.0754	-4.1	4.9	NA	IROA
Nonanoylcarnitine	[M+H]+	C16H31NO4	302.2320	-1.9	21.4	Y	Metlin
O-Acetylserine	[M+H]+	C5H9NO4	148.0600	-3.1	4.7	NA	IROA
Octanoylcarnitine	[M+H]+	C15H29NO4	288.2169	0.0	20.7	Y	Metlin
Oleic acid	[M+H]+	C18H34O2	283.2630	-0.6	25.7	Y	IROA
Oleoylcarnitine	[M+H]+	C25H47NO4	426.3567	-2.5	24.4	Y	Metlin
O-Phosphoethanolamine	[M-H]-	C2H8NO4P	140.0121	1.9	4.5	Y	IROA
Ophthalmic acid	[M+H]+	C11H19N3O6	290.1346	-0.4	6.3	Y	IROA
Ornithine	[M+H]+	C5H12N2O2	133.0970	-0.9	4.2	Y	IROA

Oxaloacetate	[M+H]+	C4H4O5	130.9979	-5.2	5.7	Y	IROA
Oxoglutarate	[M-H]-	C5H6O5	145.0144	0.8	6.2	Y	IROA
Palmitic acid	[M-H]-	C16H32O2	255.2330	0.0	25.5	Y	IROA
Palmitoylcarnitine	[M+H]+	C23H45NO4	400.3411	-2.6	24.1	Y	Metlin
p-Aminobenzoic acid	[M-H]-	C7H7NO2	136.0407	1.9	17.4	Y	IROA
Pantothenic acid	[M+H]+	C9H17NO5	220.1176	-1.7	10.5	Y	IROA
Petroselinic acid	[M+H]+	C18H34O2	283.2630	-0.6	25.7	Y	IROA
Phenylalanine	[M+H]+	C9H11NO2	166.0858	-3.0	9.6	Y	IROA
Phosphocreatine	[M+H]+	C4H10N3O5P	212.0430	-0.4	5.0	Y	IROA
Phosphoenolpyruvate	[M-H]-	C3H5O6P	166.9752	0.6	5.1	Y	IROA
Pimelylcarnitine	[M+H]+	C14H25NO6	304.1753	-0.6	14.4	Y	Metlin
Pipecolic acid	[M+H]+	C6H11NO2	130.0853	-7.6	7.3	NA	IROA
Proline	[M+H]+	C5H9NO2	116.0703	-2.8	5.4	Y	IROA
Propionylcarnitine	[M+H]+	C10H19NO4	218.1383	-1.7	11.0	Y	Metlin
Putrescine	[M+H]+	C4H12N2	89.1072	-1.4	3.9	Y	IROA
Pyridoxal	[M+H]+	C8H9NO3	168.0645	-6.1	7.3	NA	IROA
Pyrrolidonecarboxylic acid	[M-H]-	C5H7NO3	128.0358	3.8	8.2	Y	IROA
Pyruvate	[M-H]-	C3H4O3	87.0096	9.1	5.4	Y	IROA
Quinate	[M-H]-	C7H12O6	191.0559	-1.4	5.1	Y	IROA
Quinoline	[M-H]-	C9H7N	128.0506	0.0	5.2	Y	IROA
Riboflavin	[M+H]+	C17H20N4O6	377.1446	-2.6	19.0	Y	IROA
Ribose 5-phosphate	[M+H]+	C5H11O8P	229.0118	-0.5	4.5	Y	IROA
Ribulose 5-phosphate	[M+H]+	C5H11O8P	229.0118	-0.5	4.5	Y	IROA
S-Adenosylhomocysteine	[M+H]+	C14H20N6O5S	385.1288	-0.1	8.3	Y	IROA
Salicylamide	[M+H]+	C7H7NO2	138.0537	-9.2	17.7	Y	IROA
Sedoheptulose 7-P	[M+H]+	C7H15O10P	289.0316	-4.9	4.0	Y	Metlin
Serine	[M+H]+	C3H7NO3	106.0494	-4.5	4.5	Y	IROA
Spermidine	[M+H]+	C7H19N3	146.1649	-2.2	3.5	Y	IROA
Spermine	[M+H]+	C10H26N4	203.2227	-1.8	3.2	Y	IROA
Sphinganine	[M+H]+	C18H39NO2	302.3054	0.1	23.2	Y	IROA
Stearidonyl carnitine	[M+H]+	C25H41NO4	420.3093	-3.8	24.0	Y	Metlin
Stearoylcarnitine	[M+H]+	C25H49NO4	428.3727	-1.6	24.5	Y	Metlin
Suberic acid	[M-H]-	C8H14O4	173.0821	1.2	18.7	Y	IROA
Succinate	[M+H]+	C4H6O4	119.0341	2.2	8.1	Y	IROA
Taurine	[M-H]-	C2H7NO3S	124.0079	4.1	4.6	Y	IROA
Threonine	[M+H]+	C4H9NO3	120.0649	-5.1	4.7	Y	IROA
Thymidine	[M-H]-	C10H14N2O5	241.0829	-0.4	11.0	Y	IROA
Tiglylcarnitine	[M+H]+	C12H21NO4	244.1539	-1.8	16.0	Y	Metlin

Tocopherol	[M+H]+	C29H50O2	431.3867	-3.9	27.0	Y	IROA
Trigonelline	[M+H]+	C7H7NO2	138.0544	-4.3	10.1	Y	IROA
Tryptophan	[M-H]-	C11H12N2O2	203.0828	0.9	11.8	Y	IROA
Tyrosine	[M-H]-	C9H11NO3	180.0668	0.9	6.4	Y	IROA
UDP	[M+H]+	C9H14N2O12P2	405.0098	0.8	4.1	Y	IROA
UDP-glucose	[M-H]-	C15H24N2O17P2	565.0485	1.3	4.9	Y	IROA
UMP	[M+H]+	C9H13N2O9P	323.0285	-0.4	4.9	Y	IROA
Uracil	[M-H]-	C4H4N2O2	111.0206	5.1	7.4	Y	IROA
Urate	[M+H]+	C5H4N4O3	169.0351	-3.2	6.1	Y	IROA
Uridine	[M+H]+	C9H12N2O6	245.0769	0.4	6.9	Y	IROA
Valerylcarnitine	[M+H]+	C12H23NO4	246.1698	-0.9	15.4	Y	Metlin
Valine	[M+H]+	C5H11NO2	118.0860	-1.9	5.4	Y	IROA
Xanthine	[M-H]-	C5H4N4O2	151.0263	0.9	8.6	Y	IROA

SI TABLE 4.1: Annotated metabolites in zebrafish. Metabolite identities were assigned by matching accurate mass (error < 10 ppm), retention time (error < 10%), MS/MS fragmentation (library score > 70), and isotope distribution (error < 20%) with an in-house library consisting of IROA standards (IROA Technology, Bolton, MA) and other commercially available standards (650 total). Additional features were assigned by querying online databases (Metlin, HMDB). The raw data was analyzed using PeakView with XIC Manager 1.2.0 (ABSciex, Framingham, MA) for peak picking, retention time correction, and peak alignment.

SI TABLE 4.2 : Significance of Annotated Metabolites in Zebrafish					
Analyte	Control Rested vs. Nitrate Rested	Control Rested vs. Control Exercise	Control Rested vs. Nitrate Exercise	Control Exercise vs. Nitrate Exercise	Nitrate Rested vs. Nitrate Exercise
1-Aminocyclopropane-1-carboxylate	0.81479	0.37043	0.80361	0.47777	0.97059
2-Aminobenzoic acid	0.86075	0.44172	0.35912	0.76277	0.31833
2-Harenoylcarnitine	0.25994	1.74E-05	1.93E-05	0.42563	2.05E-05
3-Aminoisobutanoic acid	0.6583	0.71489	0.87423	0.57069	0.52939
3-Dehydroxycarnitine	0.6448	0.00012264	2.27E-05	0.20245	1.38E-05
3-hydroxybutyrate	0.0085138	0.0083079	0.01067	0.61313	0.86898
3-Hydroxyphenylacetic acid	0.017868	0.076992	0.20152	0.4502	0.16381
3-Nitrotyrosine	0.76577	0.65599	0.27114	0.15543	0.52523
3-phosphoglycerate	0.021921	0.49526	0.41793	0.14102	0.0067475
4-Hydroxyproline	0.72594	0.9117	0.5362	0.5881	0.9375
4-Pyridoxic acid	0.91327	0.9355	0.34703	0.32333	0.46576
5-Aminolevulinic acid	0.72594	0.9117	0.5362	0.5881	0.9375
5-Aminopentanoic acid	0.87106	0.026998	0.021935	0.87255	0.11537
5-Hydroxylysine	0.53077	0.7903	0.1773	0.43752	0.15227
5'-Methylthioadenosine	0.0090873	0.079246	0.15711	0.50906	0.093537
6-phosphogluconate	0.00087717	0.25516	0.47371	0.1255	0.018236
6-phosphogluconolactone	0.045886	0.17094	0.73334	0.10215	0.10824
AC 14:0	0.43001	4.24E-05	2.50E-05	0.2961	0.00014422
AC 14:1	0.15035	7.93E-06	6.51E-06	0.20639	0.0002069
AC 14:2	0.10065	4.39E-06	2.91E-07	0.060393	2.07E-05
AC 15:0	0.66395	7.81E-05	0.00019366	0.6877	9.94E-05
AC 16:2	0.47306	1.42E-05	4.30E-07	0.10831	6.71E-06
AC 16:3	0.23597	3.65E-05	6.04E-07	0.13857	6.14E-05
AC 17:0	0.71014	6.66E-05	0.00011916	0.68346	4.41E-05
AC 18:0-OH	0.85969	0.00012907	0.00092769	0.92548	0.00026983
AC 18:1	0.74579	2.87E-05	8.62E-06	0.3131	8.96E-06
AC 18:1-OH	0.23319	6.98E-06	1.60E-06	0.066761	4.45E-06
AC 18:3	0.50173	7.51E-06	4.72E-07	0.13861	2.74E-06
AC 20:1	0.91878	4.56E-05	9.31E-06	0.25877	2.81E-06
AC 20:2	0.85231	0.00020972	9.52E-05	0.64937	1.68E-05
AC 20:3	0.65238	0.0017835	0.0008206	0.35461	0.0028974
AC 20:4	0.46557	2.19E-05	2.75E-06	0.13379	3.26E-06
AC4:1-OH	0.092408	5.89E-05	0.0002432	0.59217	0.0031678
Acetoacetate	0.022915	0.00026272	0.2285	0.00019178	0.0062709

Adenine	0.61547	0.96969	0.35754	0.4087	0.75755
Adenosine	0.068605	0.87536	0.55383	0.0523	0.1134
Adenylosuccinate	0.74298	0.99593	0.58344	0.48694	0.82901
ADP	0.0014227	0.67785	0.47743	0.6702	0.027236
ADP-glucose	0.0022763	0.57382	0.4155	0.67368	0.027707
Alanine	0.41493	0.48018	0.87746	0.45146	0.39939
Allantoin	0.035288	0.33232	0.065225	0.46947	0.50494
Allothreonine	0.95395	0.10979	0.17228	0.63853	0.36148
Aminoadipic acid	0.67383	0.19496	0.31809	0.76213	0.74526
AMP	0.037606	0.1141	0.085563	0.031376	0.31901
Arachidonic acid	0.030012	0.49356	0.00034166	0.012954	0.0010815
Arachidyl carnitine	0.65574	0.0016081	0.0042004	0.85542	0.0036271
Arginine	0.027018	0.0011212	0.00053422	0.34332	0.010393
Argininosuccinate	0.40948	0.019478	0.00014872	0.082314	0.10755
Ascorbic acid	0.66733	0.38037	0.40838	0.88396	0.80001
Asparagine	0.5293	0.31746	0.36329	0.098071	0.17198
Aspartic acid	0.13012	0.22158	0.00072994	0.088335	0.076147
ATP	0.00085716	0.056322	0.16347	0.2271	0.00039272
Azelaic acid	0.31482	0.34452	0.088957	0.15086	0.17924
Betaine	0.031521	0.22951	0.56541	0.45349	0.056538
Biliverdin	0.69558	0.8655	0.88628	0.74234	0.5723
Bisphosphoglycerate	0.00028396	0.057209	0.73152	0.039974	0.0002795
Butenylcarnitine	0.063588	2.17E-05	9.37E-07	0.039151	2.54E-06
Butyrylcarnitine	0.47649	0.00012759	2.07E-05	0.58595	1.11E-05
cAMP	0.032255	0.077643	0.30256	0.3195	0.19436
Carnitine	0.35552	0.00057156	0.00036326	0.28024	0.0034109
Cervonyl carnitine	0.44608	5.16E-05	2.77E-05	0.36129	5.84E-05
cGMP	0.38216	0.1884	0.74532	0.23686	0.50066
cis-4-Hydroxy-D-proline	0.72594	0.9117	0.5362	0.5881	0.9375
cis-Aconitic acid	0.86068	0.1712	0.74151	0.43426	0.78493
Citrate	0.0046572	0.017362	0.0060318	0.23921	0.80843
Citrulline	0.21476	0.37626	0.71927	0.22435	0.12823
Creatine	0.83605	0.73215	0.67787	0.45263	0.56173
Cystathionine	0.78918	0.069743	0.047463	0.68633	0.073913
Cytidine	0.95941	0.46304	0.71163	0.13736	0.64356
Cytosine	0.95043	0.57217	0.69269	0.20284	0.73225
Decanoylcarnitine	0.24407	1.08E-05	2.54E-06	0.50627	1.26E-05
Dehydroascorbate	0.037681	0.36029	0.12237	0.54462	0.62564

deoxyAMP	0.52537	0.80267	0.5008	0.5973	0.88955
Deoxyuridine	0.033128	0.40348	0.066834	0.45093	0.50333
DHA	0.36928	0.31338	0.0044597	0.027428	0.0050136
Dodecanoic acid	0.23584	0.14723	0.14873	0.75241	0.61589
Dodecanoylcarnitine	0.13841	1.48E-05	2.85E-06	0.24013	3.75E-05
Elaidic acid	0.44075	0.57993	0.55131	0.99887	0.8981
EPA	0.74765	0.31887	0.0045005	0.030639	0.012048
Erythrose 4-phosphate	0.0075617	0.0055303	0.42234	0.001986	0.0024377
Ethylmalonic acid	0.10346	0.23442	0.28768	0.80776	0.45409
FAD	0.59345	0.11456	0.6932	0.3496	0.2259
Fructose 1,6-BP	9.53E-06	0.0081228	0.075191	0.31536	0.02993
Fumarate	1.95E-05	0.00057816	0.79372	0.02436	0.0058221
GABA	0.6583	0.71489	0.87423	0.57069	0.52939
GDP-glucose	0.72056	0.79344	0.97528	0.79667	0.6615
Gluconic acid	0.58063	0.16879	0.1762	0.70695	0.31873
Glucose	0.4938	0.41423	0.23748	0.69534	0.53898
Glucose 6-phosphate	0.11155	0.84206	0.33327	0.29272	0.29259
Glutamic acid	0.63658	0.84953	0.51958	0.40052	0.29278
Glutamine	0.69569	0.12359	0.39411	0.44714	0.71898
Glutaric acid	0.035643	0.028637	0.036136	0.75698	0.82094
Glyceric acid	0.044357	0.21398	0.20092	0.80031	0.2235
Glycine	0.48176	0.18286	0.22415	0.73661	0.26814
GMP	0.72708	0.051698	0.35569	0.015808	0.38062
GSH	0.48642	0.80965	0.95978	0.77416	0.528
GSSG	0.37474	0.52258	0.28168	0.59397	0.071494
Guanine	0.7162	0.80769	0.88957	0.85971	0.49001
Guanosine	0.046302	0.73643	0.43119	0.71474	0.20558
Haranoylcarnitine	0.18866	3.68E-05	9.73E-06	0.015336	5.53E-06
Heptadecanoic acid	0.19542	0.091534	0.4124	0.64477	0.050068
Hippuric acid	0.33233	0.81352	0.57713	0.81486	0.10117
Histidine	0.73112	0.31147	0.51919	0.19893	0.8144
Homoserine	0.95395	0.10979	0.17228	0.63853	0.36148
Hypotaurine	0.75136	0.79212	0.48428	0.67428	0.67212
Hypoxanthine	0.40947	0.29173	0.7228	0.33724	0.52284
Indoleacetic acid	0.34761	0.13556	0.21099	0.8778	0.75286
Inosine	0.057282	0.72256	0.27006	0.4429	0.2399
Inosinic acid	0.85311	0.221	0.25569	0.021087	0.085478
Kynurenine	0.45612	0.34861	0.67151	0.36622	0.53824

L-Acetylcarnitine	0.28657	3.72E-05	1.88E-05	0.54728	9.55E-06
Lactate	0.0022579	0.1304	0.63319	0.28193	0.011499
Leucine	0.57194	0.014797	0.055423	0.50008	0.20292
Linoleic acid	0.045173	0.16052	0.00030016	4.58E-05	0.0037068
Linolenic acid	0.24253	0.25778	0.0044432	0.0009647	0.013528
Linoleyl carnitine	0.6371	1.37E-05	1.23E-06	0.1873	4.16E-06
Lumichrome	0.010036	0.94821	0.00072497	0.00094697	0.86418
Lysine	0.90452	0.053975	0.0046173	0.27419	0.07894
Malate	8.33E-07	0.00025688	0.00092227	0.36227	0.01617
Malonic acid	0.035915	0.17925	0.058429	0.91223	0.7553
Malonylcarnitine	0.6479	0.00096906	0.00059373	0.76954	0.00024211
Mandelic acid	0.13175	0.049747	0.060333	0.92709	0.48228
Methionine	0.99335	0.071156	0.068754	0.87047	0.11183
Methyl beta-D-glucopyranoside	0.029347	0.65967	0.7355	0.99629	0.033717
Methylmalonic acid	0.039369	0.13561	0.59828	0.2644	0.076781
Myoinositol	0.4938	0.41423	0.23748	0.69534	0.53898
N-Acetylglutamic acid	0.022064	0.13845	0.43231	0.45349	0.14668
N-Acetyl-L-alanine	0.2094	0.023262	0.0026522	0.83695	0.012197
N-Acetyl-L-aspartic acid	0.0088202	0.13907	0.28536	0.54718	0.095939
N-Acetyl-L-methionine	0.22043	0.095862	0.02669	0.81799	0.23954
N-Acetyl-L-phenylalanine	0.4039	0.70964	0.18365	0.076114	0.042725
N-Acetylserine	0.55536	0.18831	0.337	0.70996	0.74618
N-Acetylserotonin	0.16899	0.28445	0.43001	0.69748	0.0685
NAD	0.32981	0.8812	0.61401	0.84489	0.24959
NADP	0.70346	0.60676	0.30756	0.78142	0.59098
Niacinamide	0.046147	0.40617	0.92033	0.49014	0.071151
Nicotinamide ribotide	0.26448	0.14371	0.68031	0.10403	0.1825
Nicotinic acid	0.34005	0.3394	0.29781	0.97763	0.052447
N-Methyl-D-aspartic acid	0.63658	0.84953	0.51958	0.40052	0.29278
N-Methyl-L-glutamate	0.67383	0.19496	0.31809	0.76213	0.74526
Nonanoylcarnitine	0.90904	0.00014294	1.39E-05	0.25763	4.26E-06
O-Acetylserine	0.63658	0.84953	0.51958	0.40052	0.29278
Octanoylcarnitine	0.25014	2.62E-05	1.44E-05	0.59901	2.27E-05
Oleic acid	0.083899	0.18153	0.0020802	0.047581	0.015341
Oleoylcarnitine	0.72851	2.84E-05	8.77E-06	0.31806	9.14E-06
O-Phosphoethanolamine	0.83892	0.83543	0.17879	0.2637	0.13743
Ophthalmic acid	0.77232	0.53827	0.4641	0.93521	0.74017
Ornithine	0.96317	0.00047984	0.0001244	0.084971	0.005741

Oxaloacetate	0.00036107	0.0028888	0.0066511	0.98327	0.18817
Oxoglutarate	0.54879	0.20748	0.15881	0.93409	0.057794
Palmitic acid	0.41242	0.4688	0.96769	0.4732	0.41405
Palmitoylcarnitine	0.79045	0.00026283	6.65E-05	0.2749	6.89E-06
p-Aminobenzoic acid	0.86075	0.44172	0.35912	0.76277	0.31833
Pantothenic acid	0.056518	0.30211	0.17701	0.8927	0.46602
Petroselinic acid	0.44075	0.57993	0.55131	0.99887	0.8981
Phenylalanine	0.88775	0.39351	0.47088	0.79442	0.68144
Phosphocreatine	0.015635	0.016858	0.5947	0.037124	0.13835
Phosphoenolpyruvate	0.00013779	0.0015886	0.0051057	0.20546	0.013211
Pimelylcarnitine	0.40247	0.00026817	2.11E-05	0.099436	8.43E-06
Pipecolic acid	0.45318	0.42817	0.68971	0.71737	0.75029
Proline	0.70948	0.32263	0.15552	0.89113	0.19372
Propionylcarnitine	0.54528	3.80E-05	5.58E-06	0.35418	2.92E-05
Putrescine	0.9668	0.66191	0.48524	0.83707	0.42443
Pyridoxal	0.25029	0.90209	0.32363	0.54758	0.058462
Pyrrolidonecarboxylic acid	0.003535	0.019213	0.033961	0.45442	0.40102
Pyruvate	0.00011936	0.24774	0.082448	0.633	0.0014899
Quinate	0.61403	0.26278	0.048423	0.46221	0.022135
Quinoline	0.82701	0.57444	0.52553	0.99716	0.72361
Riboflavin	0.88406	0.060837	0.024694	0.75617	0.097605
Ribose 5-phosphate	0.49094	0.0079378	0.011347	5.90E-05	0.0046843
Ribulose 5-phosphate	0.8219	0.010439	0.010569	6.18E-06	0.0067011
S-Adenosylhomocysteine	0.028778	0.073092	0.031049	0.78415	0.95038
Salicylamide	0.86075	0.44172	0.35912	0.76277	0.31833
Sedoheptulose 7-phosphate	0.0015023	0.0085795	0.17178	0.00062161	0.011534
Serine	0.88089	0.87356	0.16297	0.26698	0.14081
Spermidine	0.98732	0.69408	0.55553	0.94346	0.57138
Spermine	0.44508	0.43933	0.431	0.81561	0.163
Sphinganine	0.45954	0.84494	0.90709	0.93449	0.39539
Stearidonyl carnitine	0.33795	7.18E-06	9.27E-07	0.2097	2.22E-06
Stearoylcarnitine	0.86411	0.00017461	0.00061121	0.92921	0.00012036
Suberic acid	0.83973	0.84633	0.59255	0.74678	0.5928
Succinate	0.00018	3.80E-05	0.090582	0.0039763	0.0046481
Taurine	0.59639	0.40804	0.46118	0.75072	0.80567
Threonine	0.95395	0.10979	0.17228	0.63853	0.36148
Thymine	0.54121	0.35559	0.52637	0.73563	0.97899
Tiglylcarnitine	0.44654	0.00010324	9.85E-05	0.29773	5.32E-05

Tocopherol	0.017769	0.31194	0.14478	0.62127	0.49679
Trigonelline	0.54596	0.4761	0.44562	0.97636	0.94041
Tryptophan	0.32103	0.30763	0.49677	0.68672	0.65794
Tyrosine	0.44922	0.16728	0.28919	0.80237	0.78126
UDP	0.78545	0.44139	0.88782	0.24499	0.85716
UDP-glucose	0.047899	0.53898	0.075353	0.16658	0.79634
UMP	0.80828	0.10345	0.007824	0.24092	0.00050275
Uracil	0.98135	0.95411	0.828	0.78923	0.86415
Urate	0.064108	0.51605	0.73853	0.7379	0.10018
Uridine	0.03537	0.62297	0.089626	0.2954	0.5791
Valerylcarnitine	0.49959	0.0084141	7.40E-05	0.12532	0.0042706
Valine	0.87106	0.026998	0.021935	0.87255	0.11537
Xanthine	0.12921	0.80617	0.05282	0.12992	0.96125

SI TABLE 4.2: Significance of annotated metabolites in zebrafish. Statistical significance between all treatment groups was assessed with MetaboAnalyst 3.0 (Two-way ANOVA with Fisher's post-hoc and Holm FDR-correction, $p < 0.05$ indicating significance, n=9/group).

SI Table 4.3: Metabolomics Pathway Analysis Results in Zebrafish			
Pathway	Impact	Group	P-value
TCA cycle	0.398	Control: Nitrate	9.38E-06
		Control: Control Exercise	3.89E-05
		Nitrate: Nitrate Exercise	0.002076
Glycolysis or Gluconeogenesis	0.204	Control: Nitrate	1.21E-05
		Control: Control Exercise	0.0010568
		Nitrate: Nitrate Exercise	0.0026731
Pyruvate metabolism	0.188	Control: Nitrate	1.21E-05
		Control: Control Exercise	0.0010568
		Nitrate: Nitrate Exercise	0.0026731
Propanoate metabolism	0.000	Control: Nitrate	0.00018
		Control: Control Exercise	3.80E-05
		Nitrate: Nitrate Exercise	0.0046481
		Control Exercise: Nitrate Exercise	0.0039763
Pentose phosphate pathway	0.367	Control: Nitrate	0.00032975
		Control: Control Exercise	0.00085588
		Nitrate: Nitrate Exercise	0.00040558
		Control Exercise: Nitrate Exercise	7.73E-06
Butanoate metabolism	0.130	Control: Nitrate	0.001521
		Control: Control Exercise	0.0017195
		Nitrate: Nitrate Exercise	0.01625
Glyoxylate and dicarboxylate metabolism	0.592	Control: Nitrate	0.0026261
		Control: Control Exercise	0.013423
Synthesis/degradation of ketone bodies	0.600	Control: Nitrate	0.0043458
		Control: Control Exercise	0.00048865
		Control Exercise: Nitrate Exercise	0.010365
Tyrosine metabolism	0.137	Control: Nitrate	0.0072462
		Control: Control Exercise	0.0016606
		Nitrate: Nitrate Exercise	0.018801
		Control Exercise: Nitrate Exercise	0.0051759
Alanine, aspartate and glutamate metabolism	0.922	Control: Nitrate	0.015468
		Control: Control Exercise	0.044732
		Nitrate: Nitrate Exercise	0.037713
Cysteine and methionine metabolism	0.367	Control: Nitrate	0.02157
		Nitrate: Nitrate Exercise	0.04426
Arachidonic acid metabolism	0.329	Control: Nitrate	0.030012
		Nitrate: Nitrate Exercise	0.0010815
		Control Exercise: Nitrate Exercise	0.012954

Glycerolipid metabolism	0.104	Control: Nitrate	0.044357
Linoleic acid metabolism	1.000	Control: Nitrate	0.045173
		Nitrate: Nitrate Exercise	0.0037068
		Control Exercise: Nitrate Exercise	4.58E-05
Valine, Leucine, and isoleucine degradation and biosynthesis	0.666	Control: Control Exercise	0.0030564
		Control Exercise: Nitrate Exercise	0.045941
		Control: Exercise	0.026105
Arginine and proline metabolism	0.645	Control: Control Exercise	0.04331
Lysine degradation	0.015	Control: Control Exercise	0.050019
Biosynthesis of unsaturated fatty acids	0.000	Nitrate: Nitrate Exercise	0.0083608
		Control Exercise: Nitrate Exercise	0.0031808
alpha-linolenic acid metabolism	1.000	Nitrate: Nitrate Exercise	0.013528
		Control Exercise: Nitrate Exercise	0.0009647

SI TABLE 4.3: Metabolomics pathway analysis results in zebrafish. Tabulated pathway analysis results, comparing all treatment groups. Pathway analyses were performed MetaboAnalyst 3.0 using log-transformed peak intensities of all annotated metabolites detected in positive and negative ion mode (Two-way ANOVA with Fisher's post-hoc and Holm FDR-correction, $p < 0.05$ indicating significance, n=9/group).

CHAPTER 5: CONCLUSION

In this dissertation, I present novel mechanisms of nitrate with relevance to both cardiovascular health and exercise performance. Here, I discuss the utility of the mass spectrometry techniques that made these discoveries possible.

5.1. THE BENEFITS OF AN UNTARGETED APPROACH

I utilize untargeted metabolomics as a hypothesis-generating tool to elucidate novel mechanisms of the benefits of organic and inorganic nitrate. With metabolomics, I narrowed our focus to the most significantly changed pathways instead of testing hypotheses individually. This is especially important when studying nutrition, because unlike pharmaceutical compounds, nutritional interventions may not specifically interact with a single cellular target, and yet alter the flux throughout a pathway. In particular, metabolomics is useful to study deficiency or supplementation of a particular nutrient, vitamin, or mineral. Metabolomics allows for the differentiation of phenotypes better than traditional clinical endpoints (218,219). Although traditionally metabolomics was performed using NMR, it suffers from low sensitivity, small dynamic range, and only approximately 60 compounds can be detected in a biological sample (220). Mass spectrometry, in comparison, has high sensitivity and can detect more than 1000 compounds in a single sample (221).

I acknowledge that many of our original hypotheses on nitrates were not supported by the results presented here. I hypothesized that ascorbic acid would salvage 4-hydroxy-2(*E*)-nonenal (HNE)(164), protecting ALDH2 from damage and reducing intracellular oxidative stress. Although ALDH2 is inactivated in nitrate tolerance, I determined that ascorbic acid does not protect ALDH2 from damage. I then utilized untargeted metabolomics to assess metabolic changes resulting from nitrate treatment, with or without ascorbic acid supplementation. I discovered

that purine metabolism was impaired, leading us to the new hypothesis that XO, the enzyme that catalyzes the final step in purine metabolism, is inactivated during nitrate tolerance. This was surprising because although XO was known to bioactivate GTN into NO, it was perceived to be a low affinity pathway that was not physiologically relevant. Ultimately, I demonstrated that maintaining XO activity with ascorbic acid co-treatment prevents the development of nitrate tolerance. I would not have identified the link between ascorbic acid and XO without first performing metabolomics analysis.

Furthermore, my initial goal in the zebrafish project was to determine whether nitrate metabolism is altered with exercise. I demonstrated that exercise reduces nitrite levels, suggesting increased reduction into NO. Incidentally, metabolomics discovered significant changes in unexpected pathways. Nitrate treatment resulted in changes in the central pathways of energy metabolism: glycolysis, the pentose phosphate pathway, the TCA cycle, fatty acid metabolism, and purine metabolism. Metabolomics led us to the new hypothesis that nitrate increases ATP production by shifting the utilization of metabolic fuels. My work with nitrate is a prime example of a nutritional component that has many molecular targets, leading to changes in multiple metabolic pathways.

One limitation in metabolomics is that the data is challenging to interpret. With the zebrafish research, I measured elevated ATP levels. Two broad explanations of this finding are that either ATP synthesis is increased, or ATP usage is decreased. Therefore, an important step to any metabolomics approach is validation of the results. This requires complementing metabolomics with targeted mass spectrometry assays, or by assessing single targets (i.e., protein activity). Many of our chosen supplementary techniques have involved stable isotopes. For example, we intend on incubating homogenized muscle tissue from the zebrafish with ^{13}C-labeled fatty acids,

then measuring rates of β-oxidation. This allows for us to determine whether β-oxidation flux is increased or decreased in zebrafish, which is not possible with metabolomics alone. Without this validation step, metabolomics results can be ambiguous and lead to incorrect interpretations.

5.2. TRACKING THE METABOLIC FATE OF NITRATE

One overwhelming question that I was unable to answer in this work is deceptively simple - where does the nitrogen from nitrate go? I was able to demonstrate that organic nitrates were metabolized into nitrite and NO in both endothelial and epithelial cells, and that inorganic nitrate is uptaken in zebrafish and metabolized into nitrite in vivo. In both cells and zebrafish, I saw significant, and similar, changes in the metabolic profile. Nitrate altered glycolysis, the pentose phosphate pathway, fatty acid metabolism, and purine metabolism. However, with this approach we cannot determine if these changes are due to direct incorporation of nitrogen, or if these are indirect effects in response to nitrate treatment.

This seemingly simple question is challenging to answer. The only way to identify the fate of an atom is by using stable isotope precursors and quantifying with mass spectrometry. The stable isotope is, in a simplistic sense, a tracking device. The most common mass spectrometry technique to measure stable isotopes is a targeted method to quantify metabolites of interest. This removes the potential of discovering novel enrichment pathways because the analyst is limited to a subset of pre-selected metabolites. Furthermore, analytical standards are required to confirm the identity of the compound and optimize the method. My objective was to identify the fate of nitrogen in the metabolome, which is not possible with a targeted method. To address this limitation, I utilized a new technique termed “stable isotope-assisted

metabolomics".

I analyzed the zebrafish that were labeled with ^{15}N-nitrate with X^{13}CMS, a free and open-source R-package that can identify isotopically enriched metabolites (222). X^{13}CMS was published in 2014, and is the first software tool allowing for automatic identification and quantification of isotope enrichment in metabolomics data. The basis of X^{13}CMS software is that it scans for a user-defined mass difference (in this example, 0.99874 Da for ^{15}N enrichment) to identify metabolites that are enriched. Then, the user can compare the enrichment of treatment groups (in this example, control vs. exercise). In our case, it would allow us to determine the effect of exercise on nitrate metabolism (Figure 5.1, X^{13}CMS study design).

The raw chromatograms from the ABSciex 5600 TripleTOF (acquired in TOF scan mode in positive and negative mode) were pre-processed with XCMS for peak picking, retention time alignment, and grouping (223). X^{13}CMS was used to identify significantly enriched metabolites. The X^{13}CMS results were, to say the least, not promising. All of the enriched metabolites proved to either be background noise, or they were overlapped peaks that were erroneously identified as isotopologues of the same analyte. This issue arises from the fact that the resolving power of most high-resolution mass spectrometers are not sufficient to resolve the difference between a hydrogen atom and isotope enrichment, either ^{15}N, ^{13}C or otherwise. Furthermore, X^{13}CMS can only utilize full scan data, which means that MS/MS fragmentation patterns are not utilized. This leads to a high number of falsely identified enriched peaks (Figure 5.2, Incorrect identification of isotope enrichment). This high error rate means that the user must manually validate every positive result, which is a significant time commitment. This time-consuming manual validation makes X^{13}CMS infeasible for large sample sets, and reduces the utility of the software.

X^{13}CMS did not identify any significantly enriched metabolites after manual validation. This is either because there were no metabolites that incorporate nitrogen from nitrate, or that X^{13}CMS was unable to detect and quantify the changes. X^{13}CMS has been successfully used for precursor studies with ^{13}C-glucose (222) and ^{13}C-lactate (224), presumably because the percent enrichment was very high. X^{13}CMS does not appear to be sensitive enough for minor pathways, such as nitrogen incorporation in vertebrates. I perceive that this is due to the high background levels of natural isotope labeling. Recently, tools have become available that can reduce the background levels of natural isotope labeling (225), however these are challenging to integrate into the data processing workflow. This gap in the current technology provides many limitations for the use of stable isotopes in metabolomics, and there is a clear need for more suitable and accurate software. Although various vendor and open-source software packages are available to quantify isotope enrichment, tracking isotopes in an untargeted fashion remains a challenge.

Although the technology for stable isotope-assisted metabolomics may not be developed enough to track nitrate metabolism in vivo, this technique could be relatively easily applied to measure the flux throughout metabolic pathways. Metabolomics analyses are a snap-shot in time, therefore we cannot make conclusions about activity or flux through a pathway. To address this limitation, a relatively new technology called “fluxomics” utilizes stable isotope labeling to get a dynamic view of selected pathways (226,227). This analysis would be ideal for our work on inorganic nitrates because it would allow for us to examine flux through glycolysis, the TCA cycle, and fatty acid metabolism. For example, treating with ^{13}C-glucose and measuring isotope enrichment of glycolytic intermediates over time would help us determine flux through glycolysis. Unfortunately, fluxomics requires taking samples, usually blood, at regular time points to determine flux though a pathway. This is not feasible with the small size of the

zebrafish, however is relatively easily done in larger animal models and in humans.

5.3. CONCLUDING REMARKS

This dissertation is a contribution to the scientific body of knowledge because of the development of a new assay to measure ^{15}N-labeled nitrate and nitrite isotopologues, which I have now applied to study both pharmaceutical and dietary nitrates. Using stable isotopes in mass spectrometry has allowed us to quantify GTN bioactivation in both human endothelial cells and porcine epithelial cells, despite high background levels of nitrate in cell culture media. This method has also allowed us to determine that uptake and utilization of endogenous sources of nitrate is a significant pathway in zebrafish, and can account for up to 90% of the tissue nitrate content. I have provided evidence to support the identification of xanthine oxidase both as a GTN-bioactivating enzyme, a potential cause for the development of nitrate tolerance, and finally, an enzyme that stimulates NO production from inorganic nitrite during exercise. My work demonstrates that ascorbic acid, an inexpensive and simple oral supplement, may prevent the development of nitrate tolerance. Finally, my metabolomics work with zebrafish has generated new hypotheses on the mechanism of nitrate's beneficial effect on exercise. I demonstrate that nitrate reduces the oxygen cost of exercise by stimulating the differential usage of metabolic fuels. These projects present promising new mechanisms for the effects of nitrate on human health, and I look forward to validating these findings in humans.

5.4. FIGURES

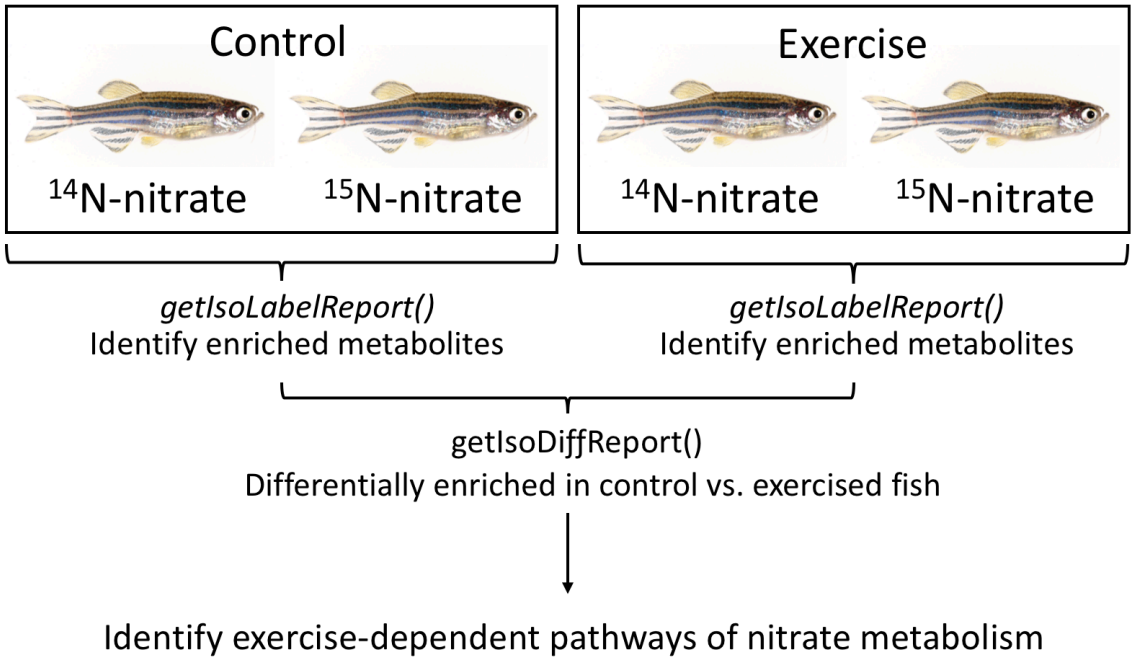

FIGURE 5.1: Study design for X^{13}CMS analysis. Zebrafish were treated with either ^{14}N-nitrate or ^{15}N-nitrate, under exercised or rested conditions. Zebrafish were extracted and analyzed with a ABSciex 5600 TripleTOF. Raw data was first pre-processed with XCMS. The X^{13}CMS code *getsioLabelReport()* was used to identify enriched metabolites in each group. The function getIsoDiffReport() was used to identify differentially enriched metabolites in control fish compared to exercised. The X^{13}CMS ultimately allows us to determine where the ^{15}N atoms go, and whether their metabolism is altered by exercise (n=9/group).

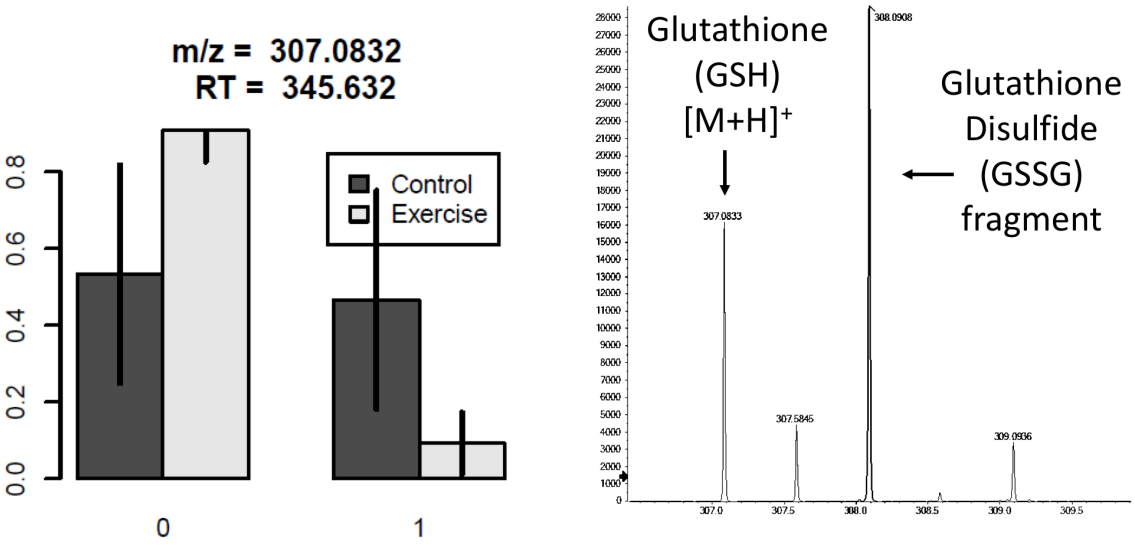

FIGURE 5.2: Incorrect identification of isotope enrichment. X^{13}CMS identified a peak with an m/z of 307.0832 as being significantly enriched, and altered with exercise. Upon manual validation, we discovered that 307.0832 was glutathione (GSH), and the "isotope" m/z 308.0908 was a fragment of oxidized glutathione (GSSG). Without manual validation, we may have erroneously concluded that GSH had incorporation of ^{15}N.

BIBLIOGRAPHY

1. Denninger, J. W., and Marletta, M. A. (1999) Guanylate cyclase and the .NO/cGMP signaling pathway. *Biochim Biophys Acta* **1411**, 334-350
2. Cai, H., and Harrison, D. G. (2000) Endothelial dysfunction in cardiovascular diseases: the role of oxidant stress. *Circ Res* **87**, 840-844
3. Lundberg, J. O. (2009) Cardiovascular prevention by dietary nitrate and nitrite. *Am J Physiol Heart Circ Physiol* **296**, H1221-1223
4. Jones, A. M. (2014) Dietary nitrate supplementation and exercise performance. *Sports Med* **44 Suppl 1**, S35-45
5. Nossaman, V. E., Nossaman, B. D., and Kadowitz, P. J. (2010) Nitrates and nitrites in the treatment of ischemic cardiac disease. *Cardiol Rev* **18**, 190-197
6. Marsh, N., and Marsh, A. (2000) A short history of nitroglycerine and nitric oxide in pharmacology and physiology. *Clin Exp Pharmacol Physiol* **27**, 313-319
7. Furchgott, R. F., and Zawadzki, J. V. (1980) The obligatory role of endothelial cells in the relaxation of arterial smooth muscle by acetylcholine. *Nature* **288**, 373-376
8. Bian, K., and Murad, F. (2014) sGC-cGMP signaling: target for anticancer therapy. *Adv Exp Med Biol* **814**, 5-13
9. Ignarro, L. J., Buga, G. M., Byrns, R. E., Wood, K. S., and Chaudhuri, G. (1988) Endothelium-derived relaxing factor and nitric oxide possess identical pharmacologic properties as relaxants of bovine arterial and venous smooth muscle. *J Pharmacol Exp Ther* **246**, 218-226
10. Palmer, R. M., Ferrige, A. G., and Moncada, S. (1987) Nitric oxide release accounts for the biological activity of endothelium-derived relaxing factor. *Nature* **327**, 524-526
11. Murad, F., Mittal, C. K., Arnold, W. P., Katsuki, S., and Kimura, H. (1978) Guanylate cyclase: activation by azide, nitro compounds, nitric oxide, and hydroxyl radical and inhibition by hemoglobin and myoglobin. *Adv Cyclic Nucleotide Res* **9**, 145-158
12. Moncada, S., and Higgs, E. A. (2006) The discovery of nitric oxide and its role in vascular biology. *Br J Pharmacol* **147 Suppl 1**, S193-201
13. Münzel, T., and Gori, T. (2013) Nitrate therapy and nitrate tolerance in patients with coronary artery disease. *Curr Opin Pharmacol* **13**, 251-259
14. Münzel, T., Daiber, A., and Gori, T. (2013) More answers to the still unresolved question of nitrate tolerance. *Eur Heart J* **34**, 2666-2673
15. Miller, M. R., and Wadsworth, R. M. (2009) Understanding organic nitrates--a vein hope? *Br J Pharmacol* **157**, 565-567
16. Azevedo, E. R., Schofield, A. M., Kelly, S., and Parker, J. D. (2001) Nitroglycerin withdrawal increases endothelium-dependent vasomotor response to acetylcholine. *J Am Coll Cardiol* **37**, 505-509
17. Chen, Z., Zhang, J., and Stamler, J. S. (2002) Identification of the enzymatic mechanism of nitroglycerin bioactivation. *Proc Natl Acad Sci U S A* **99**, 8306-8311
18. Chen, Z., Foster, M. W., Zhang, J., Mao, L., Rockman, H. A., Kawamoto, T., Kitagawa, K., Nakayama, K. I., Hess, D. T., and Stamler, J. S. (2005) An essential role for mitochondrial aldehyde dehydrogenase in nitroglycerin bioactivation. *Proc Natl Acad Sci U S A* **102**, 12159-12164
19. D'Souza, Y., Ji, Y., and Bennett, B. M. (2013) Effect of overexpression of human aldehyde dehydrogenase 2 in LLC-PK1 cells on glyceryl trinitrate biotransformation and cGMP accumulation. *Br J Pharmacol* **168**, 978-987

20. Neubauer, R., Wölkart, G., Opelt, M., Schwarzenegger, C., Hofinger, M., Neubauer, A., Kollau, A., Schmidt, K., Schrammel, A., and Mayer, B. (2015) Aldehyde dehydrogenase-independent bioactivation of nitroglycerin in porcine and bovine blood vessels. *Biochem Pharmacol* **93**, 440-448
21. De la Lande, I. S., Philp, T., Stafford, I., and Horowitz, J. D. (1996) Lack of inhibition of glyceryl trinitrate by diphenyleneiodonium in bovine coronary artery. *Eur J Pharmacol* **314**, 347-350
22. Miura, T., Nishinaka, T., Terada, T., and Yonezawa, K. (2017) Vasodilatory effect of nitroglycerin in Japanese subjects with different aldehyde dehydrogenase 2 (ALDH2) genotypes. *Chem Biol Interact*
23. Kollau, A., Hofer, A., Russwurm, M., Koesling, D., Keung, W. M., Schmidt, K., Brunner, F., and Mayer, B. (2005) Contribution of aldehyde dehydrogenase to mitochondrial bioactivation of nitroglycerin: evidence for the activation of purified soluble guanylate cyclase through direct formation of nitric oxide. *Biochem J* **385**, 769-777
24. Millar, T. M., Stevens, C. R., Benjamin, N., Eisenthal, R., Harrison, R., and Blake, D. R. (1998) Xanthine oxidoreductase catalyses the reduction of nitrates and nitrite to nitric oxide under hypoxic conditions. *FEBS Lett* **427**, 225-228
25. Doel, J. J., Godber, B. L., Goult, T. A., Eisenthal, R., and Harrison, R. (2000) Reduction of organic nitrites to nitric oxide catalyzed by xanthine oxidase: possible role in metabolism of nitrovasodilators. *Biochem Biophys Res Commun* **270**, 880-885
26. Godber, B. L., Doel, J. J., Sapkota, G. P., Blake, D. R., Stevens, C. R., Eisenthal, R., and Harrison, R. (2000) Reduction of nitrite to nitric oxide catalyzed by xanthine oxidoreductase. *J Biol Chem* **275**, 7757-7763
27. Zhang, Z., Naughton, D., Winyard, P. G., Benjamin, N., Blake, D. R., and Symons, M. C. (1998) Generation of nitric oxide by a nitrite reductase activity of xanthine oxidase: a potential pathway for nitric oxide formation in the absence of nitric oxide synthase activity. *Biochem Biophys Res Commun* **249**, 767-772
28. Harrison, R. (2002) Structure and function of xanthine oxidoreductase: where are we now? *Free Radic Biol Med* **33**, 774-797
29. Münzel, T., Daiber, A., and Mülsch, A. (2005) Explaining the phenomenon of nitrate tolerance. *Circ Res* **97**, 618-628
30. Münzel, T., Sayegh, H., Freeman, B. A., Tarpey, M. M., and Harrison, D. G. (1995) Evidence for enhanced vascular superoxide anion production in nitrate tolerance. A novel mechanism underlying tolerance and cross-tolerance. *J Clin Invest* **95**, 187-194
31. Beckman, J. S., and Koppenol, W. H. (1996) Nitric oxide, superoxide, and peroxynitrite: the good, the bad, and ugly. *Am J Physiol* **271**, C1424-1437
32. Beckman, J. S., Beckman, T. W., Chen, J., Marshall, P. A., and Freeman, B. A. (1990) Apparent hydroxyl radical production by peroxynitrite: implications for endothelial injury from nitric oxide and superoxide. *Proc Natl Acad Sci U S A* **87**, 1620-1624
33. Godber, B. L., Doel, J. J., Goult, T. A., Eisenthal, R., and Harrison, R. (2001) Suicide inactivation of xanthine oxidoreductase during reduction of inorganic nitrite to nitric oxide. *Biochem J* **358**, 325-333
34. Verhaar, M. C., Westerweel, P. E., van Zonneveld, A. J., and Rabelink, T. J. (2004) Free radical production by dysfunctional eNOS. *Heart* **90**, 494-495
35. Berry, C. E., and Hare, J. M. (2004) Xanthine oxidoreductase and cardiovascular disease: molecular mechanisms and pathophysiological implications. *J Physiol* **555**, 589-606

36. D'Souza, Y., Kawamoto, T., and Bennett, B. M. (2014) Role of the lipid peroxidation product, 4-hydroxynonenal, in the development of nitrate tolerance. *Chem Res Toxicol* **27**, 663-673
37. Schächinger, V., and Zeiher, A. M. (2000) Atherosclerosis-associated endothelial dysfunction. *Z Kardiol* **89 Suppl 9**, IX/70-74
38. Abou-Mohamed, G., Johnson, J. A., Jin, L., El-Remessy, A. B., Do, K., Kaesemeyer, W. H., Caldwell, R. B., and Caldwell, R. W. (2004) Roles of superoxide, peroxynitrite, and protein kinase C in the development of tolerance to nitroglycerin. *J Pharmacol Exp Ther* **308**, 289-299
39. Daiber, A., Oelze, M., Coldewey, M., Kaiser, K., Huth, C., Schildknecht, S., Bachschmid, M., Nazirisadeh, Y., Ullrich, V., Mülsch, A., Münzel, T., and Tsilimingas, N. (2005) Hydralazine is a powerful inhibitor of peroxynitrite formation as a possible explanation for its beneficial effects on prognosis in patients with congestive heart failure. *Biochem Biophys Res Commun* **338**, 1865-1874
40. Daiber, A., Mülsch, A., Hink, U., Mollnau, H., Warnholtz, A., Oelze, M., and Münzel, T. (2005) The oxidative stress concept of nitrate tolerance and the antioxidant properties of hydralazine. *Am J Cardiol* **96**, 25i-36i
41. Watanabe, H., Kakihana, M., Ohtsuka, S., and Sugishita, Y. (1998) Randomized, double-blind, placebo-controlled study of the preventive effect of supplemental oral vitamin C on attenuation of development of nitrate tolerance. *J Am Coll Cardiol* **31**, 1323-1329
42. Bassenge, E., and Fink, B. (1996) Tolerance to nitrates and simultaneous upregulation of platelet activity prevented by enhancing antioxidant state. *Naunyn Schmiedebergs Arch Pharmacol* **353**, 363-367
43. Bassenge, E., Fink, N., Skatchkov, M., and Fink, B. (1998) Dietary supplement with vitamin C prevents nitrate tolerance. *J Clin Invest* **102**, 67-71
44. McKnight, G. M., Duncan, C. W., Leifert, C., and Golden, M. H. (1999) Dietary nitrate in man: friend or foe? *Br J Nutr* **81**, 349-358
45. Hord, N. G., Tang, Y., and Bryan, N. S. (2009) Food sources of nitrates and nitrites: the physiologic context for potential health benefits. *Am J Clin Nutr* **90**, 1-10
46. Lundberg, J. O., Weitzberg, E., and Gladwin, M. T. (2008) The nitrate-nitrite-nitric oxide pathway in physiology and therapeutics. *Nat Rev Drug Discov* **7**, 156-167
47. Lundberg, J. O., Weitzberg, E., Lundberg, J. M., and Alving, K. (1994) Intragastric nitric oxide production in humans: measurements in expelled air. *Gut* **35**, 1543-1546
48. Benjamin, N., O'Driscoll, F., Dougall, H., Duncan, C., Smith, L., Golden, M., and McKenzie, H. (1994) Stomach NO synthesis. *Nature* **368**, 502
49. Zweier, J. L., Wang, P., Samouilov, A., and Kuppusamy, P. (1995) Enzyme-independent formation of nitric oxide in biological tissues. *Nat Med* **1**, 804-809
50. Cosby, K., Partovi, K. S., Crawford, J. H., Patel, R. P., Reiter, C. D., Martyr, S., Yang, B. K., Waclawiw, M. A., Zalos, G., Xu, X., Huang, K. T., Shields, H., Kim-Shapiro, D. B., Schechter, A. N., Cannon, R. O., and Gladwin, M. T. (2003) Nitrite reduction to nitric oxide by deoxyhemoglobin vasodilates the human circulation. *Nat Med* **9**, 1498-1505
51. Lundberg, J. O., and Weitzberg, E. (2005) NO generation from nitrite and its role in vascular control. *Arterioscler Thromb Vasc Biol* **25**, 915-922
52. Lundberg, J. O., and Govoni, M. (2004) Inorganic nitrate is a possible source for systemic generation of nitric oxide. *Free Radic Biol Med* **37**, 395-400
53. Petersson, J., Carlström, M., Schreiber, O., Phillipson, M., Christoffersson, G., Jägare, A., Roos, S., Jansson, E. A., Persson, A. E., Lundberg, J. O., and Holm, L. (2009)

Gastroprotective and blood pressure lowering effects of dietary nitrate are abolished by an antiseptic mouthwash. *Free Radic Biol Med* **46**, 1068-1075

54. Govoni, M., Jansson, E. A., Weitzberg, E., and Lundberg, J. O. (2008) The increase in plasma nitrite after a dietary nitrate load is markedly attenuated by an antibacterial mouthwash. *Nitric Oxide* **19**, 333-337
55. Weitzberg, E., and Lundberg, J. O. (2013) Novel aspects of dietary nitrate and human health. *Annu Rev Nutr* **33**, 129-159
56. Peri, L., Pietraforte, D., Scorza, G., Napolitano, A., Fogliano, V., and Minetti, M. (2005) Apples increase nitric oxide production by human saliva at the acidic pH of the stomach: a new biological function for polyphenols with a catechol group? *Free Radic Biol Med* **39**, 668-681
57. Lundberg, J. O., and Weitzberg, E. (2010) NO-synthase independent NO generation in mammals. *Biochem Biophys Res Commun* **396**, 39-45
58. Sobko, T., Marcus, C., Govoni, M., and Kamiya, S. (2010) Dietary nitrate in Japanese traditional foods lowers diastolic blood pressure in healthy volunteers. *Nitric Oxide* **22**, 136-140
59. Hord, N. G., Ghannam, J. S., Garg, H. K., Berens, P. D., and Bryan, N. S. (2011) Nitrate and nitrite content of human, formula, bovine, and soy milks: implications for dietary nitrite and nitrate recommendations. *Breastfeed Med* **6**, 393-399
60. Lundberg, J. O., Carlström, M., Larsen, F. J., and Weitzberg, E. (2011) Roles of dietary inorganic nitrate in cardiovascular health and disease. *Cardiovasc Res* **89**, 525-532
61. Larsen, F. J., Ekblom, B., Sahlin, K., Lundberg, J. O., and Weitzberg, E. (2006) Effects of dietary nitrate on blood pressure in healthy volunteers. *N Engl J Med* **355**, 2792-2793
62. Larsen, F. J., Weitzberg, E., Lundberg, J. O., and Ekblom, B. (2007) Effects of dietary nitrate on oxygen cost during exercise. *Acta Physiol (Oxf)* **191**, 59-66
63. Webb, A. J., Patel, N., Loukogeorgakis, S., Okorie, M., Aboud, Z., Misra, S., Rashid, R., Miall, P., Deanfield, J., Benjamin, N., MacAllister, R., Hobbs, A. J., and Ahluwalia, A. (2008) Acute blood pressure lowering, vasoprotective, and antiplatelet properties of dietary nitrate via bioconversion to nitrite. *Hypertension* **51**, 784-790
64. Kenjale, A. A., Ham, K. L., Stabler, T., Robbins, J. L., Johnson, J. L., Vanbruggen, M., Privette, G., Yim, E., Kraus, W. E., and Allen, J. D. (2011) Dietary nitrate supplementation enhances exercise performance in peripheral arterial disease. *J Appl Physiol (1985)* **110**, 1582-1591
65. Tsuchiya, K., Kanematsu, Y., Yoshizumi, M., Ohnishi, H., Kirima, K., Izawa, Y., Shikishima, M., Ishida, T., Kondo, S., Kagami, S., Takiguchi, Y., and Tamaki, T. (2005) Nitrite is an alternative source of NO in vivo. *Am J Physiol Heart Circ Physiol* **288**, H2163-2170
66. Kanematsu, Y., Yamaguchi, K., Ohnishi, H., Motobayashi, Y., Ishizawa, K., Izawa, Y., Kawazoe, K., Kondo, S., Kagami, S., Tomita, S., Tsuchiya, K., and Tamaki, T. (2008) Dietary doses of nitrite restore circulating nitric oxide level and improve renal injury in L-NAME-induced hypertensive rats. *Am J Physiol Renal Physiol* **295**, F1457-1462
67. Poole, D. C., and Richardson, R. S. (1997) Determinants of oxygen uptake. Implications for exercise testing. *Sports Med* **24**, 308-320
68. Lansley, K. E., Winyard, P. G., Bailey, S. J., Vanhatalo, A., Wilkerson, D. P., Blackwell, J. R., Gilchrist, M., Benjamin, N., and Jones, A. M. (2011) Acute dietary nitrate supplementation improves cycling time trial performance. *Med Sci Sports Exerc* **43**, 1125-1131

69. Cermak, N. M., Gibala, M. J., and van Loon, L. J. (2012) Nitrate supplementation's improvement of 10-km time-trial performance in trained cyclists. *Int J Sport Nutr Exerc Metab* **22**, 64-71
70. Cermak, N. M., Res, P., Stinkens, R., Lundberg, J. O., Gibala, M. J., and van Loon, L. J. (2012) No improvement in endurance performance after a single dose of beetroot juice. *Int J Sport Nutr Exerc Metab* **22**, 470-478
71. Wilkerson, D. P., Hayward, G. M., Bailey, S. J., Vanhatalo, A., Blackwell, J. R., and Jones, A. M. (2012) Influence of acute dietary nitrate supplementation on 50 mile time trial performance in well-trained cyclists. *Eur J Appl Physiol* **112**, 4127-4134
72. Bescós, R., Ferrer-Roca, V., Galilea, P. A., Roig, A., Drobnic, F., Sureda, A., Martorell, M., Cordova, A., Tur, J. A., and Pons, A. (2012) Sodium nitrate supplementation does not enhance performance of endurance athletes. *Med Sci Sports Exerc* **44**, 2400-2409
73. Peacock, O., Tjønna, A. E., James, P., Wisløff, U., Welde, B., Böhlke, N., Smith, A., Stokes, K., Cook, C., and Sandbakk, O. (2012) Dietary nitrate does not enhance running performance in elite cross-country skiers. *Med Sci Sports Exerc* **44**, 2213-2219
74. Nybo, L. (2008) Viewpoint: Fatigue mechanisms determining exercise performance: integrative physiology is systems physiology. *J Appl Physiol (1985)* **104**, 1543-1544
75. Rooks, C. R., Thom, N. J., McCully, K. K., and Dishman, R. K. (2010) Effects of incremental exercise on cerebral oxygenation measured by near-infrared spectroscopy: a systematic review. *Prog Neurobiol* **92**, 134-150
76. Rupp, T., Thomas, R., Perrey, S., and Stephane, P. (2008) Prefrontal cortex oxygenation and neuromuscular responses to exhaustive exercise. *Eur J Appl Physiol* **102**, 153-163
77. Marcora, S. M., Staiano, W., and Manning, V. (2009) Mental fatigue impairs physical performance in humans. *J Appl Physiol (1985)* **106**, 857-864
78. Presley, T. D., Morgan, A. R., Bechtold, E., Clodfelter, W., Dove, R. W., Jennings, J. M., Kraft, R. A., King, S. B., Laurienti, P. J., Rejeski, W. J., Burdette, J. H., Kim-Shapiro, D. B., and Miller, G. D. (2011) Acute effect of a high nitrate diet on brain perfusion in older adults. *Nitric Oxide* **24**, 34-42
79. Thompson, K. G., Turner, L., Prichard, J., Dodd, F., Kennedy, D. O., Haskell, C., Blackwell, J. R., and Jones, A. M. (2014) Influence of dietary nitrate supplementation on physiological and cognitive responses to incremental cycle exercise. *Respir Physiol Neurobiol* **193**, 11-20
80. Gilchrist, M., Winyard, P. G., Fulford, J., Anning, C., Shore, A. C., and Benjamin, N. (2014) Dietary nitrate supplementation improves reaction time in type 2 diabetes: development and application of a novel nitrate-depleted beetroot juice placebo. *Nitric Oxide* **40**, 67-74
81. Wightman, E. L., Haskell-Ramsay, C. F., Thompson, K. G., Blackwell, J. R., Winyard, P. G., Forster, J., Jones, A. M., and Kennedy, D. O. (2015) Dietary nitrate modulates cerebral blood flow parameters and cognitive performance in humans: A double-blind, placebo-controlled, crossover investigation. *Physiol Behav* **149**, 149-158
82. Vanhatalo, A., Bailey, S. J., Blackwell, J. R., DiMenna, F. J., Pavey, T. G., Wilkerson, D. P., Benjamin, N., Winyard, P. G., and Jones, A. M. (2010) Acute and chronic effects of dietary nitrate supplementation on blood pressure and the physiological responses to moderate-intensity and incremental exercise. *Am J Physiol Regul Integr Comp Physiol* **299**, R1121-1131
83. Peleli, M., Zollbrecht, C., Montenegro, M. F., Hezel, M., Zhong, J., Persson, E. G., Holmdahl, R., Weitzberg, E., Lundberg, J. O., and Carlström, M. (2016) Enhanced XOR

activity in eNOS-deficient mice: Effects on the nitrate-nitrite-NO pathway and ROS homeostasis. *Free Radic Biol Med* **99**, 472-484

84. Larsen, F. J., Schiffer, T. A., Borniquel, S., Sahlin, K., Ekblom, B., Lundberg, J. O., and Weitzberg, E. (2011) Dietary inorganic nitrate improves mitochondrial efficiency in humans. *Cell Metab* **13**, 149-159
85. Brown, G. C., and Cooper, C. E. (1994) Nanomolar concentrations of nitric oxide reversibly inhibit synaptosomal respiration by competing with oxygen at cytochrome oxidase. *FEBS Lett* **356**, 295-298
86. Nisoli, E., Clementi, E., Paolucci, C., Cozzi, V., Tonello, C., Sciorati, C., Bracale, R., Valerio, A., Francolini, M., Moncada, S., and Carruba, M. O. (2003) Mitochondrial biogenesis in mammals: the role of endogenous nitric oxide. *Science* **299**, 896-899
87. Bailey, S. J., Fulford, J., Vanhatalo, A., Winyard, P. G., Blackwell, J. R., DiMenna, F. J., Wilkerson, D. P., Benjamin, N., and Jones, A. M. (2010) Dietary nitrate supplementation enhances muscle contractile efficiency during knee-extensor exercise in humans. *J Appl Physiol (1985)* **109**, 135-148
88. Evangelista, A. M., Rao, V. S., Filo, A. R., Marozkina, N. V., Doctor, A., Jones, D. R., Gaston, B., and Guilford, W. H. (2010) Direct regulation of striated muscle myosins by nitric oxide and endogenous nitrosothiols. *PLoS One* **5**, e11209
89. Viner, R. I., Williams, T. D., and Schöneich, C. (2000) Nitric oxide-dependent modification of the sarcoplasmic reticulum Ca-ATPase: localization of cysteine target sites. *Free Radic Biol Med* **29**, 489-496
90. Hernández, A., Schiffer, T. A., Ivarsson, N., Cheng, A. J., Bruton, J. D., Lundberg, J. O., Weitzberg, E., and Westerblad, H. (2012) Dietary nitrate increases tetanic [Ca2+]i and contractile force in mouse fast-twitch muscle. *J Physiol* **590**, 3575-3583
91. Sen, N. P., Smith, D. C., and Schwinghamer, L. (1969) Formation of N-nitrosamines from secondary amines and nitrite in human and animal gastric juice. *Food Cosmet Toxicol* **7**, 301-307
92. Cuello, C., Correa, P., Haenszel, W., Gordillo, G., Brown, C., Archer, M., and Tannenbaum, S. (1976) Gastric cancer in Colombia. I. Cancer risk and suspect environmental agents. *J Natl Cancer Inst* **57**, 1015-1020
93. Armijo, R., Gonzalez, A., Orellana, M., Coulson, A. H., Sayre, J. W., and Detels, R. (1981) Epidemiology of gastric cancer in Chile: II - Nitrate exposures and stomach cancer frequency. *Int J Epidemiol* **10**, 57-62
94. Ohshima, H., and Bartsch, H. (1981) Quantitative estimation of endogenous nitrosation in humans by monitoring N-nitrosoproline excreted in the urine. *Cancer Res* **41**, 3658-3662
95. Correa, P., Haenszel, W., Cuello, C., Zavala, D., Fontham, E., Zarama, G., Tannenbaum, S., Collazos, T., and Ruiz, B. (1990) Gastric precancerous process in a high risk population: cross-sectional studies. *Cancer Res* **50**, 4731-4736
96. Rademacher, J. J., Young, T. B., and Kanarek, M. S. (1992) Gastric cancer mortality and nitrate levels in Wisconsin drinking water. *Arch Environ Health* **47**, 292-294
97. Comly, H. H. (1987) Landmark article Sept 8, 1945: Cyanosis in infants caused by nitrates in well-water. By Hunter H. Comly. *JAMA* **257**, 2788-2792
98. DONAHOE, W. E. (1949) Cyanosis in infants with nitrates in drinking water as cause. *Pediatrics* **3**, 308-311
99. Low, H. (1974) Nitroso compounds: safety and public health. *Arch Environ Health* **29**, 256-260

100. Magee, P. N., and Barnes, J. M. (1967) Carcinogenic nitroso compounds. *Adv Cancer Res* **10**, 163-246
101. Bartsch, H., Ohshima, H., and Pignatelli, B. (1988) Inhibitors of endogenous nitrosation. Mechanisms and implications in human cancer prevention. *Mutat Res* **202**, 307-324
102. Sobala, G. M., Schorah, C. J., Sanderson, M., Dixon, M. F., Tompkins, D. S., Godwin, P., and Axon, A. T. (1989) Ascorbic acid in the human stomach. *Gastroenterology* **97**, 357-363
103. Forman, D., Al-Dabbagh, S., and Doll, R. (1985) Nitrates, nitrites and gastric cancer in Great Britain. *Nature* **313**, 620-625
104. Knight, T. M., Forman, D., Pirastu, R., Comba, P., Iannarilli, R., Cocco, P. L., Angotzi, G., Ninu, E., and Schierano, S. (1990) Nitrate and nitrite exposure in Italian populations with different gastric cancer rates. *Int J Epidemiol* **19**, 510-515
105. Boeing, H. (1991) Epidemiological research in stomach cancer: progress over the last ten years. *J Cancer Res Clin Oncol* **117**, 133-143
106. Pobel, D., Riboli, E., Cornée, J., Hémon, B., and Guyader, M. (1995) Nitrosamine, nitrate and nitrite in relation to gastric cancer: a case-control study in Marseille, France. *Eur J Epidemiol* **11**, 67-73
107. Key, T. J., Thorogood, M., Appleby, P. N., and Burr, M. L. (1996) Dietary habits and mortality in 11,000 vegetarians and health conscious people: results of a 17 year follow up. *BMJ* **313**, 775-779
108. Corella, D., Cortina, P., Guillén, M., and González, J. I. (1996) Dietary habits and geographic variation in stomach cancer mortality in Spain. *Eur J Cancer Prev* **5**, 249-257
109. González, C. A., Sanz, J. M., Marcos, G., Pita, S., Brullet, E., Saigi, E., Badia, A., and Riboli, E. (1991) Dietary factors and stomach cancer in Spain: a multi-centre case-control study. *Int J Cancer* **49**, 513-519
110. Correa, P., and Chen, V. W. (1994) Gastric cancer. *Cancer Surv* **19-20**, 55-76
111. Johnson, C. J., and Kross, B. C. (1990) Continuing importance of nitrate contamination of groundwater and wells in rural areas. *Am J Ind Med* **18**, 449-456
112. HOWARTH, B. E. (1951) Epidemic of aniline methaemoglobinaemia in newborn babies. *Lancet* **1**, 934-935
113. Czapski, G., and Goldstein, S. (1995) The role of the reactions of .NO with superoxide and oxygen in biological systems: a kinetic approach. *Free Radic Biol Med* **19**, 785-794
114. Tsikas, D. (2005) Methods of quantitative analysis of the nitric oxide metabolites nitrite and nitrate in human biological fluids. *Free Radic Res* **39**, 797-815
115. Moorcroft, M. J., Davis, J., and Compton, R. G. (2001) Detection and determination of nitrate and nitrite: a review. *Talanta* **54**, 785-803
116. Jobgen, W. S., Jobgen, S. C., Li, H., Meininger, C. J., and Wu, G. (2007) Analysis of nitrite and nitrate in biological samples using high-performance liquid chromatography. *J Chromatogr B Analyt Technol Biomed Life Sci* **851**, 71-82
117. Kind, T., and Fiehn, O. (2006) Metabolomic database annotations via query of elemental compositions: mass accuracy is insufficient even at less than 1 ppm. *BMC Bioinformatics* **7**, 234
118. Moncada, S., and Higgs, E. A. (1991) Endogenous nitric oxide: physiology, pathology and clinical relevance. *Eur J Clin Invest* **21**, 361-374
119. Culotta, E., and Koshland, D. E. (1992) NO news is good news. *Science* **258**, 1862-1865

120. Li, H., Samouilov, A., Liu, X., and Zweier, J. L. (2003) Characterization of the magnitude and kinetics of xanthine oxidase-catalyzed nitrate reduction: evaluation of its role in nitrite and nitric oxide generation in anoxic tissues. *Biochemistry* **42**, 1150-1159
121. Ellis, G., Adatia, I., Yazdanpanah, M., and Makela, S. K. (1998) Nitrite and nitrate analyses: a clinical biochemistry perspective. *Clin Biochem* **31**, 195-220
122. Marzinzig, M., Nussler, A. K., Stadler, J., Marzinzig, E., Barthlen, W., Nussler, N. C., Beger, H. G., Morris, S. M., and Brückner, U. B. (1997) Improved methods to measure end products of nitric oxide in biological fluids: nitrite, nitrate, and S-nitrosothiols. *Nitric Oxide* **1**, 177-189
123. Di Matteo, V., and Esposito, E. (1997) Methods for the determination of nitrite by high-performance liquid chromatography with electrochemical detection. *J Chromatogr A* **789**, 213-219
124. Tsikas, D., Böhmer, A., Mitschke, A., and Araujo, P. (2013) Accurate measurement of nitrate, nitrite, and S-nitrosothiols in biological samples by mass spectrometry. *Free Radic Biol Med* **65**, 301-304
125. Shin, S., and Fung, H. L. (2011) Evaluation of an LC-MS/MS assay for 15N-nitrite for cellular studies of L-arginine action. *J Pharm Biomed Anal* **56**, 1127-1131
126. Batugo, M. R., Nardi, C. D., Johnson, T. R., Biondi, S., and Impagnatiello, F. (2009) Determination of exogenous nitric oxide using stable labeled nitrogen coupled with liquid-chromatography-mass spectrometry. AAPS J.
127. Wiersma, J. H. (1970) 2,3-Diaminonaphthalene as a Spectrophotometric and Fluorometric Reagent for the Determination of Nitrite Ion. Anal. Lett.
128. May, J. M., Qu, Z. C., and Li, X. (2004) Nitrite generates an oxidant stress and increases nitric oxide in EA.hy926 endothelial cells. *Free Radic Res* **38**, 581-589
129. Hinz, B., and Schröder, H. (1998) Vitamin C attenuates nitrate tolerance independently of its antioxidant effect. *FEBS Lett* **428**, 97-99
130. Wu, G. Y., and Brosnan, J. T. (1992) Macrophages can convert citrulline into arginine. *Biochem J* **281 (Pt 1)**, 45-48
131. Li, H., Meininger, C. J., and Wu, G. (2000) Rapid determination of nitrite by reversed-phase high-performance liquid chromatography with fluorescence detection. *J Chromatogr B Biomed Sci Appl* **746**, 199-207
132. Misko, T. P., Schilling, R. J., Salvemini, D., Moore, W. M., and Currie, M. G. (1993) A fluorometric assay for the measurement of nitrite in biological samples. *Anal Biochem* **214**, 11-16
133. Gharavi, N., and El-Kadi, A. O. (2003) Measurement of nitric oxide in murine Hepatoma Hepa1c1c7 cells by reversed phase HPLC with fluorescence detection. *J Pharm Pharm Sci* **6**, 302-307
134. Woitzik, J., Abromeit, N., and Schaefer, F. (2001) Measurement of nitric oxide metabolites in brain microdialysates by a sensitive fluorometric high-performance liquid chromatography assay. *Anal Biochem* **289**, 10-17
135. Tsikas, D. (2015) Circulating and excretory nitrite and nitrate: their value as measures of nitric oxide synthesis, bioavailability and activity is inherently limited. *Nitric Oxide* **45**, 1-3
136. Kleinbongard, P., Dejam, A., Lauer, T., Jax, T., Kerber, S., Gharini, P., Balzer, J., Zotz, R. B., Scharf, R. E., Willers, R., Schechter, A. N., Feelisch, M., and Kelm, M. (2006) Plasma nitrite concentrations reflect the degree of endothelial dysfunction in humans. *Free Radic Biol Med* **40**, 295-302

137. Tsikas, D. (2000) Simultaneous derivatization and quantification of the nitric oxide metabolites nitrite and nitrate in biological fluids by gas chromatography/mass spectrometry. *Anal Chem* **72**, 4064-4072
138. Task Force Members, M. G., Sechtem U, Achenbach S, Andreotti F, Arden C,, and al., e. (2013) ESC Guidelines on the management of stable coronary artery disease: the task force on the management of stable coronary artery disease of the European Society of Cardiology. Eur Heart J
139. Kleschyov, A. L., Oelze, M., Daiber, A., Huang, Y., Mollnau, H., Schulz, E., Sydow, K., Fichtlscherer, B., Mülsch, A., and Münzel, T. (2003) Does nitric oxide mediate the vasodilator activity of nitroglycerin? *Circ Res* **93**, e104-112
140. Núñez, C., Víctor, V. M., Tur, R., Alvarez-Barrientos, A., Moncada, S., Esplugues, J. V., and D'Ocón, P. (2005) Discrepancies between nitroglycerin and NO-releasing drugs on mitochondrial oxygen consumption, vasoactivity, and the release of NO. *Circ Res* **97**, 1063-1069
141. Rapoport, R. M., Waldman, S. A., Ginsburg, R., Molina, C. R., and Murad, F. (1987) Effects of glyceryl trinitrate on endothelium-dependent and -independent relaxation and cyclic GMP levels in rat aorta and human coronary artery. *J Cardiovasc Pharmacol* **10**, 82-89
142. Parker, J. D., Farrell, B., Fenton, T., Cohanim, M., and Parker, J. O. (1991) Counter-regulatory responses to continuous and intermittent therapy with nitroglycerin. *Circulation* **84**, 2336-2345
143. Hink, U., Oelze, M., Kolb, P., Bachschmid, M., Zou, M. H., Daiber, A., Mollnau, H., August, M., Baldus, S., Tsilimingas, N., Walter, U., Ullrich, V., and Münzel, T. (2003) Role for peroxynitrite in the inhibition of prostacyclin synthase in nitrate tolerance. *J Am Coll Cardiol* **42**, 1826-1834
144. Dikalov, S., Fink, B., Skatchkov, M., Sommer, O., and Bassenge, E. (1998) Formation of Reactive Oxygen Species in Various Vascular Cells During Glyceryltrinitrate Metabolism. *J Cardiovasc Pharmacol Ther* **3**, 51-62
145. Münzel, T., Steven, S., and Daiber, A. (2014) Organic nitrates: update on mechanisms underlying vasodilation, tolerance and endothelial dysfunction. *Vascul Pharmacol* **63**, 105-113
146. Levine, G. N., Frei, B., Koulouris, S. N., Gerhard, M. D., Keaney, J. F., and Vita, J. A. (1996) Ascorbic acid reverses endothelial vasomotor dysfunction in patients with coronary artery disease. *Circulation* **93**, 1107-1113
147. Kugiyama, K., Motoyama, T., Hirashima, O., Ohgushi, M., Soejima, H., Misumi, K., Kawano, H., Miyao, Y., Yoshimura, M., Ogawa, H., Matsumura, T., Sugiyama, S., and Yasue, H. (1998) Vitamin C attenuates abnormal vasomotor reactivity in spasm coronary arteries in patients with coronary spastic angina. *J Am Coll Cardiol* **32**, 103-109
148. McVeigh, G. E., Hamilton, P., Wilson, M., Hanratty, C. G., Leahey, W. J., Devine, A. B., Morgan, D. G., Dixon, L. J., and McGrath, L. T. (2002) Platelet nitric oxide and superoxide release during the development of nitrate tolerance: effect of supplemental ascorbate. *Circulation* **106**, 208-213
149. Johnston, C. S., Meyer, C. G., and Srilakshmi, J. C. (1993) Vitamin C elevates red blood cell glutathione in healthy adults. *Am J Clin Nutr* **58**, 103-105
150. Huang, A., Vita, J. A., Venema, R. C., and Keaney, J. F. (2000) Ascorbic acid enhances endothelial nitric-oxide synthase activity by increasing intracellular tetrahydrobiopterin. *J Biol Chem* **275**, 17399-17406

151. Millar, J. (1995) The nitric oxide/ascorbate cycle: how neurones may control their own oxygen supply. *Med Hypotheses* **45**, 21-26
152. Axton, E. R., Hardardt, E. A., and Stevens, J. F. (2016) Stable isotope-assisted LC-MS/MS monitoring of glyceryl trinitrate bioactivation in a cell culture model of nitrate tolerance. *J Chromatogr B Analyt Technol Biomed Life Sci* **1019**, 156-163
153. Frei, B., England, L., and Ames, B. N. (1989) Ascorbate is an outstanding antioxidant in human blood plasma. *Proc Natl Acad Sci U S A* **86**, 6377-6381
154. Kirkwood, J. S., Lebold, K. M., Miranda, C. L., Wright, C. L., Miller, G. W., Tanguay, R. L., Barton, C. L., Traber, M. G., and Stevens, J. F. (2012) Vitamin C deficiency activates the purine nucleotide cycle in zebrafish. *J Biol Chem* **287**, 3833-3841
155. Xia, J., and Wishart, D. S. (2016) Using MetaboAnalyst 3.0 for Comprehensive Metabolomics Data Analysis. *Curr Protoc Bioinformatics* **55**, 14.10.11-14.10.91
156. Watanabe, H., Kakihana, M., Ohtsuka, S., Enomoto, T., Yasui, K., and Sugishita, Y. (1993) Platelet cyclic GMP. A potentially useful indicator to evaluate the effects of nitroglycerin and nitrate tolerance. *Circulation* **88**, 29-36
157. Wenzl, M. V., Wölkart, G., Stessel, H., Beretta, M., Schmidt, K., and Mayer, B. (2009) Different effects of ascorbate deprivation and classical vascular nitrate tolerance on aldehyde dehydrogenase-catalysed bioactivation of nitroglycerin. *Br J Pharmacol* **156**, 1248-1255
158. Ji, Y., and Bennett, B. M. (2003) Activation of microsomal glutathione s-transferase by peroxynitrite. *Mol Pharmacol* **63**, 136-146
159. Laursen, J. B., Somers, M., Kurz, S., McCann, L., Warnholtz, A., Freeman, B. A., Tarpey, M., Fukai, T., and Harrison, D. G. (2001) Endothelial regulation of vasomotion in apoE-deficient mice: implications for interactions between peroxynitrite and tetrahydrobiopterin. *Circulation* **103**, 1282-1288
160. Kuzkaya, N., Weissmann, N., Harrison, D. G., and Dikalov, S. (2003) Interactions of peroxynitrite, tetrahydrobiopterin, ascorbic acid, and thiols: implications for uncoupling endothelial nitric-oxide synthase. *J Biol Chem* **278**, 22546-22554
161. Oelze, M., Knorr, M., Schell, R., Kamuf, J., Pautz, A., Art, J., Wenzel, P., Münzel, T., Kleinert, H., and Daiber, A. (2011) Regulation of human mitochondrial aldehyde dehydrogenase (ALDH-2) activity by electrophiles in vitro. *J Biol Chem* **286**, 8893-8900
162. Needleman, P., and Hunter, F. E. (1966) Effects of organic nitrates on mitochondrial respiration and swelling: possible correlations with the mechanism of pharmacologic action. *Mol Pharmacol* **2**, 134-143
163. Shiva, S., Oh, J. Y., Landar, A. L., Ulasova, E., Venkatraman, A., Bailey, S. M., and Darley-Usmar, V. M. (2005) Nitroxia: the pathological consequence of dysfunction in the nitric oxide-cytochrome c oxidase signaling pathway. *Free Radic Biol Med* **38**, 297-306
164. Miranda, C. L., Reed, R. L., Kuiper, H. C., Alber, S., and Stevens, J. F. (2009) Ascorbic acid promotes detoxification and elimination of 4-hydroxy-2(E)-nonenal in human monocytic THP-1 cells. *Chem Res Toxicol* **22**, 863-874
165. Shapiro, I. M., Leboy, P. S., Tokuoka, T., Forbes, E., DeBolt, K., Adams, S. L., and Pacifici, M. (1991) Ascorbic acid regulates multiple metabolic activities of cartilage cells. *Am J Clin Nutr* **54**, 1209S-1213S
166. Ohtsubo, T., Rovira, I. I., Starost, M. F., Liu, C., and Finkel, T. (2004) Xanthine oxidoreductase is an endogenous regulator of cyclooxygenase-2. *Circ Res* **95**, 1118-1124

167. Hinz, B., and Schröder, H. (1998) Nitrate tolerance is specific for nitric acid esters and its recovery requires an intact protein synthesis. *Biochem Biophys Res Commun* **252**, 232-235
168. Vita, J. A., Keaney, J. F., Raby, K. E., Morrow, J. D., Freedman, J. E., Lynch, S., Koulouris, S. N., Hankin, B. R., and Frei, B. (1998) Low plasma ascorbic acid independently predicts the presence of an unstable coronary syndrome. *J Am Coll Cardiol* **31**, 980-986
169. Nyyssönen, K., Parviainen, M. T., Salonen, R., Tuomilehto, J., and Salonen, J. T. (1997) Vitamin C deficiency and risk of myocardial infarction: prospective population study of men from eastern Finland. *BMJ* **314**, 634-638
170. Larsen, F. J., Weitzberg, E., Lundberg, J. O., and Ekblom, B. (2010) Dietary nitrate reduces maximal oxygen consumption while maintaining work performance in maximal exercise. *Free Radic Biol Med* **48**, 342-347
171. Bailey, S. J., Winyard, P., Vanhatalo, A., Blackwell, J. R., Dimenna, F. J., Wilkerson, D. P., Tarr, J., Benjamin, N., and Jones, A. M. (2009) Dietary nitrate supplementation reduces the O2 cost of low-intensity exercise and enhances tolerance to high-intensity exercise in humans. *J Appl Physiol (1985)* **107**, 1144-1155
172. Giraldez, R. R., Panda, A., Xia, Y., Sanders, S. P., and Zweier, J. L. (1997) Decreased nitric-oxide synthase activity causes impaired endothelium-dependent relaxation in the postischemic heart. *J Biol Chem* **272**, 21420-21426
173. Ostergaard, L., Stankevicius, E., Andersen, M. R., Eskildsen-Helmond, Y., Ledet, T., Mulvany, M. J., and Simonsen, U. (2007) Diminished NO release in chronic hypoxic human endothelial cells. *Am J Physiol Heart Circ Physiol* **293**, H2894-2903
174. Larsen, F. J., Schiffer, T. A., Ekblom, B., Mattsson, M. P., Checa, A., Wheelock, C. E., Nyström, T., Lundberg, J. O., and Weitzberg, E. (2014) Dietary nitrate reduces resting metabolic rate: a randomized, crossover study in humans. *Am J Clin Nutr* **99**, 843-850
175. Babcock, G. T., and Wikström, M. (1992) Oxygen activation and the conservation of energy in cell respiration. *Nature* **356**, 301-309
176. Bugel, S. M., Tanguay, R. L., and Planchart, A. (2014) Zebrafish: A marvel of high-throughput biology for 21(st) century toxicology. *Curr Environ Health Rep* **1**, 341-352
177. Kimmel, C. B., Ballard, W. W., Kimmel, S. R., Ullmann, B., and Schilling, T. F. (1995) Stages of embryonic development of the zebrafish. *Dev Dyn* **203**, 253-310
178. Amsterdam, A., Nissen, R. M., Sun, Z., Swindell, E. C., Farrington, S., and Hopkins, N. (2004) Identification of 315 genes essential for early zebrafish development. *Proc Natl Acad Sci U S A* **101**, 12792-12797
179. Howe, K., Clark, M. D., Torroja, C. F., Torrance, J., Berthelot, C., Muffato, M., Collins, J. E., Humphray, S., McLaren, K., Matthews, L., McLaren, S., Sealy, I., Caccamo, M., Churcher, C., Scott, C., Barrett, J. C., Koch, R., Rauch, G. J., White, S., Chow, W., Kilian, B., Quintais, L. T., Guerra-Assunção, J. A., Zhou, Y., Gu, Y., Yen, J., Vogel, J. H., Eyre, T., Redmond, S., Banerjee, R., Chi, J., Fu, B., Langley, E., Maguire, S. F., Laird, G. K., Lloyd, D., Kenyon, E., Donaldson, S., Sehra, H., Almeida-King, J., Loveland, J., Trevanion, S., Jones, M., Quail, M., Willey, D., Hunt, A., Burton, J., Sims, S., McLay, K., Plumb, B., Davis, J., Clee, C., Oliver, K., Clark, R., Riddle, C., Elliot, D., Eliott, D., Threadgold, G., Harden, G., Ware, D., Begum, S., Mortimore, B., Mortimer, B., Kerry, G., Heath, P., Phillimore, B., Tracey, A., Corby, N., Dunn, M., Johnson, C., Wood, J., Clark, S., Pelan, S., Griffiths, G., Smith, M., Glithero, R., Howden, P., Barker, N., Lloyd, C., Stevens, C., Harley, J., Holt, K., Panagiotidis, G., Lovell, J., Beasley, H., Henderson, C., Gordon, D., Auger, K., Wright, D., Collins, J., Raisen, C., Dyer, L., Leung, K., Robertson, L., Ambridge, K., Leongamornlert, D.,

McGuire, S., Gilderthorp, R., Griffiths, C., Manthravadi, D., Nichol, S., Barker, G., Whitehead, S., Kay, M., Brown, J., Murnane, C., Gray, E., Humphries, M., Sycamore, N., Barker, D., Saunders, D., Wallis, J., Babbage, A., Hammond, S., Mashreghi-Mohammadi, M., Barr, L., Martin, S., Wray, P., Ellington, A., Matthews, N., Ellwood, M., Woodmansey, R., Clark, G., Cooper, J., Tromans, A., Grafham, D., Skuce, C., Pandian, R., Andrews, R., Harrison, E., Kimberley, A., Garnett, J., Fosker, N., Hall, R., Garner, P., Kelly, D., Bird, C., Palmer, S., Gehring, I., Berger, A., Dooley, C. M., Ersan-Ürün, Z., Eser, C., Geiger, H., Geisler, M., Karotki, L., Kirn, A., Konantz, J., Konantz, M., Oberländer, M., Rudolph-Geiger, S., Teucke, M., Lanz, C., Raddatz, G., Osoegawa, K., Zhu, B., Rapp, A., Widaa, S., Langford, C., Yang, F., Schuster, S. C., Carter, N. P., Harrow, J., Ning, Z., Herrero, J., Searle, S. M., Enright, A., Geisler, R., Plasterk, R. H., Lee, C., Westerfield, M., de Jong, P. J., Zon, L. I., Postlethwait, J. H., Nüsslein-Volhard, C., Hubbard, T. J., Roest Crollius, H., Rogers, J., and Stemple, D. L. (2013) The zebrafish reference genome sequence and its relationship to the human genome. *Nature* **496**, 498-503

180. Palstra, A. P., Tudorache, C., Rovira, M., Brittijn, S. A., Burgerhout, E., van den Thillart, G. E., Spaink, H. P., and Planas, J. V. (2010) Establishing zebrafish as a novel exercise model: swimming economy, swimming-enhanced growth and muscle growth marker gene expression. *PLoS One* **5**, e14483
181. Palstra, A. P., Rovira, M., Rizo-Roca, D., Torrella, J. R., Spaink, H. P., and Planas, J. V. (2014) Swimming-induced exercise promotes hypertrophy and vascularization of fast skeletal muscle fibres and activation of myogenic and angiogenic transcriptional programs in adult zebrafish. *BMC Genomics* **15**, 1136
182. Gilbert, M. J., Zerulla, T. C., and Tierney, K. B. (2014) Zebrafish (Danio rerio) as a model for the study of aging and exercise: physical ability and trainability decrease with age. *Exp Gerontol* **50**, 106-113
183. Jensen, F. B. (2007) Nitric oxide formation from nitrite in zebrafish. *J Exp Biol* **210**, 3387-3394
184. Learmonth, C., and Carvalho, A. P. (2015) Acute and Chronic Toxicity of Nitrate to Early Life Stages of Zebrafish-Setting Nitrate Safety Levels for Zebrafish Rearing. *Zebrafish*
185. Voslářová E., V. P., Z. Svobodová, I. Bedáňová. (2008) Nitrite Toxicity to Danio rerio: Effects of Subchronic Exposure on Fish Growth. Acta Vet. Brno
186. Babaei, F., Ramalingam, R., Tavendale, A., Liang, Y., Yan, L. S., Ajuh, P., Cheng, S. H., and Lam, Y. W. (2013) Novel blood collection method allows plasma proteome analysis from single zebrafish. *J Proteome Res* **12**, 1580-1590
187. Moore, J. L., Aros, M., Steudel, K. G., and Cheng, K. C. (2002) Fixation and decalcification of adult zebrafish for histological, immunocytochemical, and genotypic analysis. *Biotechniques* **32**, 296-298
188. Westerfield, M. (2007) The Zebrafish Book, 5th Edition; A guide for the laboratory use of zebrafish (danio rerio). The University of Oregon, Eugene, OR
189. Knecht, A. L., Truong, L., Marvel, S. W., Reif, D. M., Garcia, A., Lu, C., Simonich, M. T., Teeguarden, J. G., and Tanguay, R. L. (2017) Transgenerational inheritance of neurobehavioral and physiological deficits from developmental exposure to benzo[a]pyrene in zebrafish. *Toxicol Appl Pharmacol* **329**, 148-157
190. Masse, A. J., Thomas, J. K., and Janz, D. M. (2013) Reduced swim performance and aerobic capacity in adult zebrafish exposed to waterborne selenite. *Comp Biochem Physiol C Toxicol Pharmacol* **157**, 266-271

191. Marit, J. S., and Weber, L. P. (2011) Acute exposure to 2,4-dinitrophenol alters zebrafish swimming performance and whole body triglyceride levels. *Comp Biochem Physiol C Toxicol Pharmacol* **154**, 14-18
192. Marit, J. S., and Weber, L. P. (2012) Persistent effects on adult swim performance and energetics in zebrafish developmentally exposed to 2,3,7,8-tetrachlorodibenzo-p-dioxin. *Aquat Toxicol* **106-107**, 131-139
193. Thomas, J. K., and Janz, D. M. (2011) Dietary selenomethionine exposure in adult zebrafish alters swimming performance, energetics and the physiological stress response. *Aquat Toxicol* **102**, 79-86
194. Lanza, I. R., and Nair, K. S. (2009) Functional assessment of isolated mitochondria in vitro. *Methods Enzymol* **457**, 349-372
195. Makrecka-Kuka, M., Krumschnabel, G., and Gnaiger, E. (2015) High-Resolution Respirometry for Simultaneous Measurement of Oxygen and Hydrogen Peroxide Fluxes in Permeabilized Cells, Tissue Homogenate and Isolated Mitochondria. *Biomolecules* **5**, 1319-1338
196. Piknova, B., and Schechter, A. N. (2011) Measurement of nitrite in blood samples using the ferricyanide-based hemoglobin oxidation assay. *Methods Mol Biol* **704**, 39-56
197. Sessa, W. C., Pritchard, K., Seyedi, N., Wang, J., and Hintze, T. H. (1994) Chronic exercise in dogs increases coronary vascular nitric oxide production and endothelial cell nitric oxide synthase gene expression. *Circ Res* **74**, 349-353
198. Matsumoto, A., Hirata, Y., Momomura, S., Fujita, H., Yao, A., Sata, M., and Serizawa, T. (1994) Increased nitric oxide production during exercise. *Lancet* **343**, 849-850
199. Patil, R. D., DiCarlo, S. E., and Collins, H. L. (1993) Acute exercise enhances nitric oxide modulation of vascular response to phenylephrine. *Am J Physiol* **265**, H1184-1188
200. Balon, T. W., and Nadler, J. L. (1997) Evidence that nitric oxide increases glucose transport in skeletal muscle. *J Appl Physiol (1985)* **82**, 359-363
201. Hellsten, Y., Hansson, H. A., Johnson, L., Frandsen, U., and Sjödin, B. (1996) Increased expression of xanthine oxidase and insulin-like growth factor I (IGF-I) immunoreactivity in skeletal muscle after strenuous exercise in humans. *Acta Physiol Scand* **157**, 191-197
202. Piknova, B., Park, J. W., Swanson, K. M., Dey, S., Noguchi, C. T., and Schechter, A. N. (2015) Skeletal muscle as an endogenous nitrate reservoir. *Nitric Oxide* **47**, 10-16
203. Piknova, B., Park, J. W., Kwan Jeff Lam, K., and Schechter, A. N. (2016) Nitrate as a source of nitrite and nitric oxide during exercise hyperemia in rat skeletal muscle. *Nitric Oxide* **55-56**, 54-61
204. Jessen, N., and Goodyear, L. J. (2005) Contraction signaling to glucose transport in skeletal muscle. *J Appl Physiol (1985)* **99**, 330-337
205. Bradley, S. J., Kingwell, B. A., and McConell, G. K. (1999) Nitric oxide synthase inhibition reduces leg glucose uptake but not blood flow during dynamic exercise in humans. *Diabetes* **48**, 1815-1821
206. Baron, A. D. (1994) Hemodynamic actions of insulin. *Am J Physiol* **267**, E187-202
207. Baron, A. D., Steinberg, H. O., Chaker, H., Leaming, R., Johnson, A., and Brechtel, G. (1995) Insulin-mediated skeletal muscle vasodilation contributes to both insulin sensitivity and responsiveness in lean humans. *J Clin Invest* **96**, 786-792
208. Almeida, A., Almeida, J., Bolaños, J. P., and Moncada, S. (2001) Different responses of astrocytes and neurons to nitric oxide: the role of glycolytically generated ATP in astrocyte protection. *Proc Natl Acad Sci U S A* **98**, 15294-15299

209. Young, M. E., and Leighton, B. (1998) Evidence for altered sensitivity of the nitric oxide/cGMP signalling cascade in insulin-resistant skeletal muscle. *Biochem J* **329 (Pt 1)**, 73-79
210. Young, M. E., and Leighton, B. (1998) Fuel oxidation in skeletal muscle is increased by nitric oxide/cGMP--evidence for involvement of cGMP-dependent protein kinase. *FEBS Lett* **424**, 79-83
211. Young, M. E., Radda, G. K., and Leighton, B. (1997) Nitric oxide stimulates glucose transport and metabolism in rat skeletal muscle in vitro. *Biochem J* **322 (Pt 1)**, 223-228
212. Ashmore, T., Roberts, L. D., Morash, A. J., Kotwica, A. O., Finnerty, J., West, J. A., Murfitt, S. A., Fernandez, B. O., Branco, C., Cowburn, A. S., Clarke, K., Johnson, R. S., Feelisch, M., Griffin, J. L., and Murray, A. J. (2015) Nitrate enhances skeletal muscle fatty acid oxidation via a nitric oxide-cGMP-PPAR-mediated mechanism. *BMC Biol* **13**, 110
213. Doulias, P. T., Tenopoulou, M., Greene, J. L., Raju, K., and Ischiropoulos, H. (2013) Nitric oxide regulates mitochondrial fatty acid metabolism through reversible protein S-nitrosylation. *Sci Signal* **6**, rs1
214. Evans, M., Cogan, K. E., and Egan, B. (2017) Metabolism of ketone bodies during exercise and training: physiological basis for exogenous supplementation. *J Physiol* **595**, 2857-2871
215. Puchalska, P., and Crawford, P. A. (2017) Multi-dimensional Roles of Ketone Bodies in Fuel Metabolism, Signaling, and Therapeutics. *Cell Metab* **25**, 262-284
216. Noh, H. S., Kim, D. W., Cho, G. J., Choi, W. S., and Kang, S. S. (2006) Increased nitric oxide caused by the ketogenic diet reduces the onset time of kainic acid-induced seizures in ICR mice. *Brain Res* **1075**, 193-200
217. Roberts, L. D., Ashmore, T., McNally, B. D., Murfitt, S. A., Fernandez, B. O., Feelisch, M., Lindsay, R., Siervo, M., Williams, E. A., Murray, A. J., and Griffin, J. L. (2017) Inorganic Nitrate Mimics Exercise-Stimulated Muscular Fiber-Type Switching and Myokine and γ-Aminobutyric Acid Release. *Diabetes* **66**, 674-688
218. Assfalg, M., Bertini, I., Colangiuli, D., Luchinat, C., Schäfer, H., Schütz, B., and Spraul, M. (2008) Evidence of different metabolic phenotypes in humans. *Proc Natl Acad Sci U S A* **105**, 1420-1424
219. Brindle, J. T., Antti, H., Holmes, E., Tranter, G., Nicholson, J. K., Bethell, H. W., Clarke, S., Schofield, P. M., McKilligin, E., Mosedale, D. E., and Grainger, D. J. (2002) Rapid and noninvasive diagnosis of the presence and severity of coronary heart disease using 1H-NMR-based metabonomics. *Nat Med* **8**, 1439-1444
220. Martin, F. P., Dumas, M. E., Wang, Y., Legido-Quigley, C., Yap, I. K., Tang, H., Zirah, S., Murphy, G. M., Cloarec, O., Lindon, J. C., Sprenger, N., Fay, L. B., Kochhar, S., van Bladeren, P., Holmes, E., and Nicholson, J. K. (2007) A top-down systems biology view of microbiome-mammalian metabolic interactions in a mouse model. *Mol Syst Biol* **3**, 112
221. Vigneau-Callahan, K. E., Shestopalov, A. I., Milbury, P. E., Matson, W. R., and Kristal, B. S. (2001) Characterization of diet-dependent metabolic serotypes: analytical and biological variability issues in rats. *J Nutr* **131**, 924S-932S
222. Huang, X., Chen, Y. J., Cho, K., Nikolskiy, I., Crawford, P. A., and Patti, G. J. (2014) X13CMS: global tracking of isotopic labels in untargeted metabolomics. *Anal Chem* **86**, 1632-1639
223. Smith, C. A., Want, E. J., O'Maille, G., Abagyan, R., and Siuzdak, G. (2006) XCMS: processing mass spectrometry data for metabolite profiling using nonlinear peak alignment, matching, and identification. *Anal Chem* **78**, 779-787

224. Gelman, S. J., Mahieu, N. G., Cho, K., Llufrio, E. M., Wencewicz, T. A., and Patti, G. J. (2015) Evidence that 2-hydroxyglutarate is not readily metabolized in colorectal carcinoma cells. *Cancer Metab* **3**, 13
225. Niedenführ, S., ten Pierick, A., van Dam, P. T., Suarez-Mendez, C. A., Nöh, K., and Wahl, S. A. (2016) Natural isotope correction of MS/MS measurements for metabolomics and (13)C fluxomics. *Biotechnol Bioeng* **113**, 1137-1147
226. Cortassa, S., Caceres, V., Bell, L. N., O'Rourke, B., Paolocci, N., and Aon, M. A. (2015) From metabolomics to fluxomics: a computational procedure to translate metabolite profiles into metabolic fluxes. *Biophys J* **108**, 163-172
227. Srivastava, A., Kowalski, G. M., Callahan, D. L., Meikle, P. J., and Creek, D. J. (2016) Strategies for Extending Metabolomics Studies with Stable Isotope Labelling and Fluxomics. *Metabolites* **6**